UNIVERSITÀ DEGLI STUDI FIRENZE

## DOTTORATO DI RICERCA IN

Scienze Biomediche

CICLO XXVI

COORDINATORE Prof. Persio Dello Sbarba

hERG1 CHANNEL AS A MOLECULAR TARGET FOR NEW ANTICANCER THERAPEUTIC APPROACHES

Settore Scientifico Disciplinare MED/04

Dottorando

Dott. Gasparoli Luca
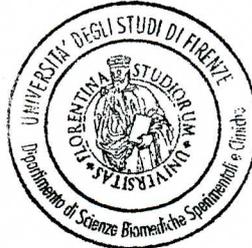
Tutore

Prof.ssa Arcangeli Annarosa

Coordinatore
Prof. Dello Sbarba Persio

Anni 2011/2013

INTRODUCTION

1. Ion channels and hallmarks of cancer

Cancer is a leading cause of death worldwide, being responsible for around 13% of all deaths in 2008 (World Health Organization, IARC). It has been extensively demonstrated, during the last 50 years, that the tumorigenesis is a multistep process, involving alterations in the genome that ultimately drive the transition from normal cells into malignant derivatives. Although there are at least 100 distinct type of cancer (Prevarskaya et al, 2010), in 2000 Hanahan and Weinberg identified six essential pathophysiological phenotypes (named "hallmarks of cancer"), which characterized the vast majority of cancer types (Hanahan & Weinberg, 2000). These hallmarks include: 1) sustaining proliferative signals, 2) evading growth suppressor, 3) resisting cell death (apoptosis), 4) limitless replicative potential, 5) inducing angiogenesis, 6) tissue invasion and metastasis. A decade later, Hanahan and Weinberg revised these six hallmarks, considering the discoveries made in understanding their mechanistic basis and including two new emerging pathophysiological phenotypes, i.e. "evading immune destruction" and "reprogramming energy metabolism" (Hanahan & Weinberg, 2011). In the same paper, the authors described two enabling characteristics, crucial for the acquisition of the above mentioned hallmarks of cancer: the first is the tumour-promoting inflammation, namely the concept that the cells of the immune system-which are present at different level in virtually all neoplastic lesion-can facilitate and contribute to tumourigenesis and cancer progression, by supplying growth and survival factors, pro-angiogenic factors and matrix-modifying enzymes (Hanahan & Weinberg, 2011). The second enabling characteristic is the genome instability and mutation, which is shared, although with several difference between different tumour type, by the great majority of human cancer (Hanahan & Weinberg, 2011). It has been widely described that genome instability can allow a succession of genetic alteration and that the mutation rate in cancer cells is greatly accelerated compared to their normal counterpart: both these characteristics could permit the onset of a subclones of cells, with different selective advantages, which can ultimately prevail on the normal cells

population. In this view, the multistep tumour progression can be also described as a succession of clonal expansions, each driven by the acquisition of a new mutant genotype (Hanahan & Weinberg, 2011).

Ion channel genes form a large superfamily (Harmar et al, 2009) which members, considering their gating mechanism, can be classified into two major categories: there are voltage-gated channels (VGICs), which open in response to the variations of membrane potential, and ligand-gated channels (LGICs), which are opened by ligands, both extracellular, such as neurotransmitters, and intracellular, such as Ca^{2+} or cyclic nucleotides. Voltage-gated ion channels, according to their ion selectivity, can be divided in three major classes: voltage-gated sodium, voltage-gated calcium and voltage-gated potassium channels.

Multiple lines of evidence in the last twenty years indicated that plasma membrane ion channels could be among the genes affected by genetic instability and mutation, during the change from normal epithelium toward cancer. Ion channels can indeed control several aspects of normal cell physiology such as cellular volume and membrane voltage (Vm) potential, proliferation and progression through cell cycle, motility and migration, differentiation and apoptosis (Becchetti, 2011) (Kunzelmann, 2005) (Li & Xiong, 2011). Thus, it's not hard to believe that genetic alteration of ion channels expression or modification in their control's mechanism during tumourigenesis, could be partly responsible for the acquisition of one or more of the above mentioned pathophysiological phenotypes (Prevarskaya et al, 2010).

As revised in 2010 by Prevarskaya et al., both calcium (Ca_v) and sodium (Na_v) voltage-gated channels are implicate in several hallmarks of cancer; as an example, different type of Ca_v channels seems to be involved in the self sufficiency of growth signals, in the acquisition of the limitless replicative potential and in the mechanisms of tissue invasion and metastasis (Prevarskaya et al, 2010) (Cuddapah & Sontheimer, 2011). In the latter malignant phenotypes also Na_v channels seems to play a crucial role: indeed altered expression of different sodium channels, mostly in their embryonic isoforms (Diss et al, 2005) (Fraser et al, 2005), has been detected in highly metastatic cancer-derived cell lines and in several biopsies of breast, prostate and cervical tumours (Diss et al, 2005) (Fraser et al, 2005).

2. Potassium channels families

In the voltage-gated ion channels superfamily, K^+ channels account, with 78 members, for about half of this extended gene superfamily (Wulff et al, 2009). According to the IUPHAR classification, K+ channels can be divided into four structural types, based on the mechanism of activation and the number of trans-membrane segments (TM), which constitute each channel subunit: a) inwardly rectifying, 2 TM, (K_{ir}), b) two-pore, 4 TM, (K_{2P}), c) calcium-activated, 6 or 7 TM, (K_{Ca}), and d) voltage-gated, 6 TM, (K_V).

Inward rectifier potassium channels (K_{ir}) are formed by four subunits, each constituted by two domains, linked by a P-loop; the physiological role of this channel family comprises the regulation of cell excitability in neurones and muscle cells and the repolarisation of cardiac action potential (Yang et al, 1995); they also contribute to development and myelination of oligodendrocytes (Neusch et al, 2001). K_{ir} channels were found to be expressed in different types of human cancer, particularly in astrocytic-type brain tumours, where they seems to have a stage-specific expression pattern, and in non-small cell lung cancer (NSCLC) in which, as an example, K_{ir} 3.1 correlates with tumour progression (D'Amico et al, 2013).

Fifteen distinct genes have been identified so far belonging to the K_{2P} channel family; two pore domain potassium channels family shares a common structure, with 4 transmembrane domains and two pore forming regions arranged in tandem (D'Amico et al, 2013). Given their K^+ selectivity, the voltage-independent gating and other peculiar biophysical characteristics, K_{2P} currents are thought to be responsible for mediating leak (also referred as background) K+ currents (Enyedi & Czirjak, 2010). The involvement of two pore domain potassium channels in cancer emerged recently with the discovery of the amplification of K_{2P} 9.1 in breast cancer (Kim et al, 2004), followed by the indication that other K_{2P} channels (in particular 3.1, 1.1 and 2.1) are expressed in prostate cancer and neuronal tumours (Ohya et al, 2009) (Voloshyna et al, 2008).

Calcium-activated potassium channels (K_{Ca}) included eight different members, divided in two well distinct major groups: the SK group comprises three "small-conductance" and one "intermediate-conductance" channels (respectively named K_{Ca} 2.1, 2.2, 2.3 and 3.1), while the BK group includes K_{Ca} 1.1, 4.1, 4.2 and 5.1. Native BK channels are usually formed by the assembly of four α subunits, which is the pore forming portion of

the channel, and four β subunits. Functional SK channels are instead composed by the assembly of four α subunits, each formed by six transmembrane domains (S1-S6), with the pore region in S5-S6 linker (Tanaka et al, 1998) (Toro et al, 1998). Member of the calcium-activated potassium channel family are involved in several physiological function, such as control of cell volume, synaptic plasticity, learning and memory formation. K_{Ca} 3.1 channels exert also a fundamental role in cell cycle, in particular during S and G2 phases, in normal angiogenesis and in vasodilatation, and they are over-expressed during lymphocytes activation. Given these pleiotropic functions, it is not surprising that K_{Ca} channels are aberrantly expressed in different types of lymphomas and leukemias, in neuroblastomas and melanomas, as well as in epithelial-derived carcinomas (for more details see (D'Amico et al, 2013)).

Voltage-gated potassium channels (K_V) are formed by four α subunits, each containing six transmembrane domains (S1-S6), which surround a central pore. The S4 domain is the voltage-sensor domain, while the residues between S5 and S6 are named P(pore)-loop or H5 domain and provide an important contribution to ion selectivity (D'Amico et al, 2013). The classification into different subfamilies of K_V channels is based on the difference in the α subunits. There are also accessory β subunits, which functions seem to be independent of the K^+ conductance and probably rely in protein recruitment and scaffolding (Li & Xiong, 2011). K_V channels exerts pleiotropic function in normal cells: they are involved in maintaining the membrane potential and modulating the electrical activity in excitable cells and in the cell volume regulation; their activity is fundamental in the progression of the cell cycle through G1/S phase (Becchetti, 2011)and in cell proliferation (Kunzelmann, 2005); they are also involved in the apoptotic signalling cascade (Pal et al, 2003) (Pal et al, 2006), in muscle contractility and some of them has a crucial role in heart physiology (for more details see below). Voltage-gated potassium channels are expressed in a broad type of human cancer, including epithelial-derived tumours, neural crest-derived, lymphomas and leukemias (Arcangeli et al, 2009) (D'Amico et al, 2013).

Several detailed reviews (Arcangeli et al, 2009) (Prevarskaya et al, 2010) (Stuhmer & Pardo, 2010) and some special issue (Arcangeli & Yuan, 2011) have deeply analysed the involvement of all the K^+ channels family described above in almost all the various

hallmarks of cancer, as well as in one of the enabling characteristics. A summary of the major findings is figured in Figure 1.1.
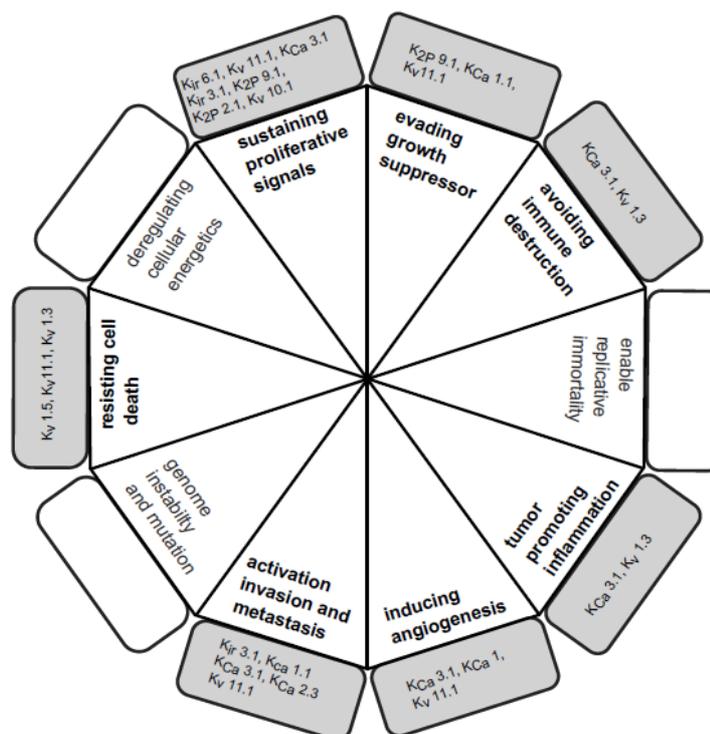
Figure 1.1: Potassium channels and the hallmarks of cancer. In the figure are reported all the potassium channels found to be involved in the different hallmarks of cancer (from (D'Amico et al, 2013)).

3. The hERG1 channel

3.1 hERG1 gene

The human ether-à-go-go-related gene (hERG) channel, also referred to as K_V 11.1 according to IUHPAR nomenclature or as KCNH2 by HGNC (HUGO Gene Nomenclature Committee), is a delayed rectifier voltage-gated potassium channels. hERG1, together with the other two member of its subfamily K_V 11.2 (hERG2) and K_V 11.3 (hERG3), is a member of the ether-à-go-go (EAG) family of voltage-dependent K^+

channels, which comprises also K$_V$ 10.1-2 (EAG1 and EAG2) and K$_V$ 12.1-3 (ELK or ether-à-go-go like) channels.

The human *KCNH2* gene is located on chromosome 7, in the region q36.1 (accession no. NG_008916), and contains 15 exons and 14 introns totalling about 33 kb (see Figure 1.2).
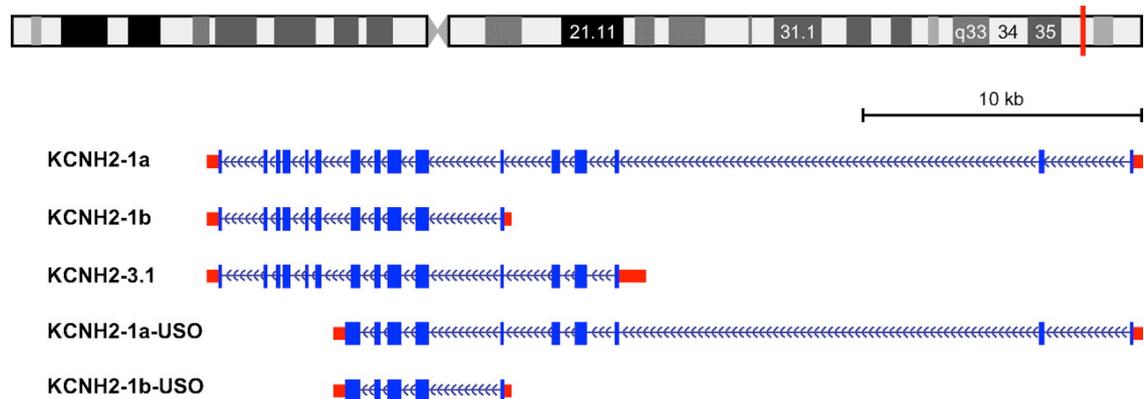
Figure 1.2: *KCNH2* **genomic structure.** In the genome browser view of the chromosome 7 in red is identified the q36.1 region. Below are listed all the KCNH2 isoform known to date (from (Vandenberg et al, 2012)).

As reported in Figure 1.2, *hERG1* gene has two additional transcription starts, besides to the one of full length hERG1A: the first is on intron 5 and the resulting transcript, named hERG1B, lacks of the first 5 exons and has an alternative and unique exon b (Lees-Miller et al, 1997); the second transcription starts is on the intron 2 and the resulting mRNA, named hERG 3.1, is missing the first two exons and has six peculiar amino acids at 5' end of exon 3 (Huffaker et al, 2009). There is also an alternative termination site, along with the stop codon in exon 15 of hERG1A: the exon 9 can be "be translated for an additional 88 unique amino acids followed by a 3'UTR within intron 9 of the KCNH2–1a transcript" (Vandenberg et al, 2012). The resulting transcripts have a premature COOH-terminal truncation and are identified as hERG1$_{USO}$.

3.2 hERG1 protein

The hERG1A transcript is translated into a 1,159 amino acids protein, which constitutes an α subunit (Figure 1.3). Each α subunit is formed by six transmembrane domains (S1-

S6), with the S4 containing six positive charges typical of K_V channels and the first four helices (S1–S4) forming the voltage sensor domain which is coupled to a central K^+ selective pore domain. This is composed of an outer helix (S5) and inner helix (S6) connected by a pore α-helix (or H5 domain) and a selectivity filter, which contains the highly conserved sequence Thr-Ser-Val-Gly-Phe-Gly. In addition the these transmembrane domains, the hERG1A protein has large NH2-terminal and COOH-terminal domains. N-terminus contains a Per-Arnt-Sim (PAS) domain, characteristic of the ether-à-go-go subfamily, while the C-terminus contains a cyclic nucleotide binding domain (cNBD), which has homology with to one of cyclic nucleotide-gated (CNG) and hyperpolarisation activated channels (HCN).
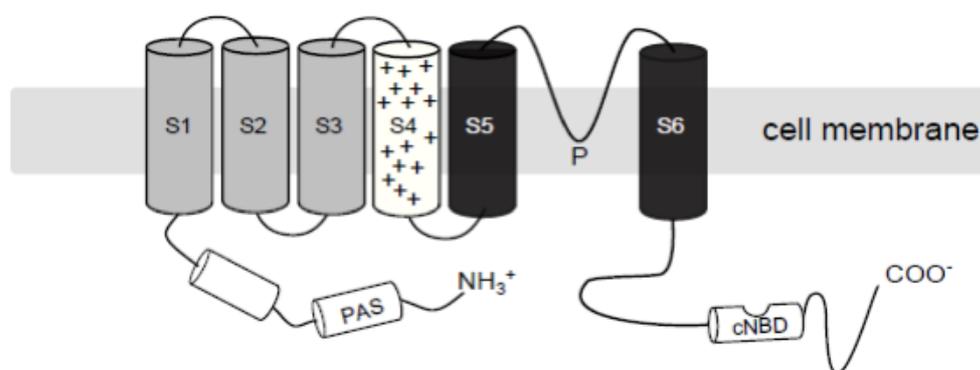
Figure 1.3. Molecular structure of one α subunit of hERG1 channels. The functional channel is a tetramer of four α subunits.

3.3 hERG1 protein assembly and tetramerisation

The functional hERG1 channel is a tetramer, formed by the assembly of four α subunits which surround a central pore. It has been demonstrated that tetramerisation can occur as homotetramers or heterotetramers of different isoforms (London et al, 1997) (Jones et al, 2004) (Phartiyal et al, 2007). Since in canonical voltage gated potassium channels the interaction of N-terminus domain can facilitate subunit assembly, the role of the two cytoplasmic domains, NH2-terminal and COOH-terminal, in hERG1 protein assembly and tetramerisation was investigated. In 1997 Li et al. suggested a contribute of N-terminus in this process, since they found a subunit interaction domain (named NAB) in the NH2-terminal which can form tetramer in absence of the rest of the hERG1 protein

(Li et al, 1997). However, in 1998, Wang et al. reported that the deletion of most of the N-terminus did not affect the normal trafficking (Wang et al, 1998). Given these opposite results, the attention was switched to the C-terminus domain. In a paper by Kupershmidt et al., the authors shown that a ligation of a portion of the distal COOH terminus (residues 1018-122, also known as the recapitulation domain) in COOH-terminus lacking channels is able to rescue both hERG1 trafficking and current (Kupershmidt et al, 1998). However, subsequent works have shown that these residues are not crucial for the functional tetramers (Akhavan et al, 2003). Therefore both cytoplasmic domains may be not essential but could contribute to tetramers stabilisation. Recently, it has been proposed that cNBD domain could have a role in the tetramerisation process, since mutations or partial deletion of this domain resulted in trafficking defects. Furthermore, Gustina and Trudeau have recently demonstrated that both intersubunit interactions can involve PAS and cNBD domains (Gustina & Trudeau, 2011).

3.4 Gating of hERG1 channel and its molecular basis

3.4.1 Activation

The process of activation of a voltage-dependent K^+ channel (VGK) begins when changes in the transmembrane electric field cause outward movement of the voltage sensing domain (VSD), which comprises the first four transmembrane domains (S1-S4). This structural rearrangements are transferred to the pore domain of the channels through the physical interaction of the S4-S5 linker with the cytoplasmic terminals of the S6 domain, which is responsible of the opening and closing of the activation gate. This briefly described mechanism of potassium channels activation is shared also by hERG1 channels concerning the role of VSD, S4-S5 linker and S6 domain (Vandenberg et al, 2012). Nevertheless, there are some differences in hERG1 activation gating in comparison to other VGK channels.

Activation gate

By analysing the crystal structure of several potassium channels it has been demonstrated that the COOH-termini of the inner helices are packed in the close state and subsequently spread out in the open state (Vandenberg et al, 2012). There are two hypothetical hinge points: the first is a highly conserved glycine residue (Gly 648 in

hERG1), while the second is a Pro-X-Pro motif which plays a crucial role in the movement of the activation gate (hERG1 channel has instead a second glycine in position 657). However, mutagenesis experiments, performed by Mitcheson's group, found that substitution of both S6 glycine residues did not altered the voltage dependence rates of activation and did not prevent channel opening (Mitcheson et al, 2005) (Hardman et al, 2007). These data suggest that the two glycine in position 468 and 657 are more important for helical packing rather than as a hinge of the channel pore. Another difference between hERG1 and VGK channels in the COOH-termini of the S6 domain includes the presence of two micro domains crucial for the hERG1 gating (Wynia-Smith et al, 2008). The first and innermost is a ringed domain, constituted by Gln664, Tyr667 and Ser668, in which Gln664 is responsible of the occlusion of the conduction pathway in the closed state. The second micro domain contains the residue Val659, which is buried, in the closed state, in a pocket formed by S5, S6 and S4-S5 linker. Mutations in this residue reduce the slope of voltage dependence activation, suggesting a crucial role of this residue in the coupling of the voltage sensor and the activation gate (Wynia-Smith et al, 2008).

Voltage sensing domain

The S4 domain is deeply involved, in most of the VGK channels, in the voltage sensing process, containing four positively charged residues. In K_V 11.1 these four residues are Lys525, Arg528, Arg531 and Arg537: mutation of any of these residues to glutamine, i.e. a neutralisation of the positive charge, changes the voltage dependence of activation gating (Subbiah et al, 2004). In particular, A531Q mutation (arginine to glutamine) causes a shift towards the closed state, while mutation in Lys525 shifted the equilibrium towards open state, thus suggesting that Lys525 and Arg531 are responsible of the stabilisation of respectively the closed and the open states in wild type channels. Subbiah et al. also demonstrated the crucial specificity of the lysine in position 525 in the voltage dependence of activation by showing that replacement of this lysine with another positively charged amino acid (e.g. an arginine) did not restore the wild type phenotype (Subbiah et al, 2004). In the same year Zhang and Tseng (Zhang et al, 2004) showed, by examining the contribution to activation of each of the charged residues in the S4, "that only the outermost three residues contributed to activation gating charge" (Vandenberg et al, 2012).

As reported above one peculiar characteristic of hERG1 channels is the very slow activation gating. Several hypothesis have been suggested to explain this feature: slow activation could be due to slow movement of the voltage sensing domain or to inefficient coupling between VSD movement and opening of the S6 domain or to both factors together. Smith and Yellen (Smith & Yellen, 2002) before and Piper at al. (Piper et al, 2003) the following year demonstrated that the slow kinetics of hERG1 channel activation can be explained by slower movement of the VSD domain compared to the *Shaker* channels. These findings shifted the attention to the origin of VSD slow movement. Two main hypothesis were proposed: the slow movement could be due intrinsic properties of the domain or to addition constraints on the voltage sensor. Subbiah et al and Zhang et al. both investigated the hypothesis of internal constraints, the first suggesting that the movement of the S4 helix could be limited by steric hindrance of surrounding protein domains (Subbiah et al, 2005) and the second hypothesising the presence of internal salt bridges between the positively charged residues in S4 and negative charges in the S1-S3 transmembrane helices (Zhang et al, 2004). However, the hypothesis by Subbiah et al. was not verified by experimental data, since it turned out that the S4 helix has not close interaction with other domain in the voltage sensor. Regarding the second hypothesis, different groups have identified several residues in S1, S2 and S3 domains involved in the folding of the VSD and contributing to the gating movement. In K_V 11.1 these residues are Asp411 in S1, Asp456, 460 and 466 in S2 and Asp501 and 509 in S3. Mutation of each of these residues causes changes in the biophysical properties of activation: in particular Asp460 e Asp509 seems to act by stabilising the open state, while Asp411 is involved in stabilisation of the close state (Vandenberg et al, 2012). Together with the previous findings of the involvement of Lys525 and Arg531 for the stabilisation of respectively the closed and the open state, Lys525-Asp411 and Arg531-Asp460/Asp509 could represent possible salt bridges between VSD and the S1-S3 domains (Zhang et al, 2004); (Piper et al, 2008). Moreover, it has been shown that also external factors, such as S4S5 linker, can limit the VSd movement in hERG1 channels (Van Slyke et al, 2010).

Coupling of voltage sensing domain and activation gate

As reported above, it is thought that the rearrangements of the voltage sensing domain are transferred to the activation gate through the interaction of the S4-S5 linker and the S6 helices (Tristani-Firouzi et al, 2002). Indeed, several mutation have been identified in this linker in two amino acids residues, Asp450 and Glu544, altering both activation and deactivation gating. Using one of these mutant, D450K, Tristani-Firouzi et al. investigated the interaction between S4-S5 and S6 helices and demonstrated that Arg665 residue in S6 is the unique amino acids involved in the activation gating of the D450K mutant. These findings suggested that, in wild type channels, the interaction between S4-S5 and S6 helices, which mediates the coupling of VSD and activation gate, can occur through electrostatic interaction between Asp50 and Arg665 (Tristani-Firouzi et al, 2002).

3.4.2 Deactivation

Like the corresponding process of activation, also the deactivation gating is characterised by a very slow kinetic. However, the mechanism of slow closure of hERG1 does not entirely depends on the slow movements of the voltage sensing domain; indeed some of the unique cytosolic domains of hERG1 channel have been shown to modulate the kinetic of channel deactivation.

NH_2 terminus

The role of the NH_2 terminus in the process of channel deactivation has been proposed after the discovery that deletion of the NH_2 cytoplasmic domain resulted in a great acceleration of deactivation kinetic (Schonherr & Heinemann, 1996) (Spector et al, 1996). In particular, the attention has been focused on the PAS domain of the NH_2 terminus, since several papers have demonstrated that acceleration of the deactivation kinetics was due to point mutations in this domain (Morais Cabral et al, 1998) (Gustina & Trudeau, 2009). Moreover, the work of Morais Cabral et al. showed that the addition of recombinant protein corresponding to the PAS domain resulted in substantial reduction of the fast deactivation kinetic of the hERG Δ2-373 mutant channels (Morais Cabral et al, 1998). The findings by Morais Cabral on the importance of the PAS domain have been recently confirmed by Gustina and Trudeau: they showed that genetically encoded PAS domain, but not mutant PAS domain construct, is able to

restore the wild-type slow deactivation kinetics to a hERG Δ2-354 mutant channel (Gustina & Trudeau, 2009).

With the PAS domain starting at residue 26, also the preceding 25 amino acids seems to play a role in the regulation of hERG1 channel deactivation. Indeed, deletion of these 25 residues results in a phenotype similar to that seen with the deletion of the entire NH_2-terminus and numerous point mutation within these residues greatly accelerate the deactivation rates (Muskett et al, 2011) (Ng et al, 2011). The NMR resolution of the PAS domain revealed that these first 25 amino acids formed a α-helical element, whose disruption resulted in an acceleration of deactivation comparable to the one obtained with the truncation of the entire 25 residue tail (Ng et al, 2011). All these findings strongly indicate that the NH_2 terminus plays a crucial role in slow deactivation of the hERG1 channels. The hypothesised mechanism suggests that a stable interaction of the PAS domain with the core of the channel could bring the NH_2 terminal tail near to "the central conduction axis" where it can regulate the activation gating (Vandenberg et al, 2012).

Numerous hypothesis have been proposed regarding the interaction site of both PAS domain and NH_2 tail with the channel. One possible site of interaction was identified by Gustina and Trudeau, since they demonstrated that deletions of the cNBD resulted in a deactivation kinetic as fast as with deleted PAS mutants. Moreover they showed that addition of a recombinant PAS domain to channels lacking of both PAS domain and cNBD did not restore slow deactivation (Gustina & Trudeau, 2011). These findings suggest that a possible site of interaction, in the regulation of deactivation gating of hERG1 channel, is between cytoplasmic PAS and cNDB domains. The importance of this interaction was further supported by the identification of hydrophobic patch on the surface of cNBD, in which modification of the charged residues led to a strong increase in deactivation rate (Al-Owais et al, 2009). A similar hydrophobic patch was also identified in the surface of PAS domain (Morais Cabral et al, 1998), thus providing a possible site for stable interaction between the two domains.

A possible site of regulation of the deactivation gating was thought to be the S4-S5 linker: mutations in this linker indeed resulted in modification of the deactivation kinetics (Wang et al, 1998) (Wang et al, 2000). As an example, the introduction of a cysteine in position Gly546 in S4-S5 linker caused an acceleration of the deactivation

similar to the one reported for the Δ2-354 mutant (Wang et al, 1998). In 2010, Li et al. showed that titration of the PAS domain protein in presence of some amino acids of the S4-S5 linker modified the peaks of heteronuclear single quantum coherence spectroscopy (HSQC) spectrum and argued that a specific interaction could exist between S4-S5 linker and PAS domain residues (Li et al, 2010). Another proposed site interaction between NH_2 terminus and the rest of the hERG1 channel was identified, using cysteine mutagenesis, by de la Pena et al. (de la Pena et al, 2011). The authors showed that Val3Cys in the NH_2 tail is able to form disulfide bridges with the Tyr542Cys in the S4-S5 linker, thus suggesting that these residues could be in close proximity.

3.4.3 Inactivation

The inactivation process of hERG1 channels is analogous to C-type inactivation of *Shaker* channels, since it is "sensitive to external application of TEA and ion occupancy of the selectivity filter" (Schonherr & Heinemann, 1996) (Spector et al, 1996)). However, hERG1 inactivation process has also some unique features including fast and voltage-dependent rates of inactivation and recovery from inactivation and potassium sensitivity (Smith et al, 1996) (Schonherr & Heinemann, 1996) (Spector et al, 1996). As discussed before (see "physiological role of hERG1 in heart" chapter) the presence of inactivation gating was first suggested by Shibasaki in 1987 and its very fast kinetic was thought to be the basis of the "hook" shape of the I_{Kr} current following repolarisation. Moreover, in 1996 it turned out that the unique features of hERG1 C-type inactivation could explain the mechanism of inward rectification identified by several groups in both native I_{Kr} and heterologous systems (Smith et al, 1996) (Schonherr & Heinemann, 1996) (Spector et al, 1996). At date, the role of the different channel domains in the process of inactivation has been well described.

Role of the selectivity filter

The importance of the selectivity filter in fast inactivation was demonstrated by the discovery that several mutation within this region abolished inactivation. As an example, in the double S631C:G628C or in the single S620T mutant channels the inactivation was completely removed (Smith et al, 1996) (Schonherr & Heinemann, 1996) (Herzberg et al, 1998). Herzberg et al. also demonstrated that removing the region

of the pore helix and the selectivity filter form hERG1 channel and adding the same region to EAG channel conferred rapid inactivation to the latter and abolished it in hERG1 (Herzberg et al, 1998).

In the last years the molecular basis of gating at the selectivity filter have been deeply analysed in both *Shaker* and KcsA channels and numerous residues have been identified to be crucial for both ion selectivity and C-type inactivation. These residues form a network of hydrogen bonds and van der Waals interactions between NH_2 terminus of the pore helix and the selectivity filter, contributing to the maintenance of the selectivity filter conformations and stabilising it in both open and/or inactivated states (Doyle et al, 1998) (Cuello et al, 2010) (Cordero-Morales et al, 2007). However, none of these residues have been found in hERG1 channels and the lacking of the corresponding hydrogen bonds seems to be responsible for the more "collapsing" feature of hERG1 selectivity filter which causes faster rate of inactivation (Fan et al, 1999).

The tight relationship between ion selectivity and inactivation in hERG1 channels was further confirmed by the identification of several mutation which alter both the inactivation process and the ionic selectivity (Lees-Miller et al, 2000) (Liu et al, 2002) (Tseng, 2006). For these reasons it has been proposed that inactivation process could be constituted by two different steps, name P-type and C-type, characterised by a decrease in selectivity for K^+ over Na^+; P-type steps corresponds to "the initial closure of the selectivity filter" while C-type "refers to the stabilisation of the inactive state" (Gang & Zhang, 2006).

Role of the pore outer mouth

The pore outer mouth was first identified as an important regulator of C-type inactivation in *Shaker* channels, in particular in its residue Thr449. Mutation in the corresponding residue in hERG1, i.e the Ser631, resulted in either a strong shift in the $V_{1/2}$ of inactivation (the S631A mutation) or in complete destruction of inactivation (the S631E or S631K) (Zou et al, 1998) (Fan et al, 1999).

Role of the S5 Pore domain

The role of the S5P linker in hERG1 channels inactivation was suggested by the discovery that mutation in two histidine residues (His578 and His687) in this region resulted in altered inactivation features (Jiang et al, 1999). The same authors, however, noticed that some mutations in His687 did not affect hERG1 gating properties, while the same mutations in His578 had a deep impact on both inactivation and ion selectivity. These findings raised the question of how mutation in the S5P linker could affect inactivation and ionic selectivity, since S5P is quite far from pore and selectivity filter in the primary protein structure (Vandenberg et al, 2012). A possible explanation to this question comes from the NMR resolution of this region, which revealed the presence, suggested by different authors, of a helical component in the middle part of the linker (Torres et al, 2003). This helical structure is thought to run parallel to the membrane and with the NH_2 terminus in close proximity to the central pore (Jiang et al, 2005). Jiang et al. also proposed that S5P helical domains could physically contribute to ion conduction termination during inactivation by steric hindrance or through the interaction of hydrophobic residues along S5P helices, which create a local electrostatic potential unfavourable to K+ ion flux (Jiang et al, 2005).

Role of the eag domains

Recently Gustina and Trudeau investigated the involvement of eag domain in the regulation of hERG1 channel inactivation (Gustina & Trudeau, 2013). Using different hERG1 mutant lacking of only the eag domain or the entire NH_2 terminus (Δ2-135 or Δ2-354) and co-expressing them with eag domain-containing fragments, they demonstrated that eag domain-containing fragments were able to restore inward rectification, inactivation rate, recovery from inactivation and steady-state inactivation to wild type-like values. All these findings suggested that eag domain plays a crucial role in the inactivation process, through a direct interaction with the channel (Gustina & Trudeau, 2013).

Voltage sensitivity of inactivation

As stated above, one of the peculiar feature of hERG1 channels is the voltage dependence of inactivation. Two main hypothesis have been considered concerning the origin of this voltage dependence. The first suggested that voltage dependence could be due to the coupling with the S4 voltage sensor, in particular of the fast component of the

voltage sensor movement (Piper et al, 2003); the second proposed the presence of an inactivation-voltage domain different from the activation voltage sensor (Clarke et al, 2006). Despite the use of numerous approaches, including voltage-clamp fluorometry and the use of different hERG1 mutants, the first hypothesis was never confirmed by experimental data, thus leaving unresolved the possible link between VSD movement and voltage dependence of inactivation. The attention was then switched to the SP5 linker as a candidate for the inactivation voltage sensor (Torres et al, 2003) (Clarke et al, 2006). The hypothesis of Tseng et al. is that SP5 linker could act as a bridge, coupling the VSD and the outer mouth of the pore: during depolarisation, the SP5 helices are moved toward the channel pore by the upward motion of the voltage sensor, thus forming a barrier to ion conduction (Liu et al, 2002). This hypothesis was further reinforced by the discovery that the introduction of positive and negative charged residues in all the hydrophilic residues in the SP5 α-helix dramatically shifted the voltage range of inactivation. Moreover, the interchange of the SP5 domains between hERG1, EAG and hELK-2 resulted in a large effect of the voltage dependence of inactivation (Clarke et al, 2006).

The C-type inactivation in hERG1 is thought to be a complex process, involving the role of numerous domains throughout the channel. Recently, Wang and colleagues showed that hERG1 channel inactivation started with the efflux of K+ from the selectivity filter, and followed with conformational rearrangements of S5 helix, extracellular turret region, S4 domain, S4-S5 linker and pore domain inner helix. The last step of this process could be collapse of the selectivity filter, which may stabilise the inactivation state (Wang et al, 2011).

3.5 Physiological role of hERG1 in heart

hERG1 channels, like other VGK potassium channels, can reside in three different states: closed, open and inactivated state. However, as described above, hERG1 channels display some peculiar gating kinetics: indeed the transitions between closed and open state are slow, while the transitions from open to inactivated states are very fast and voltage dependent. These unusual kinetics confer to hERG1 channels some distinctive characteristics, such as the presence of a hooked tail current upon repolarisation, that were first identified in cardiac isolated myocytes. The presence of a rectifying K+ current, contributing to repolarisation of the cardiac action potential

(cAP), has been repeatedly reported between 1969 and 1980. In 1987 Shibasaki identified, in rabbit sinoatrial node cells, the current now known as the rapid component of the delayed rectifying current I_{Kr}. Shibasaki demonstrated the presence of a voltage-dependent activation gate and suggested, based on the lifetime of the open state, the presence of a second different gate, i.e. the inactivation gate; he also proposed that the existence of a "hook" current was due to " a quick removal of inactivation" during the repolarising pulse (Shibasaki, 1987). During the following years the above mentioned characteristics of hERG1 current in cardiac myocytes were deeply analysed by several groups, by both electrophysiological and pharmacological method, until Sanguinetti and Jurkiewicz in 1990 "coined the term I_{Kr} to describe this component of the repolarising I_K" (Sanguinetti & Jurkiewicz, 1990).

To date the hERG1 role in cardiac action potential is fully characterised. The ventricular cardiac action potential is composed by five distinct phases. Phase 1 is the rapid upstroke due to activation of Na channels. Repolarisation then takes place during the next three phases. There is an initial fast repolarisation (phase 1) due to activation of transient outward K^+ current (I_{TO}), which lasts only a few milliseconds, followed by a very slow repolarisation (phase 2) that gives rise to the prolonged action potential plateau, and then the final repolarisation (phase 3) that terminates the action potential and returns membrane potential back to the resting membrane potential (phase 4). Phases 2 and 3 are so prolonged, in part because of the slow inactivation of L-type calcium current, but also because the K^+ currents responsible for repolarisation are small in amplitude, slow to activate or have a low conductance at depolarised potentials. The long duration of the cardiac action potential is important for allowing excitation-contraction coupling to occur, but also makes ventricular muscle refractory to premature or unsynchronised depolarisations. I_{Kr} is the most important of the K^+ currents for terminating the action potential. In the early part of phase 2, at depolarised membrane potential hERG1 channel slowly activates and rapidly enters in a non-conducting inactivate state, thereby passing little current through the channel. At the beginning of the repolarisation phase, hERG1 channel quickly recovers from inactivation and, due to the very slow deactivation kinetic, allows more current to flow through, thus contributing to shape the repolarising AP phase (Spector et al, 1996). At the end of the repolarisation hERG1 channel fully deactivates. These properties, i.e the slow

activation/deactivation kinetics and the very rapid inactivation and recovery from inactivation, enable hERG1 channel either to determine the duration of plateau phase of the action potential and to rapidly respond to depolarising stimuli, making the cardiac myocytes refractory to premature excitation (Sanguinetti & Tristani-Firouzi, 2006).

3.5.1 Importance of hERG1B isoform in native IKr

The gating features described above in isolated myocytes have been also recapitulated in heterologous systems, through the expression of the hERG1A isoform in both mammalian cells and *Xenopus* oocytes. I_{Kr} and heterologous hERG1 current display quite similar biophysical properties, such as $V_{1/2}$ of activation, inward rectification and paradoxical activation by external K^+ (Vandenberg et al, 2012). However, regional heterogeneity it has been described in the kinetics properties of native I_{Kr} in heart (Gintant, 2000). A possible explanation of this heterogeneity is native I_{Kr} being the result of heterotetramerisation of both hERG1A and hERG1B subunits (London et al, 1997); (Lees-Miller et al, 1997). As discussed above, the hERG1B transcripts lacks of the first 5 exons and has an alternative exon b. The corresponding protein is 340 amino acids shorter than the full length hERG1A and has 34 unique amino acids in the N-terminus, with no homology with the N-terminus of hERG1A (Lees-Miller et al, 1997). This peculiar domain determines the fast deactivation typically observed in hERG1B (Lees-Miller et al, 1997) (Morais Cabral et al, 1998). In 2008, two groups independently shown that heterotramers of hERG1A and hERG1B isoforms have faster activation, deactivation and recovery from inactivation compared to the homotetramers of hERG1A subunits (Larsen et al, 2008) (Sale et al, 2008). Moreover, a few years later, Larsen and Olesen demonstrated that heterogeneity of native I_{Kr} can be reproduced by varying the ratio of hERG1A and hERG1B isoforms and that the relative abundance of these two isoform has also an effect on cardiac action potential duration (cAPD) (Larsen & Olesen, 2010). These findings, together with the detection at both RNA and protein level of the hERG1B isoform in human heart (Larsen et al, 2008); (Jones et al, 2004) and the demonstration that the two isoforms preferentially coassemble through interaction of the NH_2-termini (Phartiyal et al, 2007), strongly supported the hypothesis that native I_{Kr} is composed of hERG1A/hERG1B heterotetramers.

3.6 Non-cardiac roles of hERG1 channels

3.6.1 hERG1 in neuronal and smooth muscle cells

Numerous data emerged in the last years on the functional role of hERG1 currents in the non cardiac cell populations where ERG expression has been detected (Schwarz & Bauer, 2004). In neurones, hERG1 can regulate cell firing in several types of neuronal cells (Chiesa et al, 1997) (Sacco et al, 2003). hERG1 current also regulates hormonal secretion in neuroendocrine cells (Rosati et al, 2000) (Lecchi et al, 2002) (Gullo et al, 2003), mainly through the regulation of Ca^{2+} concentration. In these cells, hERG1 displays an inhibitory activity on secretion of the specific hormone and the blockade of hERG1 currents suddenly leads to increase hormone secretion. Moreover, a primate-specific hERG1 isoform, named hERG 3.1, was recently identified by Huffaker et al. in human brain (Huffaker et al, 2009). This isoform, which lacks of the N-terminal domain, resulted to be over-expressed in hippocampus from individuals with schizophrenia and induced a high-frequency, non-adapting firing pattern in primary neurones. These findings suggest a possible role of hERG 3.1 isoform in neurological disorders (Huffaker et al, 2009).

Finally, hERG1 controls smooth muscle cells contraction. In particular, hERG1 currents have an active role in the control of membrane potential in smooth muscle cells: hence, the pharmacological block of hERG1 current in these cells depolarises the membrane potential, with an increase in muscle contraction (Farrelly et al, 2003).

3.6.2 hERG1 channels and cancer

The first indication of the presence of hERG1 channel in cancer derived from patch-clamp experiments on neuroblastoma cell lines: a K^+ current constitutively and highly expressed in these cells was identified, having the same biophysical and pharmacological properties of the cardiac I_{Kr}. Moreover, the same K^+ current governs the resting potential (V_{rest}) of neuroblastoma cells and is modulated in the different phases of the cell cycle (Arcangeli et al, 1995). These findings were further reinforce by the identification of the same current in tumours with different histogenesis but not in the healthy counterpart of the same tissues (Bianchi et al, 1998). In the following years hERG1 channels was found to be frequently over- and/or mis-expressed in many tumour cell lines as well as in primary human cancers. In 2000 Cherubini et al.

demonstrated that both *herg1* gene and hERG1 protein are expressed at high level in primary samples of human endometrial cancer as compared to normal and hyperplastic endometrium (Cherubini et al, 2000). Different groups have enlightened the expression and the role of hERG1 channels in both leukaemia cell lines and primary samples of Acute Myeloid Leukaemia (AML) (Smith et al, 2002) (Pillozzi et al, 2002); (Pillozzi et al, 2007), as well as in primary tumour and in cell lines of acute lymphoblastic leukaemia (ALL) (Pillozzi et al, 2011). The overexpression of hERG1 channels in both primary tumours and cancer cell lines was also demonstrated in colorectal and gastric cancer (Lastraioli et al, 2004) (Shao et al, 2008), in glial tumours, especially in high-grade astrocytic tumour (Masi et al, 2005) and in human melanomas (Afrasiabi et al, 2010); (Arcangeli et al, 2013), as well as in human mammary carcinoma cell line MCF-7 (Roy et al, 2008). Moreover, in 2012 Menendez et al. demonstrated that hERG1 is frequently aberrantly expressed in primary samples and in carcinoma-derived cell lines of head and neck squamous cell carcinomas (Menendez et al, 2012).

Given the hERG1 channel broad expression in such different human cancer, it is not surprising that hERG1 plays a crucial role in different hallmark of cancer (Figure 1.1) and in numerous other features of neoplastic cell behaviour.

Control of voltage membrane potential (V_m)

Conversely to what occurs in slowly proliferating or non-proliferating cells, in which the resting membrane potential is between -70 and -90 mV, a voltage membrane potential between -30 and -50 mV is typical of highly proliferative cycling cells (Binggeli & Weinstein, 1986). The biophysical features of hERG1 channel result in a maximal steady-state open probability (the peak of the ''window current'') around -40 mV, due to the intersection of activation and inactivation curves (Schonherr et al, 1999); this characteristic suggested that hERG1 channel could spend, in highly proliferating cells like cancer cells, most of the time in the open state, thus being the main actor in controlling the V_m (Arcangeli & Becchetti, 2010). Moreover, when hERG1 currents are mainly represented by hERG11B isoform, like in leukaemia cells, the faster rates of deactivation and inactivation typical of this isoform confer to the steady state current a more depolarised values (around -20 mV) (Guasti et al, 2008); (Schonherr et al, 1999). These V_m values were confirmed, by patch-clamp experiments, in both leukaemia and neuroblastoma cell lines (Arcangeli et al, 1995) (Schonherr et al, 1999).

Control of cell proliferation

The link between membrane potential, ion channels and cell cycle was clarified in the early nineties (Wonderlin & Strobl, 1996) and all the following observation have supported the notion that specific ion channels could affect different aspects of cell proliferation in both normal and cancer cells (Becchetti, 2011). hERG1 channels seems to be crucial in both the transition between G_0/G_1 and G_1/S phase (Becchetti, 2011), when a K^+ channels-mediated hyperpolarisation is required for Ca^{2+} entry; in addition, the hyperpolarisation of cell membrane is crucial for the establishment of the electrical gradient necessary for Na+-dependent transport of metabolic substrates and ions across the plasma membrane, which is necessary for DNA synthesis (Jehle et al, 2011). In this view, overexpression of hERG1 channels could confer a selective growth advantage to cancer cells, leading to loss of proliferative control and to increase of cell cycle rate. The crucial role of the hERG1 channels in cell cycle and proliferation was confirmed by the inhibition of hERG1 channels: indeed both treatment of leukaemic and neuroblastoma cell lines with either E-4031 or WAY 123,398 or silencing hERG1 with shRNA or siRNA in neuroblastoma and gastric cell lines induces arrest of the cell cycle in G1 phase (summarised in (Jehle et al, 2011)). Moreover, several lines of evidence indicated that hERG1 channels could exert control on cell cycle and proliferation not only by controlling V_m but also by switching on or modulating signalling pathways, through the formation of macromolecular complexes (Pillozzi & Arcangeli, 2010). An example of such macromolecular complex is the one formed by β1 integrins, VEGFR-1 (FLT-1) and hERG1 channels in acute myeloid leukaemia, which regulates cell proliferation and invasion (Pillozzi et al, 2007).

Invasion and metastasis

hERG1 channels were found to be involved in the regulation of cell migration, invasion and metastasis in different cancer cell lines. In acute myeloid leukaemia the control of cell invasion is exerted by the same macromolecular complex outlined above, i.e. the one between β1 integrins, VEGFR-1 (FLT-1) and hERG1 channel (Pillozzi et al, 2007). Indeed, the migration induced by the addition of VEGF and by the concomitant stimulation of integrins was inhibited by hERG1 specific blockers WAY and E-4031 (Pillozzi et al, 2007). hERG1 activity seems to be crucial for cells invasion also in colorectal cancer, since it has been demonstrated that pharmacological inhibition of the

channel by WAY reduces cell migration in H630, HCT116 and HCT8 (Lastraioli et al, 2004). The same results, i.e. a reduction of cell migration and invasion, were obtained *in vitro* treating melanoma cells MDA-MB-435S with either specific hERG1 blocker and with siRNA against hERG1 (Afrasiabi et al, 2010) and by siRNA mediated knockdown in head and neck squamous carcinoma-derived cell lines (Menendez et al, 2012). Recently, Crociani et al. also demonstrated that hERG1 activity is able to regulate cell invasion and metastatic spread of colorectal cancer cells *in vivo* (Crociani et al, 2013).

Inducing Angiogenesis

The relationship between hERG1 channels and the well-known prototypes of angiogenesis inducers, i.e. the vascular endothelial growth factor-A (VEGF-A), was firstly identified by Masi et al. in glioblastoma cell lines (Masi et al, 2005). They presented evidence that hERG1 expressing cells U138 secretes VEGF-A in the culture medium and that treatment with hERG1 blocker WAY decreases the secretion in dose dependent manner, whereas WAY treatment does not inhibit VEGF secretion in non hERG1 expressing neuroblastoma cells A172 (Masi et al, 2005). This evidence was further supported by the discovery of a significant correlation between *herg1* expression and VEGF secretion in both AML primary blast and AML cell lines, as well as by the identification of the β1 integrins, VEGFR-1 (FLT-1) and hERG1 channels macromolecular complex (Pillozzi et al, 2007).

Resisting cell death

Evading or reduced apoptosis is a crucial stage in carcinogenesis process and it has been underlined that potassium channel blockers can induce apoptosis of tumour cells (Choi et al, 1999). Different groups have investigated the role of hERG1 channels in cell programmed death and it turned out that hERG1 inhibition, both pharmacological and siRNA mediated, resulted in a significant increase in cell apoptosis in different cancer cell lines (Shao et al, 2005) (Shao et al, 2008) (Pillozzi et al, 2011) (Zhang et al, 2012). The importance of hERG1 channels in the apoptotic pathways has been demonstrated by Thomas et al. in HEK293 hERG1 transfected cells, in which they shown an increase in apoptosis following treatment with doxazosin, a α1-adrenoceptor antagonist with hERG1-blocking features (Thomas et al, 2008). The mechanisms of the doxazosin-induced apoptosis has been investigated in HL-1 cardiomyocytes and involved the

endoplasmic reticulum pathway: in brief the phosphorylation of p38 mitogen-activated protein kinase induces a cascade of different proteins activations, dimerisation and nuclear translocations which end in the activation of caspase 3 and in the cleavage of the protein-tyrosine kinase FAK (focal adhesion kinase); the loss of FAK compromises cell adhesion and starts apoptosis (Eiras et al, 2006). It has been demonstrated that FAK proteins co-assemble with hERG1 channel and β1 integrins and that cell adhesion activates hERG1 channels, leading to FAK phosphorylation (Cherubini et al, 2005). Moreover, FAK and hERG1 overexpression in different tumours "has been independently related to enhanced dissemination and invasiveness" (Kornberg, 1998) (Lastraioli et al, 2004). Based on these evidences some authors hypothesised that FAK phosphorylation, following hERG1 activation, could confer to cancer cells the ability to avoid apoptosis in the absence of cell adhesion to extracellular matrix (Jehle et al, 2011); the blockade of hERG1 channel by doxazosin thus may lead to inhibition of FAK phosphorylation, depriving transformed cells of a mechanism to circumvent cell apoptosis (Jehle et al, 2011). However, pro-apoptotic hERG1 blockers such as imatinib (Zheng et al, 2012) and cisapride (Shao et al, 2008) could activate different pathways and their mechanisms of action are still unclear.

Chemotherapy resistance

Intrinsic or acquired resistance to chemotherapy is becoming, in the last years, one of the major limit to the good outcome of cancer therapy, in both solid tumours and leukemias (Pommier et al, 2004). In leukaemic cells, a contribute to drug resistance can be exerted by bone marrow mesenchymal cells (MSCs) (Kumagai et al, 1996). It has been recently demonstrated that hERG1 channels plays also a critical role in the development of chemotherapy resistance in acute lymphoblastic leukaemia (ALL). A macromolecular complex between hERG1 channels, β1 integrins and CXCR4 was found to be expressed on the plasma membrane of leukaemia cells and to be activated by culture of leukaemic cells with MSCs. The activation of such complex modulates downstream signalling pathways, including ILK, ERK1/2 MAP kinases and Akt (Tabe et al 2007), which in turn produces anti-apoptotic effects thus counteracting the effects of classical chemotherapeutic drugs such as doxorubicin, prednisone or methotrexate (Pillozzi et al, 2011). The role of hERG1 channels in this process is further reinforced by the demonstration that hERG1 specific blockers, such as E-4031, WAY and

erythromycin, resulted in a reduction of the protective effect of MSCs and, more important, in an enhancement of the effect of chemotherapeutic drugs (Pillozzi et al, 2011).

3.7 hERG1 channels and drugs development: hERG1 as an anti-target

As described above (see Physiological role of hERG1 in heart) hERG1 channels plays a crucial role during cardiac action potential (cAP) being one of the major regulator of the action potential repolarisation in cardiac cells. The importance of hERG1 channels in heart physiology was further strengthened by the discovery that inherited mutations in the *herg1* gene cause long QT syndrome (LQTS); LQTS is a cardiac repolarisation disorder defined by the prolongation of the electrocardiographic (ECG) QT interval, which represents the time needed for ventricular repolarisation during a single cardiac cycle, and by an increased risk of ventricular fibrillation (Sanguinetti & Tristani-Firouzi, 2006).

LQT can also be acquired (aLQT) as a side effect of the treatment with different drugs, including both anti-arrhythmic (such as class I and III drugs) and non anti-arrhythmic compounds, such as antihistamines, antipsychotics and antibacterials drugs. The main mechanisms underlying the drug-induced LQT turned out to be the reduction of the hERG1 channel currents, because of a direct blockade of the I_{Kr} currents in cardiac ventricular cardiomyocytes (Keating & Sanguinetti, 1996) (Recanatini et al, 2005) (Witchel, 2011), of the disruption of the channel trafficking to cell membranes (Eckhardt et al, 2005), or of some indirect mechanisms (Mitcheson, 2008) (Witchel, 2011). The most critical consequence of the QT prolongation is the onset of the polymorphic ventricular tachyarrhythmia known as *Torsades de pointes* (TdPs), a potentially life-threatening arrhythmia which can degenerate into ventricular fibrillation and sudden death (Viskin, 1999) (De Bruin et al, 2005); (Raschi et al, 2008). As defined by Viskin, TdPs "denotes a ventricular tachycardia, with QRS complexes of changing amplitude that appear to twist around the isoelectric line" (Viskin, 1999).

After the discovery of the role of hERG1 channels in cardiac repolarisation, the hypothesised mechanism of how LQTS could lead to sudden death was that hERG1 channel block could cause cardiac action potential prolongation and subsequently QT prolongation, which could then increase the risk of TdPs and sudden death (Witchel,

2011). Based on this hypothesis, a wide number of different compounds associated with QT prolongation or TdPs were tested for their ability to block hERG1 channels. It emerged that hERG1 channels has a surprisingly "pharmacological promiscuity", mainly due to the presence of a large inner cavity with both aromatic and polar residues that can interact with a wide pharmacological range of molecules (Mitcheson, 2008). The screening of such wide number of different compounds have highlighted some key findings about hERG1 blockade: 1) the vast majority of drugs which target hERG1 channels require channels opening to gain access to the inner cavity of the pore (Vandenberg et al, 2012); one extremely interesting exception to this are hERG1 channel toxins. 2) The inactivation process turned out to play a role, at least for some drugs, in hERG1 channel block, although the preferential binding to inactivate state seems to be drug-dependent (Perrin et al, 2008). 3) The closure of the activation gate during repolarisation is responsible for the retention of drugs within the pore of the channel, a mechanism defined as drug trapping. An important consequence of drug trapping is the use dependent block, i.e. the onset of hERG1 channel block due to the accumulation of undissociated drugs during repetitive depolarizations, such as during repetitive action potentials (Vandenberg et al, 2012). 4) Some hERG1 blockers displayed a slow recovery from block (e.g. bepridil, domperidone, E-4031, MK499), probably due to the trapping in the closed state or to a stronger binding, in the inactivate state, to some residues (Vandenberg et al, 2012). 5) At least two aromatic residues, Phe656 and Tyr652, and two polar residues, Thr623 and Se624, were found to be crucial site for the binding to the hERG1 channels (Vandenberg et al, 2012). In particular the contribution of the polar residues seems to be compound-specific (Perry et al, 2004) whilst the aromatic residues are crucial for high affinity block by wide chemical range of molecules (Vandenberg et al, 2012). All these findings concerning hERG1 channels binding and blocking mechanisms by different drugs add a further level of complexity to the relationship between hERG1 blockade and the onset of side effects (Fermini & Fossa, 2003) (Bell & Bilodeau, 2008).

However, it is worth noting for the that not all the hERG1 blockers are arrhythmogenic (Wallis, 2010) and not all the LQT-inducer compounds act by acute hERG1 channel inhibition (Raschi et al, 2008). Moreover, the relationship between QT prolongation and the generation of arrhythmia and TdPs is still incomplete (Raschi et al, 2008);

(Arcangeli & Becchetti, 2010). At date, growing body of evidences have revealed an extremely complex scheme, suggesting that TdPs could depend on several concurrent risk factors such as genetic mutation, electrolyte imbalance, drugs interactions or concurrent diseases (Raschi et al, 2008) (Witchel, 2011). In 1998, Roden suggested the concept of "repolarisation reserve", i.e. the presence, in normal ventricle, of redundant mechanisms, which ensure a large repolarisation reserve, thus abolishing the risk of TdPs. The concomitant presence of multiple risk factors, which reduce the repolarisation reserve, and the blockade of I_{Kr} can resulted in a marked QT prolongation, leading to TdPs (Roden, 1998).

3.8 hERG1 channels and drugs development: <u>hERG1 as a target</u>

3.8.1 hERG1 as a target in excitable cells

hERG1 channels turned out to be a evaluable target in arrhythmology since the identification that several mutations in *herg1* gene may be responsible, in cardiac tissue, for the occurrence of a number of diseases characterised by gain or loss-of-function in hERG1 channels. As an example, hERG1 blockers belonging to the class III antiarrhythmic drugs can be useful tools in the treatment of the short QT syndrome (SQTS). SQTS is characterised by the a shortened QT interval, associated with sincopes, atrial fibrillations and life-threatening arrhythmias (Raschi et al, 2008). The molecular mechanism responsible for the shortened QT seems to be a mutation in N588 residues which confers a gain-of-function to hERG1 channels (Gussak et al, 2000). The gain-of-function of hERG1 channels could produce an increase in the outward current, so the blockade of that current may represent a therapeutic approach for SQTS (Raschi et al, 2008). Based on this hypothesis numerous hERG1 blockers were tested in patients: sotalol, flecainide and ibutilide failed to restore the physiological QT duration, whilst quinidine was proven to be effective in both patients (Wolpert et al, 2005) and rabbit model of SQTS (Milberg et al, 2007).

In the last years several hERG1 activators have been identified (Kang et al, 2005) (Casis et al, 2006) (Su et al, 2009) (Gessner et al, 2010), even displaying hERG1 isoforms specificity (Larsen et al, 2010). hERG1 activators enhance hERG1 currents mainly by attenuating inactivation and severely slowing the rate of channel deactivation (type I activators) (Perry et al, 2007) or by shifting the voltage dependence of inactivation to

more depolarised membrane potentials and a slowing of the onset rate (type II activators) (Perry & Sanguinetti, 2008). Two exceptions are mallotoxin and the amiodarone derivative KB130015, which act by accelerating the rate of activation and shifting its voltage dependence to more negative potentials (Gessner et al, 2010). The pharmacological properties of hERG1 activators could be, at least theoretically, used for the treatment of long QT syndromes (Grunnet et al, 2008): it should be possible to achieve, by enhancing the hERG1 K^+ current, a shortening of the QT interval. Several groups have already demonstrated the anti-arrhythmic effects of some hERG1 activators in single cell preparations, isolated cardiac tissue, Langendorff perfused hearts and in-vivo models (Grunnet, 2010) (Szabo et al, 2011). However, some pro-arrhythmic action of hERG1 activators have also been reported (Bentzen et al, 2011).

hERG1 could also represent a target for pharmacological treatment due to its role in pathophysiological process in neuronal cells. In particular, Chiesa et al. demonstrated a spike-frequency adaptation of the firing of neuroblastoma cells expressing hERG1 channels, when clamped with long depolarisation (Chiesa et al, 1997). They also showed that class III antiarrhythmic hERG1 blockers are able to convert the adaptive firing into regular firing (Chiesa et al, 1997). Thus, defective or null expression of hERG1 channels may be responsible of some hyper-excitable states (Chiesa et al, 1997) (Raschi et al, 2008), suggesting a possible therapeutic use of the newly discovered hERG1 activators. Moreover, the recent identification of a high-frequency, non-adapting firing induced by the expression of the hERG 3.1 isoform (see "hERG1 in neuronal and smooth muscle cells") together with its overexpression in schizophrenic hippocampus (Huffaker et al, 2009), provide a rationale for hERG1 channels as a new psychotherapeutic drug target.

3.8.2 hERG1 as a target in oncological diseases: a balance between therapeutical and side effects

As extensively discussed above, hERG1 channels are deeply involved in several hallmarks of cancer (Arcangeli et al, 2009) (D'Amico et al, 2013). Blocking hERG1 in different cancer cell lines results in the arrest of cell cycle and proliferation, in the block of the invasiveness of colon cancer and of the VEGF-A secretion from cultured glioma cells and myeloid leukaemia cells (Arcangeli & Becchetti, 2010). hERG1 blockade can also induce a significant increase in cell apoptosis in different cancer lines (revised in

(Jehle et al, 2011)), can overcome the MSC-induced drug resistance to apoptosis and is synergistic with some chemotherapeutic drugs, such as doxorubicin, prednisone and methothrexate (Pillozzi et al, 2011). Thus, targeting hERG1 channels could represents a very promising tool for new anticancer therapeutic approaches. However, the adverse risks of TdP by hERG1 blockers have to be considered (Witchel, 2011) (Raschi et al, 2008); indeed, notwithstanding several hERG1 blockers, such as E-4031, dofetilide and WAY 123,398, have shown very clear and relevant anti-tumour effects both *in vitro* and *in vivo* models, they also induce severe side effects, including long QT and TdPs. For these reasons, there is an urgent need to identify or synthesise newly hERG1 blockers, devoid of cardiotoxicity and pro-arrhythmogenic effects, to be used in cancer therapy.

Some different strategies, to circumvent the problems that therapeutic use of hERG1 blockers may cause, have been proposed (Arcangeli et al, 2009) (Arcangeli & Becchetti, 2010) (Arcangeli et al, 2012) (D'Amico et al, 2013).

1) Use of non-arrhythmogenic compounds

hERG1 channel blockers comprise many different pharmacological categories, including class III antiarrhythmics, antihistaminics, prokinetics, antibiotics and antipsychotics compounds, because of its "pharmacological promiscuity". It is worth nothing that not all of these compound produce arrhythmogenicity (Arcangeli & Becchetti, 2010). As an example, verapamil, a class IV antiarrhythmic compound, is a strong hERG1 inhibitor but does not produce lengthening of the QT interval in both humans and animals, probably because hERG1 blockade is counteract by a concomitant block of voltage-dependent Ca^{2+} channels, which in turn can reduce the action potential duration (Chouabe et al, 1998). Another hERG1 blocker, the antipsychotic sertindole, produces QT elongation without inducing torsadogenic effects (Shah, 2005). This evidence should not be surprising since our knowledge about the mechanistic relationship between QT prolongation and the generation of arrhythmia and TdPs is still incomplete. A possible explanation of the non torsadogenic potency of sertindole could be its very high affinity for hERG1 channels (Rampe et al, 1998): it is possible that the higher torsadogenicity of other hERG1 blockers depends on their lower specificity, which may cause supplementary effects on other ion channels (Arcangeli & Becchetti, 2010). The chemical structure of sertindole can therefore be attractive for pharmacological development of other more specific hERG1 inhibitors.

2) Targeting different conformational states

Most of the voltage gated ion channels can reside in three different states: closed, open and inactivated state. Therefore, in cells having distinct Vm dynamics, the same channel isoform may be present in very different distribution of conformational states. Since many drugs preferentially bind to a precise conformational state, it should be possible to target certain cell types (Arcangeli & Becchetti, 2010). This approach is currently used in the treatment of neuropathic pain and can be applied also to cancer therapy.

Conversely to what occurs during cardiac action potential, in which hERG1 is for most of the time either deactivated (at negative Vm) or inactivated (during the depolarised plateau), in cancer cells hERG1 channel spends most of the time in the open state, because of the very depolarised voltage membrane potential of these cells. Therefore, compounds with a specific open state affinity could target hERG1-expressing tumour cells, without affecting cardiac myocytes (Arcangeli & Becchetti, 2010). This is the case of R-roscovitine, a cyclin-dependent kinase inhibitor currently tested as an anticancer agent, which quickly and reversibly blocks hERG1 channels in open state (Ganapathi et al, 2009). R-roscovitine affinity for the open state could explain the absence, at clinically relevant concentrations, of pro-arrhythmic effects.

3) Targeting different channel domains

Most of the hERG1 inhibitors act by the intracellular side of the channel protein and are retained, during repolarisation, within the pore of the channel due to the closure of the activation gate (drug trapping). This mechanism could cause a use dependent block, another supplementary problem of many hERG1 blockers. To overcome this further complication a way can be to develop new compounds starting from the structure of recently discovered peptide toxins (Arcangeli & Becchetti, 2010). Two of these toxins, named BeKm-1 and ErgTx-1, display a high affinity for hERG1 channels and a rapid onset and reversibility of block, indicating that they bind to an external vestibule when the channel is closed. The binding resulted in the shifting of hERG1 activation curve to more positive membrane potentials and, when the channel opens, in the obstruction of the channel pore (Milnes et al, 2003) (Zhang et al, 2003). Mutagenesis studies and NMR spectroscopy have suggested the outer mouth of the pore as well as the S5P-linker as the possible binding sites of these toxins (Pardo-Lopez et al, 2002) (Tseng et al,

2007). The sea anemone toxin APETx1 is also specific for hERG1 channels (Diochot et al, 2003). This toxin act as a gating modifier, impairing hERG1 activation through the binding to the voltage sensor paddle, which is comprised of S3b to S4 helices (Zhang et al, 2003).

4) Targeting the "tumor" hERG1 isoforms

As described before (see "Importance of hERG1B isoform in native I_{Kr}") hERG1B isoform is expressed in human heart and forms hERG1A/hERG1B heterotetramers, which are thought to originate the native I_{Kr}. However, in the heart hERG1A isoform is expressed at higher level compared to hERG1B. Conversely, in tumour cells, especially leukaemia and neuroblastoma, the hERG1B isoform often prevails (Guasti et al, 2008) (Pillozzi et al, 2007) and in neuroblastoma cells hERG1B isoform is also significantly up-regulated during the S phase of the cell cycle (Crociani et al, 2003) (Guasti et al, 2008). Based on these evidence, another possible strategy is design drugs which selectively block the hERG1B isoform. Moreover, as already discussed before, the high expression of hERG1B isoform confers to the steady state current a more depolarised values (around -20 mV), thus increasing the fraction of channels in the open state; hence, compounds which also demonstrated a preferential binding to the open channel might produce significant cumulative effects on hERG1B-expressing tumour cells and could be applied at lower concentrations (Arcangeli et al, 2009).

3.9 hERG1 liability screening

During the last twenty years QT prolongation, together with hepatotoxicity, resulted to be responsible of more than 60% of drug withdrawals (Raschi et al, 2008). Since hERG1 channels blockade represents the most important and the most investigated mechanism of drug-induced TdPs and due to the increased evidences of hERG pharmacological promiscuity, it is "now common practice for pharmaceutical companies to screen compounds for hERG1 channel activity early during preclinical safety assessment" (Sanguinetti & Tristani-Firouzi, 2006).

The "gold standard" technology for the early screening of drug-induced inhibition of hERG1 channels is the patch clamp electrophysiology in the voltage clamp mode and the determination of the IC_{50}, i.e. the half-maximal inhibitory drug concentration, of drug-induced hERG1 blockade (Witchel, 2011). Several other technologies include

hERG binding assays, fluorescence polarisation assays, K^+ efflux assays and fluorometric voltage-sensitive dyes; although these techniques are routinely used, the final of hERG liability are based on electrophysiology (Witchel, 2011). A fundamental improvement in the hERG screening is the recent development of the planar patch clamp, which had allow for substantial automation and increased throughput. In 2005, the International Conference on Harmonization (ICH) published the ICH S7B Guideline for the non-clinical strategy to investigate the QT prolonging potential of novel products; the core of the testing system are, together with other non clinical approaches, the *in vitro* assay of the I_{Kr}, in isolated cardiomyocytes, and the *in vivo* study in laboratory animals (Raschi et al, 2008). In the preclinical screening of new compounds effects it is also important to establish safety margins; in 2003 Redfern et al. compared published data on hERG activity, action potential duration *in vitro* (APD) and QT prolongation *in vivo* in dogs against QT effects and reports of TdP in humans for about 100 drugs. These data were then set against the available free plasma concentrations attained during clinical use. From this analysis it turned out that drugs with little or no margin between peak free therapeutic plasma concentrations and hERG (or I_{Kr}) IC_{50} are frequently associated with *Torsades de pointes* in humans, whereas drugs with a large margin are not. Their data suggest that a 30-fold margin between hERG IC_{50} and peak free therapeutic plasma concentrations may be sufficient to exclude a clinical effect on cardiac repolarisation (Redfern et al, 2003). However, the authors stated that a more integrated assessment of both *in vitro* and *in vivo* effects is crucial for the prediction of the torsadogenic potential of a new drugs (Redfern et al, 2003). Indeed, it is now clear that drug-induced block of hERG channels does not always produce lengthening of the QT interval or induce TdPs and that some drugs with a QT prolonging effect do not seem to block hERG acutely, thus leading to the concept that hERG liability is "neither absolutely necessary nor sufficient for a drug to have risk for torsadogenesis" (Witchel H.J., 2011). For these reasons, there is an increase need for a more multidisciplinary approach, which shall include in the early screening also the other ion channels found to be crucial in cardiac action potential, as well as QT liability. To do so, several novel techniques are available, allowing the *in vitro* measuring of physiological cardiac action potentials, such as the Multielectrode assays (MEAs) or the cardiomyocytes derived

from either human embryonic stem (hES) cells or induced pluripotent stem cells (iPS) (Witchel, 2011).

AIMS OF THE THESIS

In the last decade growing evidences indicated a crucial role of ion channels in the hallmarks of cancer (Prevarskaya et al, 2010), thus suggesting a rationale for targeting them in anticancer therapies. Among these channels, hERG1 turned out to be aberrantly expressed in numerous human cancers (Arcangeli et al, 2009) and to regulate several aspects of cancer cell behaviour (Arcangeli et al, 2009) (D'Amico et al, 2013). For these reasons, targeting hERG1 channels in cancer could represents a very promising tool for new anticancer therapeutic approaches. However, hERG1 is also considered as an anti-target for drugs development, due to the serious cardiac side effects, including long QT syndrome and TdPs, that follow its blockade; indeed hERG1 channels plays a crucial role during cardiac action potential (cAP), being one of the major regulator of the action potential repolarisation in cardiac cells (Sanguinetti & Tristani-Firouzi, 2006). For these reasons, there is an urgent need to identify or synthesise newly hERG1 blockers, devoid of cardiotoxicity and pro-arrhythmogenic effects, to be used in cancer therapy.

The main aim of this research project was the screening of new compounds that behave as hERG1 blockers, but devoid of cardiotoxicity, to be used in cancer therapy. In a first phase we tested, through patch-clamp technique, all the available compounds looking for specific hERG1B blockers, i.e the isoform mostly expressed in leukaemia and neuroblastoma cells, and we investigated the biophysical properties and the mechanisms of action of such compounds. Parallel experiments were performed to test the biological activity *in vitro* on viability, proliferation and apoptosis of different tumour cell lines. In a second phase, the compounds that demonstrated relevant characteristics (i.e preference for the block on hERG1B isoform and significant biological activity) were tested *in vivo* in a preclinical leukemia mouse model. Finally, the torsadogenic liability of the successful compounds was evaluated on an *in vitro* model of cardiac action potential. The second aim of this thesis was the electrophysiological evaluation of the role of hERG1 channels on colorectal cancer (CRC). In particular we focus our attention onto two key aspects of CRC; the first is a signalling pathway, involving hERG1 and β1 integrins, that sustains angiogenesis and progression in CRC, while the

second concerns a pharmacological strategy to overcome chemotherapy resistance in colorectal cancer.

MATERIALS AND METHODS

1. In vitro experiments

Cell culture.

Leukemic cell lines FLG 29.1, HL60, REH, 697, NB4, KG1 and RS were cultured in RPMI (Lonza, Basel, Switzerland) plus 10% defined FBS (Foetal Bovine Serum; Euroclone, Milan, Italy) and 2% L-glutamine (Euroclone, Milan, Italy). Colorectal cancer (CRC) cell lines HCT116 were cultured in RPMI 1640 (Euroclone; Milan, Italy) with 10% Fetal Calf Serum (FCS) (Euroclone Defined; Euroclone; Milan, Italy). HEK 293 (Human Embryonic Kidney) and CHO (Chinese Hamster Ovary) cells were cultured in DMEM high glucose (Euroclone, Milan, Italy), plus 10% FBS and 4% L-glutamine. Human bone marrow–derived MSCs were cultured as in (Pillozzi et al, 2011). Cell lines were grown in their corresponding cell culture media in a humidified 5% CO_2 atmosphere at 37°C. For electrophysiology, the adherent cells were harvested using 0.25% trypsin/EDTA (Invitrogen, Carlsbad, USA). All cells were plated into 35 mm culture dishes (Corning, NY, USA) that served as the recording chamber.

Cells transfection and selection.

HEK 293 and CHO were transfected with Lipofectamine 2000 Reagent (Invitrogen, Carlsbad, USA) according to the manufacturer's protocol. HEK 293 were stably transfected with pcDNA3.1 hERG1A, pcDNA3.1 hERG1B, pcDNA 3.1 hERG Δ2-370 and transiently with pALTER MAX hERG G628C:S631C (Jiang et al, 1999). HEK 293 were also stably transfected with pcDNA 3.1 KCa 3.1. CHO cell line were transiently transfected with pIND hERG1 F656A vector (Milnes et al, 2003). The selection of the stably transfected cells was achieved by the addition of 800mg/ml geneticin (Life Technologies, Carlsbad, USA).

For the *in-vivo* leukemic mouse model experiments, HL60 cells were transfected with firefly luciferase gene using pGL4.51[luc2/CMV/Neo] plasmid (Promega, Madison, USA). $3,5 \times 10^6$ cells were mixed with 20 ng of plasmid into a total volume of 400 μl and the mixture was transferred into 4 mm Biorad Gene Pulser cuvette, and electroporated by Gene Pulser X cell Electroporation system (BioRad, US) using "Mammalian 12"

protocol. After electroporation an appropriate amount of the complete medium was added to the cells that were rapidly re-plated into a 6 well cluster. After 24 hours the cells were moved into a 25 cm^2 flask and geneticin was added to obtain cell selection.

Coculture of leukemic cells and MSCs.

Coculture of leukemic cells and MSCs were essentially performed as in (Pillozzi et al, 2011) For signalling experiments cells were cocultured with MSCs for 30 minutes, 1 and 6 hours. At the end of the incubation, cells were harvested and proteins were extracted as in "Protein extraction and Western Blotting" (see below).

Cells adhesion experiments.

For patch-clamp experiments, colorectal cancer (CRC) cell lines HCT116 were seeded for different time (15 minutes, 1, 2 and 5 hours) into 35 mm culture dishes previously coated with TS2/16 (20 μg/ml), i.e. the β1 integrin activating antibody, or BSA (250 μg/ml). At the end of the incubation hERG current recordings were performed as described in "Patch-clamp recording of hERG currents" (see below).

RNA interference.

FLG 29.1 cells were cultured as in "Cell cultures" in 6-well cell clusters (Costar, Corning). Twenty-four hours after plating, cells were transfected with a mix of anti-hERG1 siRNAs (44858 anti-hERG1 siRNA1; 44762 anti-hERG1 siRNA3; Ambion; 100nM final concentration), and siRNA scramble (50nM final concentration, Silencer Negative control #1, 4611, Ambion) according to the manufacturer's instructions. After 5 hours, the medium was changed and cells were harvested and processed for both electrophysiology and pharmacology experiments.

Leukemic B and Peripheral Blood Mononuclear cell isolation.

Cells were isolated from freshly heparin-anticoagulated whole blood and leukemic B cells were purified using RosetteSep human B cell enrichment cocktail (Stem Cell Technologies, Vancouver, Canada) and ficoll-Hypaque density gradient centrifugation. Cells were resuspended in either Hybridoma Serum Free medium (SFM; Invitrogen) or

SFM with 10% FBS as in Levesque et al., (Levesque et al, 2001). Peripheral Blood Mononuclear Cells (PBMC) were isolated from Buffy Coat preparation of 2 independent healthy donors, using Ficoll–Hypaque (Pharmacia, Uppsala, Sweden) gradient centrifugation. Mononuclear cells were recovered at the interphase, washed, counted and then used in the viability experiments.

Cell Viability.

To assess cell viability the WST1 cell viability assay (Roche Diagnostics, Mennheim, Germany) was used. Cells were serum-starved for 16 hours with 1% FBS EU and were subsequently seeded at $3x10^4$/well in 96-well plates, and incubated with the different drugs for 24 hours. Peripheral Blood Mononuclear Cells (PBMC) cells were seeded ($6x10^4$/well) in 96-well plates, and incubated for 6 hours without stimulation. In both cases at the end of incubation the WST1 reagent was added (1:10) and absorbance was measured at 450 nm with microplate reader ELX 800 (BioTek Instruments,Winooski, United States). The mean and standard deviation was calculated for each group and average data were fitted using a Hill-type equation (see below). The ED_{50} value was calculated from the dose-response curve interpolating the experimental data (Microcal Origin 8.0 software).

Cell Cytotoxicity.

For the cytotoxicity assay CLL cells ($2.5x10^5$ cells/well) were placed in 96-well plates in triplicates and cultured in the presence and absence of CD-160130 (0.1-100 μM) for 72 hours. Cytotoxicity was detected using the tetrazolium compound 3-(4,5-dimethylthiazol-2-yl)-5-(3-carboxymethoxy-phenyl)-2-(4-sulfophenyl)-2H-tetrazolium, inner salt (MTS) with a "CellTiter 96 Aqueous One Solution Cell Proliferation Assay" kit (Promega). Optical densities were read at 490 nm using a plate reader spectrophotometer. The effective CD-160130 concentration that induced death of 50% of CLL cells (EC_{50}) was calculated using mean OD_{490} values from triplicates. The EC_{50} value was determined from a two point linear regression of the two concentrations of CD-160130 that induced greater and less than 50% CLL cell death. The EC_{50} was the concentration on the linear regression curve that corresponded to 50% viability.

Cell Proliferation.

To assess cell proliferation $1x10^4$/well cells were seeded in 96-well plates and treated with CD-160130 at time 0 (single treatment) or at both time 0 and 48 (double treatment). Following incubation, cells were harvested and counted using a Bürker Chamber with viable cells identified as Trypan Blue negative.

Bromodeoxyuridine (BrdU) Assay.

BrdU assay was performed to asses cell proliferation. Cells were serum-starved for 16 hours with 1% FBS EU and were subsequently seeded at $3x10^4$/well in 96-well plates, and incubated with the different drugs for 24 hours. At the end of the incubation, cells were collected and resuspended in 500 μL of the appropriate medium (without FBS) and were cytocentrifuged at 800g for 15 minutes at 4°C. Cells were then fixed with 4% paraformaldehyde for 10 minutes at room temperature (RT). Cells were permeabilised with PBS-Triton X 0,1% for 5 minutes at RT and subsequently washed three times (5 minutes each) with PBS 1x. DNA was denatured incubating cells with HCL 2M for 30 minutes at 37°C. Cells were therefore washed three times with PBS 1x and incubated with Hoechst 33258 (1:2000 in distilled water) for 40 minutes at RT in the dark. Nonspecific binding sites were blocked by incubating cells with PBS-BSA 3%- Triton X 0.1 % for 1 hour at RT. The cells were stained with anti-BrdU antibody (Sigma Aldrich) 1:1000 in PBS-BSA 3% over night at 4°C. After the incubation with primary antibody cells were washed twice with PBS-Triton X 0.1% for 15 minutes each and the incubated with Cy3 anti-mouse antibody (1:800 in PBS- BSA 3%) for 1 hour at RT in the dark. After another three wash with PBS, coverslips were mounted on microscope slides with ProLong Gold antifade reagent (Life Technologies, Carlsbad, USA). Images were acquired with a Bio-Rad MRC 1024 ES Confocal Laser Scanning microscope (Bio-Rad, Hercules, CA).

Apoptosis Analysis.

The effects of the different compounds on leukemic cell line apoptosis was investigated, in both suspension and coculture with MSCs, through annexin V/propidium iodide (Annexin-VFLUOS staining kit; Roche Diagnostics, Mennheim, Germany). Cells were

seeded at $1*10^5$/well in 24-well plates and incubated with different drugs for 24 hours (suspension) or 48 hours (coculture). Cells were then harvested, washed with PBS and then re-suspended in 100 µL of binding buffer and incubated with FITC-conjugated annexin V and propidium iodide for 15 min. Flow cytometric analysis were performed with BD FACSCanto (Becton Dickinson, NJ, USA) and analysed with BD FACSDiva Software 6.1.3. Each experiment was performed in triplicate.

Clonogenic assay.

Bone marrow (BM) aspirates from patients in complete remission were obtained from the Oncohematology Laboratory of the Department of Woman and Child Health, University of Padova (under informed consent). BM cells were cultured on MethoCult GF H4034 (StemCell Technologies, Vancouver, Canada), designed to support growth of CFU-GEMM, CFU-GM, CFU-G, CFU-M, CFU-E and BFU-E colonies, testing two different CD-160130 concentrations (5µM and 10µM). CD-160130 was pre-incubated with $2x10^4$ BM cells/35mm dishes for 15 minutes. Cells were then maintained in a humidified atmosphere and 5% CO_2. Colonies were enumerated using an inverted microscope after 18 days of culture according to the manufacture's protocol. Results were average of three independent experiments from three different patients.

Guinea pig cardiac myocyte isolation.

Adult male Dunkin Hartley guinea pigs (Harlan Laboratories, UK) weighing 400–465 g were sedated with hypnorm (1 ml/kg) (Roche Diagnostics, Mennheim, Germany) and hypnovel (1 ml/kg) (VetaPharma Ltd, Leeds, UK) and sacrificed by cervical dislocation. The heart was excised, and retrogradely perfused via the aorta with Ca^{2+} free Tyrode for 4-6 minutes, enzyme solution (1.04 mg/ml type I collagenase, 0.62 mg/ml type XIV protease and 1.67 mg/ml bovine serum albumin) for 7-10 minutes and then with Ca^{2+} free Tyrode for 1-2 minutes. Following tissue digestion the left ventricle was dissected into small pieces and mechanically agitated in 2 mM Ca^{2+} Tyrode to disperse single cells. Tyrode solution contained (in mM): 0 or 2 $CaCl_2$, 4 KCl, 135 NaCl, 1 $MgCl_2$, 0.33 NaH_2PO_4, 5 Na^+ pyruvate, 10 glucose, 10 HEPES; pH adjusted to 7.4 with NaOH.

[³H]Astemizole Binding Assay.

HEK 293 cells stably expressing hERG channels were maintained as outlined in Cell Culture and Transfection with membranes being prepared as described by Finlayson et al. (Finlayson et al, 2001a). [³H]Astemizole binding to hERG channels was performed in incubation buffer containing: 10 mM HEPES, pH 7.4, 0.1% BSA, 5mM KCl, 0.8 mM MgCl₂, 130 mM NaCl, 1 mM EGTA, 10 mM Glucose. Assay buffer or CD-160130 was incubated with 1.5 nM [³H] Astemizole and 150 μl of membranes for 60 minutes at 25°C. Non-radiolabeled astemizole (10 μM) was used to determine non-specific binding. The subsequent steps of this assay were performed as described in Finlayson et al. (Finlayson et al, 2001b).

PDE-4 inhibition assay.

Human recombinant PDE-4A catalytic domain comprising amino acids 342-704 was expressed as previously described by Richter et al., (Richter et al., 2000). PDE-4A activity was determined by the scintillation proximity assay (SPA) as described by the manufacturer (Amersham Biosciences, GE Europe GmbH, Munchen, Germany) and by Horton and Baxendale (Horton & Baxendale, 1995). The reaction mixtures contained 100 mM TrisHCl (pH 7.5), 5 mM MgCl₂, 3.8 mM 2-mercaptoethanol, 1 μM cAMP as substrate and the inhibitors at different concentrations. The reaction was started by adding the enzyme. The operating volume was 100 μl in the wells of a 96-well plate. All test substances were produced as stock solutions in DMSO. After reaction initiation samples were incubated at 22°C for 20 minutes. The reaction was stopped by the addition of SPA bead suspension which contains the zinc sulphate concentration provided according to the manufacturer. Afterwards, the beads were allowed to sediment for 30 minutes and the plates were analysed on a luminescence microliter plate reader (Fluostar Optima, BMG Labtechnologies GmbH, Ortenberg/Germany).

Total RNA extraction.

Total RNA was extracted from different cell lines following the TRIzol® Reagent protocol (Life Technologies, Carlsbad, USA). RNA concentration was quantify by

measuring the optical density (OD) at 260 and 280 nm and RNA purity was determined by ratio of the absorbance values at 260 nm and 280 nm (A260/A280).

Reverse Transcription (RT-PCR).

Total RNA was reverse transcribed to cDNA, in a 20 μl reaction mixture, using Random Primers and SuperScript™ II Reverse Transcriptase (Invitrogen, Carlsbad, USA).

The mixture contains:

• 1-2 μg of total RNA

• 2 μl of Random Primers (from 3 μg/μl stock)

• Distilled water up to 12 μl

This mixture was heat to 75˚C for 10 minutes and quick chilled on ice. To the mixture were then added:

• 4 μl of 5X First-Strand Buffer

• 1 μl (200 units) of SuperScript™ II RT

• 1 μl of dNTP (from a 10mM stock)

• 2 μl of distilled water

The mixture was incubated at 25˚C for 10 minutes, then at 42˚C for 50 minutes and finally at 75˚C for 10 minutes. The synthesised cDNA was then stored at -20˚C until use.

Polymerase Chain Reaction (end point PCR).

cDNA (2 μl) was amplified by polymerase chain reaction using Platinum® PCR SuperMix (Invitrogen, Carlsbad, USA), following manufacturer's protocol. Primers final concentration was 200 nM (from a stock solution of 10 μM) in a 25 μl reaction mixture. All the primers used in this experimental work were designed using the software Primer3 (Table 1).

Gene	Sequence	Amplicon size
K$_V$ 1.3 Forward Reverse	CGGGAACAAGTGAACTCCAT ACTGGGGAAAGTAGCCTGGT	175 bp
K$_V$ 1.5 Forward Reverse	ACTTGCGGAGGTCCCTTTAT GGGAGGAAAGGAGTGAAAGG	198 bp
K$_{Ca}$ 3.1 Forward Reverse	CCCAGACCCCTTTCAAAAC TGGGATTATTGTTCGTGGTG	239 bp

Table 3.1. Sequence and amplicon size of all the primers used for end point PCR.

Real time PCR.

hERG1A and *hERG1B* mRNAs in both primary samples and cell lines were quantified by real-time quantitative polymerase chain reaction (RQ-PCR), with the PRISM 7700 sequence detection system (Applied Biosystems) and the SYBR Green PCR Master Mix Kit (Applied Biosystems) as in (Pillozzi et al, 2007).

Protein extraction and Western Blotting.

Protein extraction. Whole cell protein was extracted by using the following protocol: cells were washed twice with ice-cold phosphate-buffered saline and scraped using a cell lifter. Cells were lysed on ice with 500 μl of Lysis Buffer supplemented with protease inhibitors Roche Complete Mini (Roche Diagnostics, Mannheim, Germany) for twenty minutes. Cell lysates were centrifuged for 10 minutes at 16,000 × g at 4°C, and supernatants were collected. Protein concentration was determined by using the Bradford protein assay method (Bio-Rad, Hercules, CA). Lysis Buffer composition

(mM): 150 NP40, 150 NaCl, 50 TrisHCl pH 8.0, 5 EDTA, 10 NaF, 10 $Na_4P_2O_7$, 0.4 Na_3VO_4.

Sodium dodecyl sulphate polyacrylamide gel electrophoresis (SDS-PAGE). Lysates were loaded to a 4% stacking gel (534 μl acrylamid (30%)-bisacryamide (0.8%), 1 ml 0.5 M Tris-HCl pH 6.8, 40 μl 10% SDS, 20 μl 10% ammonium persulfate, 4 μl TEMED, 2.4 ml H_2O). Stacking gel was purred on the resolving gel (2.34 ml acrylamid (30%)-bisacryamide (0.8%), 1.75 ml 1.5 M Tris-HCl pH 8.8, 70 μl 10% SDS, 35 μl 10% ammonium persulfate, 3.5 μl TEMED, 2.76 ml H_2O). Electrophoretic run was performed at 150 V.

Western blotting. SDS-PAGE gels were transferred to PVDF membranes (Amersham, GE healthcare) for western blotting analysis in Transfer Buffer (14.4 g Glicine, 3.03 g TrisHCl, 200 ml methanol, 800 ml H_2O) at 100 V for one hour. Membranes were then washed in T-PBS (PBS 0.1% Tween) and blocked with T-PBS 5% BSA for four hours. Membranes were exposed to primary antibody diluted in T-PBS 5% BSA overnight at 4°C and then washed with T-PBS. Membranes were then incubated with secondary antibodies peroxidase-coupled for one hour at room temperature. Signals were visualised using ECL reagent (Amersham). In the signalling experiments, 30 μg of total lysates were used. For pAkt, pGSK3β, pERK1/2 and pSTAT3 detection, the anti-pAkt1/2/3 (Thr308)R (Santa Cruz Biotechnologies, dilution 1:500), the anti-pGSK3β (Ser9) (Cell Signaling, dilution 1:1000), the anti-phospho-p44/42 MAP kinase (Thr202/Tyr204) (Cell Signaling, dilution 1:500) and the pStat3 (Tyr705, D3A7) (Cell Signaling, dilution 1:500) primary antibodies were used. For tAkt, tERK and tSTAT3 detection, the anti-tAkt1/2/3 (H-136) (Santa Cruz Biothecnologies, dilution 1:500), the ERK1 (C-16) (Santa Cruz Biothecnologies, dilution 1:200) and the Stat3 (79D7) (Cell Signaling, dilution 1:1000) primary antibodies were used. Anti-rabbit peroxidase-conjugate (Sigma-Aldrich, dilution 1:10000) was used as secondary antibody. Western blotting images were acquired with an Epson 3200 scanner, and the relative bands analyzed with ImageJ 1.47v free software (developed at the National Institutes of Health). The intensity of the bands related to the phosphorylated proteins were normalized to the intensity of the bands related to the correspondent total proteins. Ratios reported in the graphs were mean ± SD of at least three different analyses. For the experiments reported

in Figure 5S, 20 μg of total lysates were used decorated with the anti-HERG1 COOH-terminus primary antibody (1:1000 dilution, developed in our laboratory, (Lastraioli et al, 2004)). The secondary antibody was anti-rabbit peroxidase-conjugate (Sigma-Aldrich, 1:10000 dilution). The intensity of the bands was normalized to the intensity of the bands that corresponds to the α-tubulin protein (Sigma-Aldrich). The control cells ratio was set as one. For each condition, at least three experiments were analyzed separately. The mean intensity of the bands for hERG1B was reported as arbitrary units.

Electrophysiological experiments.

Patch-clamp recording of hERG currents. Membrane currents were recorded in the whole-cell configuration of the patch-clamp technique, at room temperature (about 25°C). Electrodes were pulled from borosilicate glass capillaries (inside diameter 0.86 mm, outside diameter 1.5 mm; Harvard Apparatus, Holliston, MA, USA), using a PC-10 pipette puller (Narishige, Tokio, Japan). Electrodes typically had a resistance of 3.5-5 MΩ. Series resistance was always compensated up to approximately 80%. Currents were amplified and filtered using a Axopatch-1D (Molecular Devices, Sunnyvale, CA) interfacing with a Digidata 1440A (Molecular Devices) and a computer with pClamp 10.3 software (Molecular Devices). Currents were low-pass filtered at 2 kHz and digitized online at 10 kHz. Data were subsequently analysed off-line with pClamp and Origin 8.0 (Microcal Inc., Northampton, MA, USA) software.

Solutions. The pipette solution contained (in mM): K^+ aspartate 130, NaCl 10, $MgCl_2$ 2, $CaCl_2$ 2, HEPES 10, EGTA 10, titrated to pH 7.3 with KOH. During the experiments, cells were usually perfused with an extracellular solution containing (in mM): NaCl 130, KCl 5, $CaCl_2$ 2, $MgCl_2$ 2, HEPES 10, Glucose 5, adjusted to pH 7.4 with NaOH. In this case, the potassium equilibrium potential (E_K) was -80 mV. When necessary, a high extracellular $[K^+]$ was applied to increase the amplitude of inward hERG1 currents measured at -120 mV, thus avoiding the necessity of applying excessively negative test potentials. In this case, the NaCl and KCl concentrations were, respectively, 95 and 40 mM (E_K = -30 mV).

Protocols. The current-voltage relationships for channels (in the inward direction) were determined from measurements of peak tail current amplitude at -120 mV (for 1.1–s), following 15-s conditioning potentials (applied in 10 mV increments) from 0 mV to -70

mV. The time between consecutive trials in the same stimulating protocol was 4 s at 0 mV. The same stimulation protocol was used to determine the concentration-response relations for different drugs.

The current-voltage relationships for channels (in the outward direction) were determined from measurements of peak tail current amplitude at -50mV. The protocol for the measurement of the hERG1 outward tail currents consists in 11 episodes, each with one preconditioning step at -80mV, followed by steps ranging from -60 to +40 mV (with 10 mV intervals) and a final step at -50mV, during which outward tail currents are elicited.

To study the voltage-dependence a stimulation protocol, previously used to analyze the voltage-dependence of ERG toxin (Gurrola et al, 1999), was applied. The blocker was applied at different conditioning potentials (between +30 and -110 mV). Next, channels were briefly (250 ms) held at +40 mV to obtain full activation, and then Vm was brought to -120 mV, to measure the hERG1 tail current.

For hERG G628C:S631C mutant, i.e. the non-inactivating hERG channel, currents were elicited, from a holding potential of -80 mV, by a 120 s step to +40 mV. Next, Vm was stepped back to -80 mV, to reveal the inward tail currents. Drugs were applied after the current had reached the steady-state at +40 mV.

For briefness was only reported the drug effect on the tail currents elicited after conditioning at 0 mV. Each compound was applied for at least 4 minutes (or until steady state inhibition was attained), with each concentration being tested on at least 5 different cells. At the end of each application, drugs were removed through continuous perfusion with extracellular solution for at least 2 minutes. As internal controls, the selective hERG blocking agent E4031 was utilised as a positive control and DMSO, which served as the solubilising agent for all drugs, as a negative control.

Patch-clamp recording of KCa 3.1 and KCa 1.1 currents. Membrane currents were recorded in the whole-cell configuration of the patch-clamp technique, at room temperature (about 25°C). Electrodes were pulled from borosilicate glass capillaries (inside diameter 0.86 mm, outside diameter 1.5 mm; Harvard Apparatus, Holliston, MA, USA), using a PC-10 pipette puller (Narishige, Tokio, Japan). Electrodes typically had a resistance of 3.5-5 MΩ. Series resistance was always compensated up to

approximately 80%. Currents were amplified and filtered using a Axopatch-1D (Molecular Devices, Sunnyvale, CA) interfacing with a Digidata 1440A (Molecular Devices) and a computer with pClamp 10.3 software (Molecular Devices). Currents were low-pass filtered at 2 kHz and digitised online at 10 kHz. Data were subsequently analysed off-line with pClamp and Origin 8.0 (Microcal Inc., Northampton, MA, USA) software.

Solutions. The pipette solution contained (in mM): K^+ aspartate 145, $MgCl_2$ 2, HEPES 10, EGTA 10, $CaCl_2$ 5.96 (250 nM free Ca^{2+}) or 8.55 mM $CaCl_2$ (1 µM free Ca^{2+}), titrated to pH 7.2 with NaOH. During the experiments, cells were usually perfused with an extracellular solution containing (in mM): NaCl 160, KCl 4.5, $CaCl_2$ 2, $MgCl_2$ 1, HEPES 5, adjusted to pH 7.4 with NaOH.

Protocols. KCa 3.1 currents were elicited, from a holding potential of -80mV, by 200-ms voltage ramps from -120 to 40 mV applied every 10 s, and the -fold increase of slope conductance at -80 mV by drug was taken as a measure of channel activation. KCa1.1 currents were elicited by 200-ms voltage steps from -80 to 60 mV applied every 10 s (1 µM free Ca^{2+}), and channel modulation was measured as a change in mean current amplitude.

Perforated patch recordings of cardiac myocyte action potentials. Borosilicate standard wall without filament glass electrodes (Harvard Apparatus, UK) were pulled to a resistance of 1.5-2.5 MΩ. Electrodes were tip-filled (2-3 mm) with amphotericin-B-free solution and back filled with amphotericin-containing (Apollo Scientific, Stockport, UK) intracellular pipette solution. Current-clamp recordings were made using an Axopatch 200B amplifier, Axon 1322A digidata (Axon Instruments, USA) and Clampex software (version 8.2, Molecular Devices, USA). Action potentials (APs) were stimulated at 2 Hz in physiological Tyrode solution and at 37 °C, APs were sampled at 10 kHz and on-line filtered at 5 kHz. 20 APs were signal averaged after stabilizing in control or CD-160130-containing Tyrode.

Analysis of electrophysiological experiments. The concentration-response relations on hERG currents for the different drugs were obtained by plotting the percentage residual currents versus the drug concentration. The residual currents were calculated through

the following formula: 100 x ($I_{max\ drug}$/ $I_{max\ contr}$), where $I_{max\ drug}$ is the maximal hERG tail current in the presence of a given drug concentration and $I_{max\ contr}$ is the maximal hERG tail current in the absence of the drug; the maximal hERG tail current is the current at peak subtracted from the steady-state current. The mean and standard error of mean was then calculated for each drug concentration and the average data points were fitted using a Hill-type equation. $y= A_0+ [(A_0-A_1)\ x^n/k^n+x^n]$, where A_0 is the minimum and A_1 is the maximum of the function; x is the drug concentration; k is the IC_{50} value; n is the Hill coefficient. The IC_{50} value was calculated from the concentration-response curve interpolating the experimental data using Microcal Origin software.

2. *In vivo experiments.*

In vivo leukemia model. The AML cell line HL60 expressing luciferase (HL60-luc2) was injected intraperitoneally (i.p.) in 4-6 weeks old female SCID mice (5×10^6 cells/ mouse). To track the HL60-luc2 cells, bioluminescent optical imaging was performed weekly using Photon Imager system (Biospace Lab, Paris, France) including a cooled charge-coupled device (CCD) camera from day 3 to day 38 post cells injection. Prior to image acquisition, mice were anaesthetised by i.p. injection of 275 mg/kg Avertin (2,2,2,Tribromoethanol, Sigma Aldrich, Milano, Italy). Bioluminescent images were acquired for a total of 3 minutes, in ventral position, 5 minutes after i.p. injection of D-luciferin (150 mg/Kg, XenoLight RediJect D-Luciferin, Caliper Life Sciences, Villepinte, France). Optical images were analysed with M3 Vision software (Biospace Lab, Paris, France): counts per minute (CPM) values were determined for each single animal using the ROI (region of interest) tool. Imaging values at day 3 were used to distribute mice in five different treatment groups having a comparable average CPM signal. Starting from day 5, mice were treated daily for fourteen consecutive days with the following schedule: controls, 100 µl of Ora-Plus® (Paddock, Minneapolis, MN) by oral gavage (o.g.); cytarabine, 100 µl of cytarabine (6.25 mg/Kg, i.p.); CD160130 minced in Ora-Plus at two different doses o.g. (1 mg/Kg; 10 mg/kg).

Plasma pharmacokinetics. Nine female wistar rats (Janvier Labs, St Berthevin, France) were treated with a single dose (50mg/kg dissolved in Ora-Plus®) of CD-160130 by

oral gavage. Blood samples (approximately 0.5ml each) were collected from the retro-orbital plexus with Pasteur pipettes after 30 min, 1h, 2h, 4h, 6h, 8h, 24h, 48h. After sampling, the blood was kept in ice for 20 min and then centrifuged at 10,000g for 10 min. CD-160130 plasma concentration was determined by HPLC-UV (Waters Alliance 2695 separation module with Waters 2696 PDA, Waters Corp., Milford, USA) after protein precipitation with MeOH. The HPLC column was a Nova-Pak C18, 60 Å, 4 μm, 3.9x150 mm (Waters Corp., Milford, USA) with pre-column LiChroCart 4-4 (Merck, Darmstadt, Germany). Flow rate was 1.0 ml/min and the detection was performed at 337 nm at 40°C. The retention time for CD-160130 was 13.6 min and 16.0 min for its metabolite M1.

3. Chemicals and drugs.

Unless otherwise indicated, chemicals were purchased from Sigma Chemicals (Saint Louis, MO, USA). Stock solutions (5 and 10 mM) of CD-160130 and CD-140793 (BlackSwanPharma GmbH, Leipzig, Germany) were prepared in DMSO. The same applies to and amphotericin B (60 mg/ml). E4031 (Alomone Labs, Jerusalem, Israel) was dissolved in water (stock solution of 5 mM). Stock solution of Cytarabine, Doxorubicin (Amesham, GE healthcare; vial containing 50mg of doxorubicin chlorohydrate in NaCl, pH3) and Fludarabine used in the co-culture experiments were prepared in distilled water.

4. Statistical Analysis.

All averaged data are presented as mean ± SEM. The statistical significance of differences between experimental group was calculated with the Mann-Whitney test, with a $p < 0.05$ being considered as statistically significant.

All human and animal studies were approved by local Ethics Committee.

RESULTS AND DISCUSSION

1. hERG1 channels in colorectal cancer

1.1 hERG1 channels and β1 integrins in colorectal cancer (CRC)

hERG1 turned out to trigger and modulate intracellular cascade signalling in different human cancers (Pillozzi & Arcangeli, 2010), by forming macromolecular complexes with integrin subunits (Cherubini et al., 2005) and receptors for growth factors (Pillozzi et al, 2007) or chemokines (Pillozzi et al, 2011). The association between hERG1 channels and intergrins, in particular the β1 integrin, can modulate the activity of both proteins with two different mechanisms: hERG1 channels can modulate integrin-dependent signalling and, vice versa, β1 integrin can activate hERG1 channels (Pillozzi & Arcangeli, 2010). The latter mechanism was demonstrated in both human neuroblastoma (Arcangeli et al, 1996) and in a human preosteoclastic leukemia cell line, FLG 29.1 (Hofmann et al, 2001). We thus investigated whether β1 integrin might exert the same effect on hERG1 channels also in colorectal cancer cells, in which hERG1 was found to be overexpressed and to regulate cell migration and invasion (Lastraioli et al, 2004).

The effect of β1 integrin activation was analysed in HCT116 cells: cells were seeded onto TS2/16, i.e. the β1 integrin activating antibody, or BSA, taken as control, for different time (see Materials and Methods) and hERG current density was evaluated through patch-clamp technique. The time course of hERG current density is reported in Figure 1.1A. β1 intergrin activation induces an initial increase in hERG1 current density after 60 minutes of incubation on TS2/16 coating, to which follows a significant increase, as compared with the controls, of hERG1 current density after 120 minutes of incubation. The hERG current density turned out to be decreased after 300 minutes of incubation with TS2/16, due to the decline of the activating effect of TS2/16. Typical hERG1 currents, obtained in HCT116 cells seeded onto TS2/16 or BSA for 120 minutes, are reported in Figure 1.1B. These results are in agreement with the ones observed in leukaemias and neuroblastomas and clearly indicated that β1 intergrin

activation can in turn activate hERG1 channels also in colorectal cancer cells, being the first step of a more complex signalling cascade that sustains angiogenesis and progression in colorectal cancer (described in (Crociani et al, 2013)).
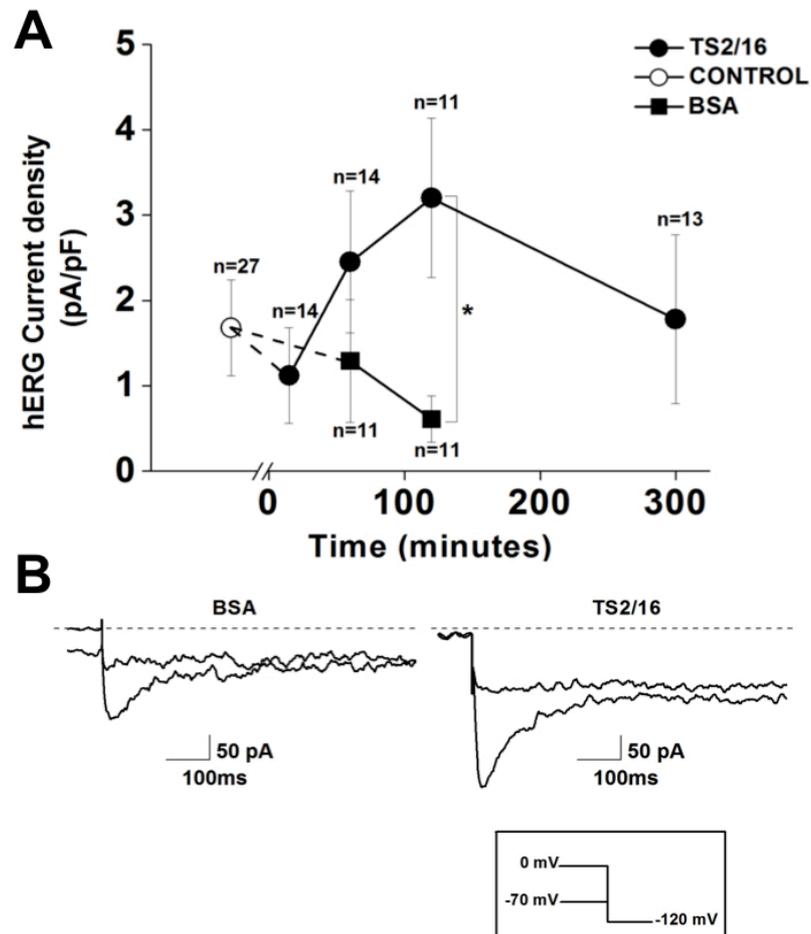

Figure 1.1. **Panel A**: Time course of hERG1 current density in HCT116 cells. HCT116 cells were seeded on TS2/16 (20 μg/ml) or BSA (250 μg/ml) for different time (15, 60, 120 and 300 minutes). hERG1 current density was measured as in Materials and Methods. Data are reported as mean ± SEM calculated on the number of cells shown above each experimental point. Time point 0 refers to the time at which cells were seeded on the different substrates. Control cells are those seeded in standard conditions (RPMI + 10% FBS) for 120 min. **Panel B**: Typical hERG1 currents obtained in HCT116 seeded onto BSA and TS2/16 for 120 minutes. In the inset is shown the protocol used for the patch-clamp recordings.

1.2 hERG channels and the overcome of cisplatin resistance in CRC

Cisplatin is a drug widely used for cancer chemoterapy, being effective for the treatment of different types of cancer, including colorectal carcinomas (Andre & de Gramont, 2004). However, the major limitation in the use of cisplatin has been the pre-existance of drug refractoriness and the frequent development of cisplatin resistance by tumours (Boulikas & Vougiouka, 2003) (Siddik, 2003). Several mechanisms of cisplatin resistance have been identified so far (revised in (Siddik, 2003) and in (Boulikas & Vougiouka, 2003)), and therefore there is an increasing need for new therapeutic protocols aimed at overcoming the development of resistance to cisplatin. Among these, combinations of platinum drug treatments with other drugs (e.g. the one with gemcitabine, paclitaxel, doxorubicin, as revised in (Boulikas & Vougiouka, 2003)) are becoming increasingly interesting. Ion channels have been described to modulate the response of cancer cells to cisplatin treatment (Marklund et al, 2001) (Siddik, 2003) (Shimizu et al, 2008), and in particular activators of the intermediate conductance calcium activated potassium channel K_{Ca} 3.1 turned out to mediate the response to cisplatin treatment in epidermoid cancer cells (Lee et al, 2008).

These findings prompted us to evaluate whether riluzole, an ion channels modulator, could regulate the cisplatin resistance in colorectal cancers. Several studies indicated that riluzole, which is already in use for the treatment of amyotrophic lateral sclerosis, exerts different effects on different ion channels: more specifically, it activates $K_{Ca}2$, $K_{Ca}3$ and K_{2p} channels, while it inhibits some Na^+ and K^+ channels, including hERG (Sankaranarayanan et al, 2009). Thus, the aim of the electrophysiological analysis performed in this experimental work was the evaluation of riluzole effects on different native K^+ channels in colorectal cancer cells HCT116.

We first evaluated the effects of riluzole on hERG channel, whose currents in HCT116 were already described (see above). hERG currents were studied by measuring tail currents at -120 mV, after depolarising voltage steps ranging at -70 mV and 0 mV, lasting 15 s (Fig. 1.2, inset). Riluzole (45 μM) significantly inhibits hERG currents in HCT116 (Figure 1.2) of about 43.8 ± 7.02 % (n=7), in agreement with the IC_{50}

(inhibitory concentration 50) of about 50 ± 4 μM obtained in the HEK 293 transfected with hERG1 channels (Sankaranarayanan et al, 2009).
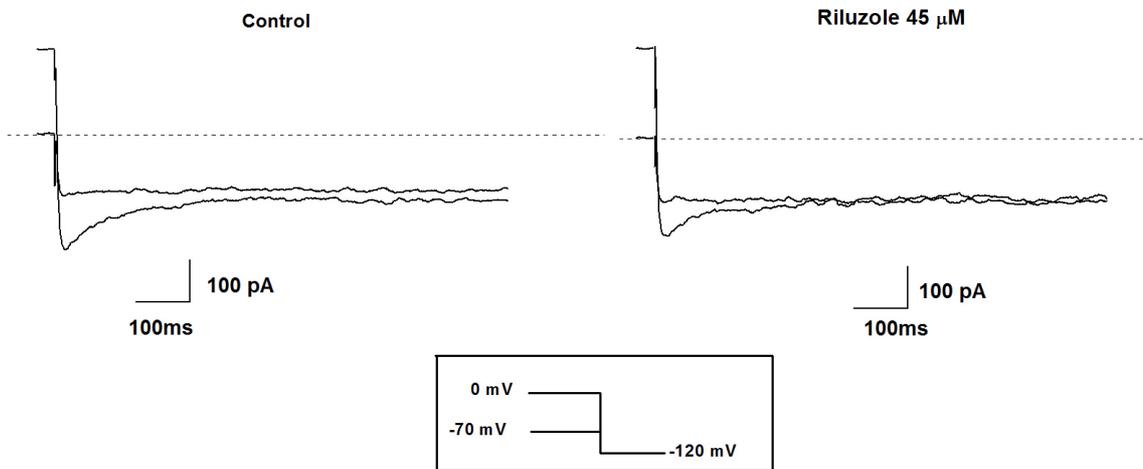
**Figure 1.2**. Typical hERG1 currents obtained in HCT116 and effect of riluzole (45 μM). Riluzole induces a significant inihibition of about 43.8 ± 7.02 % (n=7) of the hERG current, as compared with the controls. In the inset is shown the protocol used for the patch-clamp recordings.

We then analysed the effect of riluzole on the K_{Ca} 3.1 and K_{Ca} 1.1 currents elicited in HCT116, using the solutions and the protocols described in (Sankaranarayanan et al, 2009). K_{Ca} 3.1 channels are voltage-independent channels: therefore in these experiments the increase of the slope conductance at -80 mV was taken as indication of channels activation (Sankaranarayanan et al, 2009).

The results reported in Figure 1.3A indicated that riluzole activates K_{Ca} 3.1 channels in HCT116 cells, as evidenced by the significant increase of the slope conductance at -80 mV. Overall, riluzole 45 μM induces a three fold increase in the slope conductance of K_{Ca} 3.1 channels, as compared with the controls (controls slope is 4.1 ± 1.2, while riluzole treated is 12.6 ± 1.7 and, n=7).

We next examined the effects of the same concentration of riluzole (45 μM) on the K_{Ca} 1.1 currents in HCT116. Since K_{Ca} 1.1 channels are voltage-dependent, channels modulation was measured as a change in mean currents amplitude. It emerged that riluzole is able to activate also K_{Ca} 1.1 channels (Figure 1.3B), strongly increasing the current amplitude (as measured at +30mV). Taken together, these results are in agreement with the previous demonstration that riluzole activates K_{Ca} 2/3 and K_{Ca} 1.1

channels in heterologous systems (e.g. the HEK 293), and supported the notion that riluzole is able to maintain its selectivity also in colorectal cancer cells.
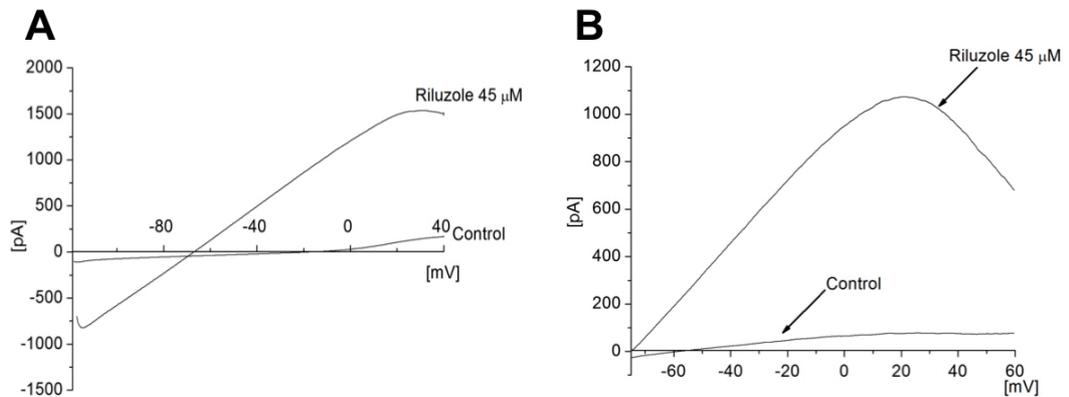
Figure 1.3. **Panel A**: K_{Ca} 3.1 current obtained in HCT116 and effect of riluzole (45 μM). Riluzole induces a significant activation, as compared with the control, of K_{Ca} 3.1 channels, as demonstrated by the increase in the slope conductance. **Panel B**: KCa 1.1 current obtained in HCT116 and effect of riluzole (45 μM). Riluzole induces a significant activation of KCa 1.1 channels, as demonstrated by the increase in mean current amplitude.

These results provided the rationale for the evaluation of the effects of riluzole, in combination with cisplatin, on HCT116 cisplatin-resistant colorectal cancer cells (for further details see Fortunato A. PhD thesis, 2013).

2. hERG1 channels as a target in anticancer drugs development

2.1. Dofetilide analogues.

The main aim of this research project was the screening of new compounds that behave as hERG1 blockers, but devoid of cardiotoxicity, to be used in cancer therapy. In particular, our strategy was based on the identification of specific hERG1B isoform blockers.

The initial screening by patch-clamp in whole cell configuration was performed on both hERG1A and hERG1B currents elicited in heterologous systems, e.g. the transfected HEK 293 cells. The effects of different compounds on hERG1A currents were examined with specific protocols on both outward, i.e. the physiological one, and inward directions (see Materials and Methods). Conversely, the effects of different molecules on hERG1B currents were mainly investigated on inward direction, because the biophysical characteristics of hERG1B currents prevented us from eliciting the currents in outward direction. The evaluation of drugs effects in the inward direction was also crucial when making the comparison between the effects on hERG1 currents in heterologous systems and in native tumour cell lines, in which hERG1 specific currents could be analysed only by increasing the external K^+ concentrations and by eliciting the currents in inward direction.

We initially tested the effects on both hERG1A and hERG1B channels, heterogously expressed in HEK 293 cells, of different analogous of dofetilide (kindly provided by Dr. A.P. IJzerman, Leiden University, The Netherlands; see (Guo et al, 2009)). Dofetilide is a member of a methanesulphonanilide class of antiarrhythmic drugs, approved for the conversion of and maintenance of sinus rhythm in patients with atrial fibrillation and atrial flutter (Lenz & Hilleman, 2000). It has been demonstrated that dofetilide has a high affinity for hERG channels, that blocks the rapid component of the delayed rectifier potassium current, I_{Kr} (Carmeliet, 1992), leading to the increase of the action

potential duration (APD) (Jurkiewicz & Sanguinetti, 1993). Moreover, dofetilide has been associated with acquired long QT syndrome and *Torsades de Pointes* (TdP) in 0.3-10.5% of patients (Lenz & Hilleman, 2000).

To determine the overlap between our experimental conditions and the data reported in literature, we first tested the effect of the native dofetilide (D1, 0.1-100nM) on the hERG currents elicited in HEK 293 hERG1A transfected cells. As shown in Figure 2.1A, 5nM D1 blocks more than 50% of the hERG1 current while 100nM D1 completely abolishes it. The IC_{50} values obtained from the dose-response curves (Figure 2.1B) for D1 were approximately 3.5 ± 0.3 nM for the outward and 5.3 ± 0.9 for the inward currents. The results gathered on the outward currents are in agreement with the one previously reported by (Guo et al, 2009). Moreover no significant difference was observed in the inhibition between outward and inward currents by D1.
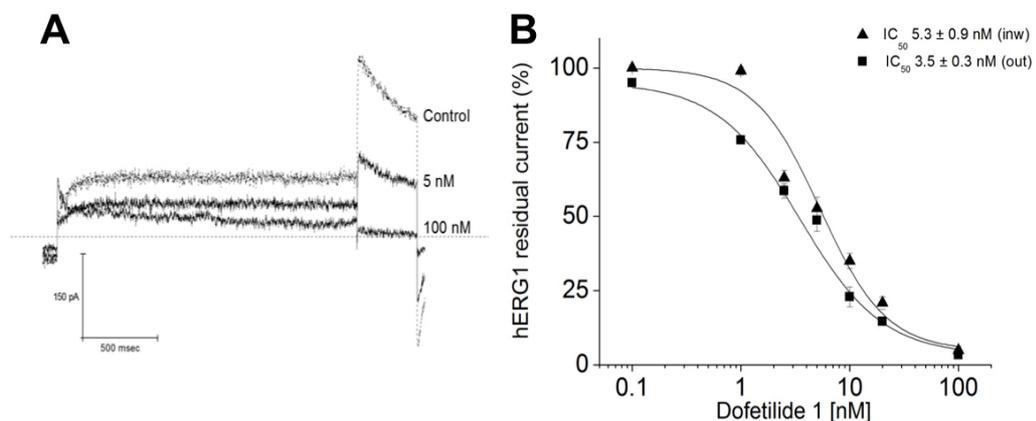

Figure 2.1. **Panel A:** Typical hERG1 currents obtained in HEK 293 hERG1A cells and effect of Dofetilide 1 (D1) on the tail current at -50 mV, after a 2 seconds preconditining step at +40 mV. **Panel B**: concentration-response curves and IC_{50} values obtained with D1 on both inward and outward current on transfected HEK 293.

After verifying that our experimental conditions were robust and replicable, we then tested four different analogous of D1, synthesised by Guo and colleagues (Guo et al, 2009) starting from the scaffold of D1.

Each of these analogues was modified in either the phenyl ring substituents and the methanesulphonamide groups (D30 and D34) or the nitrogen substituents (D57), which are hypothesised to interact respectively with Tyr652, Phe656 and the OH groups of Thr623, Ser624, Ser469 and Tyr652 in the inner pore of the channels. Evidences have

also revealed that the spacing between the basic nitrogen and the aromatic groups is important to cover the separation between the Phe656 and Tyr652 side chains in the pore region (Guo et al, 2009). Therefore another group of analogues has a modification in the carbon chain length (D79). hERG1 affinity was then evaluated with radioligand binding assay; the values for all the tested analogues are reported in Table 2.1, as in (Guo et al, 2009).

Compound	K_i [nM] or displacement %
D1	4.1 ± 0.9
D30	37% at 10 μM
D34	0.31 ± 0.28
D57	100 ± 12
D79	1.8 ± 1.0

Table 2.1. Dofetilide and analogues affinity values (K_i) obtained in radioligand binding assay to hERG1 channels (from (Shagufta et al., 2009).

We then tested the effects of analogous D30, in which the substitution of both the R' and R'' 4-NHSO$_2$CH$_3$ (i.e. the methanesulphonamide group) in the phenyl rings with two hydrogen residues causes almost a complete abolition of the affinity for hERG1 channels. Patch-clamp experiments performed with analogous D30 on both hERG1A and hERG1B currents confirmed the evidences gathered with radioligand binding assay: indeed only a 38-40% current inhibition was achieved at 200 μM (Figure 2.2A), a concentration 50 times greater than the IC$_{50}$ obtained for D1 (Figure 2.2B). Moreover, we did not observed any significative difference in the percentage of current inhibition between hERG1A and hERG1B.

These results also confirm the crucial role of the methanesulphonamide groups in the binding of dofetilide to hERG channel. Indeed, removing both the 4-NHSO$_2$CH$_3$ groups from the phenly rings prevented the binding to Phe656 or Try652, thereby impairing the inhibitory effects on hERG currents.
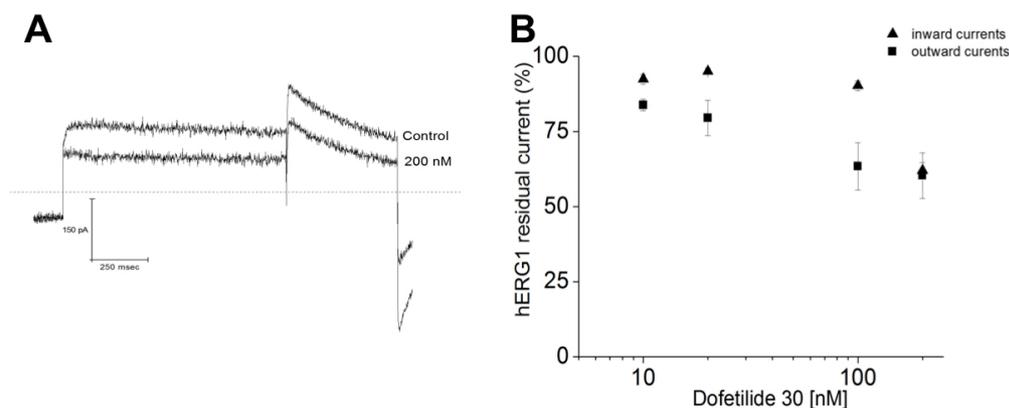
Figure 2.2. **Panel A:** Typical hERG1 currents obtained in HEK 293 hERG1A cells and effect of D30 (200nM) on the tail current at -50 mV, after a 2 seconds preconditining step at +40 mV. **Panel B**: concentration-response data obtained with D30 on both inward and outward current on transfected HEK 293 hERG1A.

The R' and R'' methanesulphonamide groups in analogous D34 were substituted by two 3,4 dichloro residues, with an increase of ten fold in the affinity for the hERG1 channels, as compared with D1. However, when tested on hERG1A currents, D34 turned out to have an effect smaller than D1, with a substantial reduction of the current only at concentration greater than 100 nM (Figure 2.3A); the IC_{50} values were quite similar considering inward and outward directions, being respectively 86.8 ± 0.3 nM and 86.5 ± 1.5 nM (Figure 2.3B). We next tested the effects of analogous D34 on hERG1B currents and we obtained quite similar results, with a substantial reduction at concentration greater than 100 nM and an IC_{50} value of 69.1 ± 1.5 nM (Figure 2.4C). The relative small effects on hERG1 currents by D34 could be explain by a less stable binding of the two 3,4 dichloro substituents with the Tyr652 and/or the Phe656 residues in the inner cavity of the pore channel. Based on the ten fold increase affinity of D34, Shagufta and colleagues suggested that a 3,4 dichloro groups as substituents of the phenyl rings could be optimal for a high hERG1 channel affinity (Guo et al, 2009); nevertheless the lack of any correlation between K_i and IC_{50} values in D34 seems to require further investigation on the mechanisms and binding sites of this analogous.
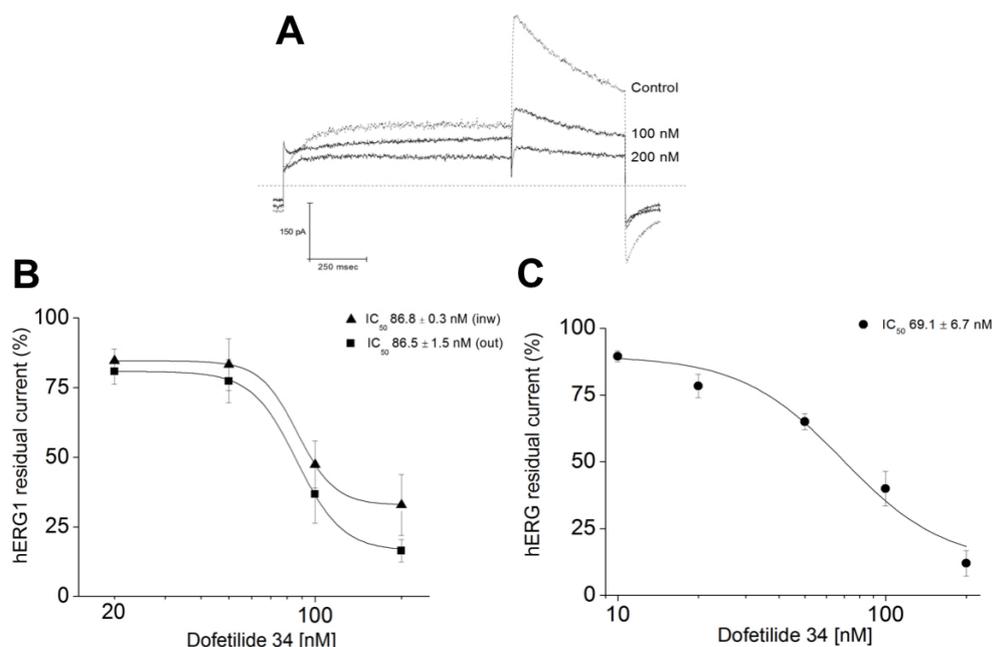
Figure 2.3. **Panel A:** Typical hERG1 currents obtained in HEK 293 hERG1A cells and effect of D34 on the tail current at -50 mV, after a 2 seconds preconditining step at +40 mV. **Panel B**: concentration-response curves and IC_{50} value obtained with D30 on both inward and outward current on transfected HEK 293 hERG1A. **Panel C**: concentration-response curves and IC_{50} value obtained with D34 on inward current on transfected HEK 293 hERG1B.

Analogous D57 was shynthetised with a modification of the central nitrogen atom, in which the hydrogen atom was substituted with a CH_2CN residues. It is worth remembering that the central nitrogen residues are thought to interact with both Thr623 and Ser624, two crucial residues for the binding of several other hERG blockers (Vandenberg et al., 2012). Indeed the affinity of D57 for the hERG1 channels decreases ($K_i = 100nM$) as compared with the unsubstituted analogous ($K_i = 48nM$) (Shagufta et al., 2009). We then tested the effect of D57 on hERG1A currents and we obtained IC_{50} values in the same range of the K_i, being 76.8 ± 12.2 nM and 76.2 ± 19.6 nM respectively for inward and outward currents (Figure 2.4A). However, we were not able to obtain a complete inhibition of the hERG1 current neither at the highest concentration used (i.e. 250 nM). Dose-response curve obtained with D57 on hERG1B currents instead revealed a slight decrease in the IC_{50} value (41.5 ± 5.3) with a significative difference observed between the effects produced on hERG1A or hERG1B at both 50 nM and 100 nM ($p < 0.05$, n= 6). However, the overall small decrease in the IC_{50} value of hERG1B channel inhibition and the absence of any correlation between

hERG1 current inhibition and the effects on cell viability (discussed below), seem to rule out a possible specificity of D79 for the hERG1B channel.
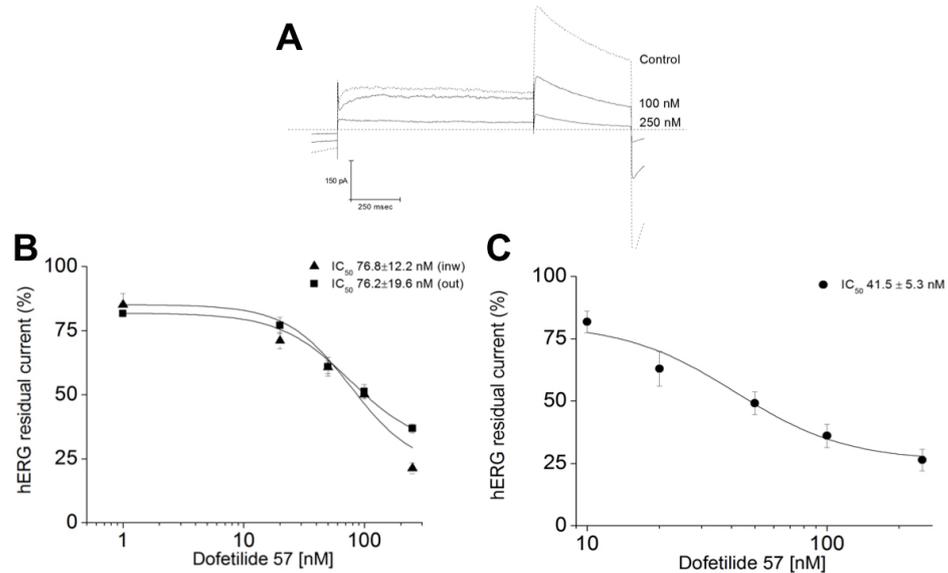

Figure 2.4. **Panel A:** Typical hERG1 currents obtained in HEK 293 hERG1A cells and effect of D57 on the tail current at -50 mV, after a 2 seconds preconditining step at +40 mV. **Panel B**: concentration-response curves and IC_{50} value obtained with D57 on both inward and outward currents on transfected HEK 293 hERG1A. **Panel C**: concentration-response curves and IC_{50} value obtained with D57 on inward current on transfected HEK 293 hERG1B.

The last tested analogous, D79, is characterised by an increase in the chain carbon length. This modification led to an increase in the affinity of D79 for hERG1 channel, as compared to reference compound (K_i are respectively 1.8 ± 1.0 nM for D79 and 5.7 ± 1.0 nM for the reference compound, see (Guo et al, 2009)). Dose-response curve obtained with D79 on hERG1A currents in inward and outward direction turned out to be extremely different (Figure 2.5B): indeed D79 seems to be more effective on inward currents rather than on outward currents. This finding was further supported by almost a ten fold increase in the IC_{50} values, which were respectively 3.6 ± 1.0 nM for inward currents (a value quite similar to the K_i) and 48.8 ± 9.2 nM for outward currents. When tested on hERG1B currents in inward direction, the full dose-response curve (Figure 2.5C) reveal a three times increase in the IC_{50} values for D79 (10.8 ± 3.3 nM). Moreover, D79 turned out to be more effective in blocking the hERG1A than the hERG1B ($p< 0.05$ at 10 nM, n= 6).
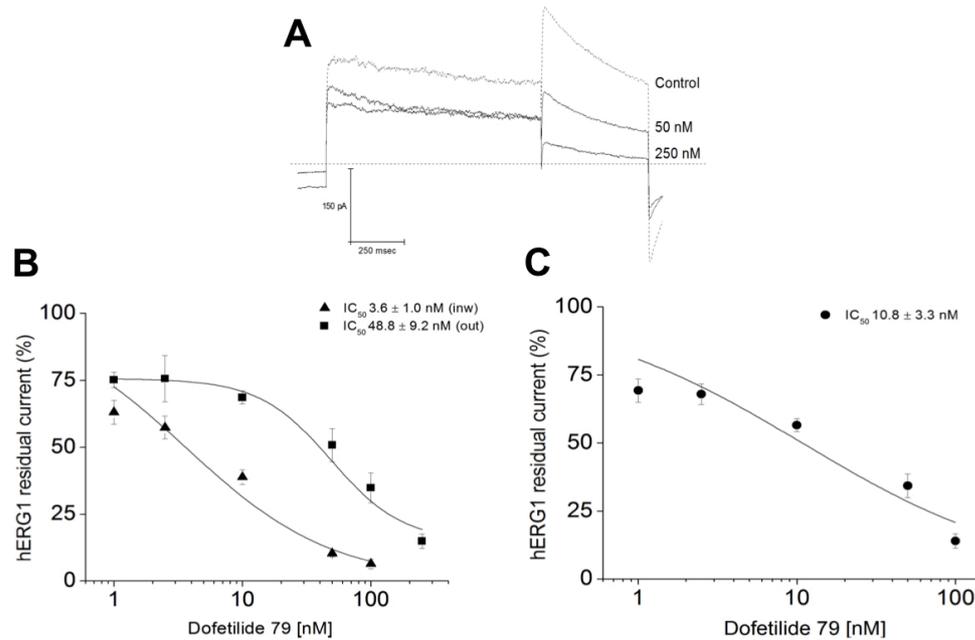
Figure 2.5. **Panel A:** Typical hERG1 currents obtained in HEK 293 hERG1A cells and effect of D79 on the tail current at -50 mV, after a 2 seconds preconditining step at +40 mV. **Panel B**: concentration-response curves and IC_{50} value obtained with D79 on both inward and outward currents on transfected HEK 293 hERG1A. **Panel C**: concentration-response curves and IC_{50} value obtained with D79 on inward current on transfected HEK 293 hERG1B.

Taken together these findings seems to indicate that D79 has a preferential block towards the hERG1A isoform, at least when currents were elicited in inward direction. Moreover, D79 inhibition of the hERG1 channels seems to be more pronounced on inward currents, as indicated by the ten fold increase in the IC_{50} values. The reason of such different effects could reside in the less stable interaction, due to the lengthening of the carbon chain, with the canonical residue Phe656 and Tyr652. A less stable binding could cause a deeper positioning of D79 within the inner pore when currents flow in inward direction, thus resulting in a significative increase of the current blockade.

To fully characterised the impacts of dofetilide analogues on hERG channels, we analysed the effect of hERG currents inhibition on the biophysical properties of hERG1 channels. To this purpose, we determined the current-voltage relationship by plotting the maximal tail current at -50 mV against the voltage membrane values applied during the preconditining steps. The experimental data were then fitted with Boltzmann equation and $V_{1/2}$, which indicates the half maximal voltage of activation, and dx, which is the slope of the curve, were extrapolated. No differences in these biophysical properties were identified for the native dofetilide or the analogues D30, D34 and D57.

Conversely, when examining the current-voltage relationship for the analogous D79, it emerged an increasing inhibitory effect of D79 on hERG1 current at membrane voltage between +10 mV and +40 mV, as compared with the control. This enhanced inhibition at high depolarised values was identified at both saturated concentrations (250 nM) as well as near to the IC_{50} value for outward activation (i.e. 50 nM), but was absent at lower (1-10 nM) tested concentrations (Figure 2.6). At both 1 nM and 50 nM, D79 causes a small but significant shift (respectively p= 0.02 and p< 0.001, n=6) in the voltage required for the half maximal activation of hERG1 (i.e. the $V_{1/2}$, obtained by fitting the experimental data with Boltzmann equation), whilst there was no difference in the slope factor of the curves.
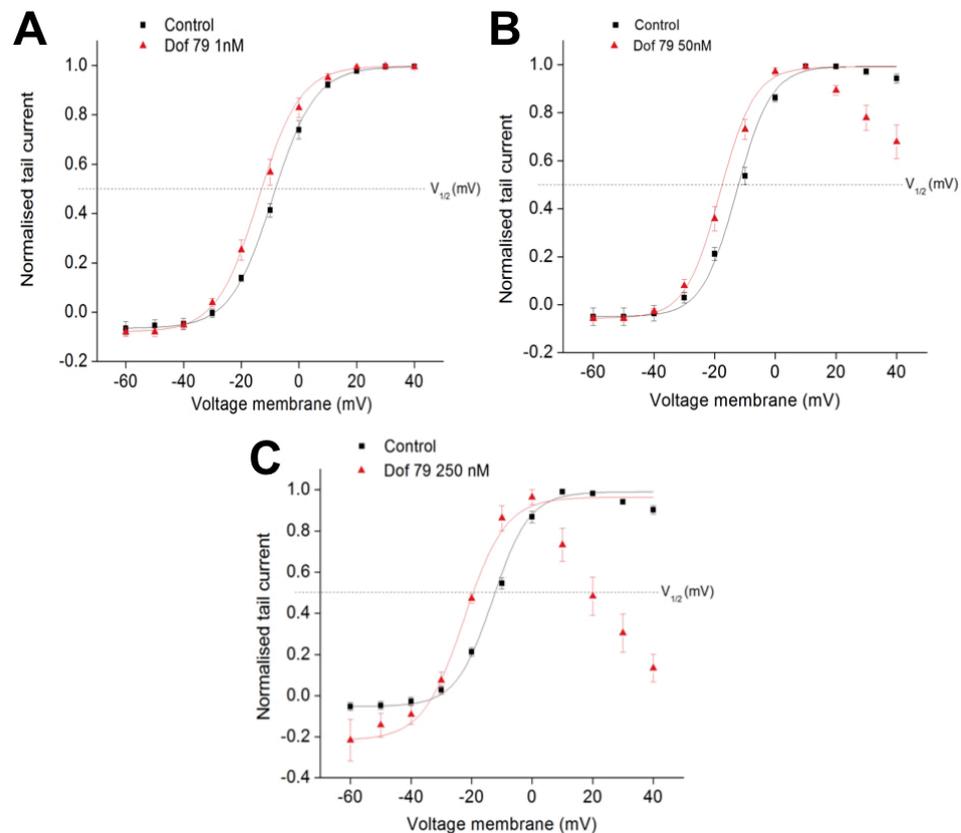
Figure 2.6. **Panel A:** Current-voltage relationship for control (black square) and 1 nM D79 (red triangle). $V_{1/2}$ of control: -8.5 ± 1.0; $V_{1/2}$ of 1 nM D79: -13.5 ± 1.6, p= 0.02, n=6. **Panel B**: Current-voltage relationship for control (black square) and 25 nM D79 (red triangle). $V_{1/2}$ of control: -12.5 ± 0.9; $V_{1/2}$ of 50 nM D79: -17.2 ± 1.0, p< 0.001, n=6. **Panel C:** Current-voltage relationship for control (black square) and 250 nM D79 (red triangle). $V_{1/2}$ of control: -8.5 ± 1.0; $V_{1/2}$ of 250 nM D79: not determined. Normalised tail currents are plotted versus membrane voltages. Experimental data were fitted using Boltzmann equation.

These results prompted us to evaluate the voltage dependency of block by D79. We thus analysed the hERG1 current inhibition at four different membrane voltages, from -20 mV to +40 mV: it clearly emerged that D79 (50nM) blocked hERG current, but the effect depend on the degree of depolarisation (Figure 2.7). Indeed the block was weaker at -20 mV (mean= 11.6 ± 8.5 %, n=6) and reached the maximum at +40 mV (mean 52.2 ± 7.4, n=6). These results, although preliminary, seems to suggest that D79, conversely to dofetilide (Tsujimae et al, 2004), exert a voltage dependent block on hERG1 currents.
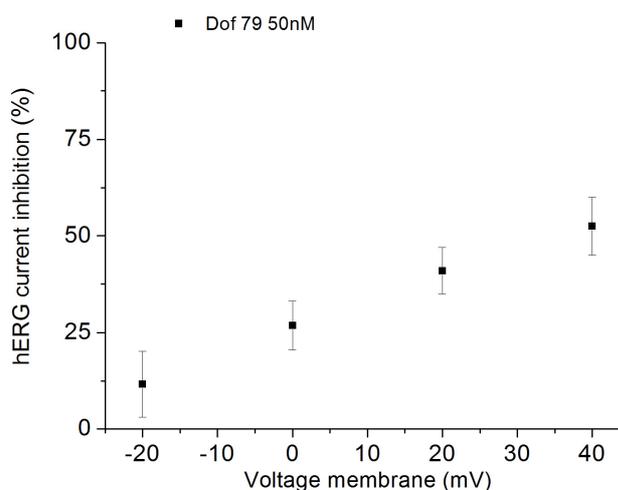
Figure 2.7. comparison of hERG1 current inhibition induced by 50 nM D79 at different membrane voltages from -20 mV to +40 mV. Black squares and bars indicated mean ± SEM. hERG current inhibition at -20mV : 11.6 ± 8.5%; at 0 mV: 26.8 ± 6.3%; at =20 mV: 41 ± 6.1%; at +40mV: 52.2 ± 7.4%.

As stated above, the spacing between the basic nitrogen and the aromatic groups is important to cover the separation between the Phe656 and Tyr652 side chains in the pore region. Therefore a possible explanation for the peculiar voltage-dependent inhibition of hERG1 current exhibited by D79, could reside on the lengthening of the carbon chain: indeed, both the basic nitrogen and the aromatic groups could interact with different residues, besides Phe656 and Tyr652, within the inner pore of the channels, thus leading to a modification of hERG1 biophysical properties.

Finally, we investigated the effects of Dofetilide 1 and all the analogues reported above on the viability of two different leukaemia cell lines, 697 and FLG 29.1, both expressing the hERG1 channels (Hofmann et al, 2001) (Pillozzi et al, 2011). Cell viability, as

examined by WST-1 assay, turned out to be markedly reduced by all the tested compounds in the nanomolar range (ED_{50} values are summarised in Table 2.2).

Dofetilide	ED_{50} 697 [nM]	ED_{50} FLG 29.1 [nM]
1	4.6 ± 0.4	3.6 ± 0.2
30	7.2 ± 0.5	3.7 ± 0.2
34	2.8 ± 0.2	1.8 ± 0.1
57	4.3 ± 0.4	3.8 ± 0.1
79	4.4 ± 0.2	2.0 ± 0.1

Table 2.2. Mean ED_{50} values and SEM obtained with WST-1 cell viability assay on leukemic cell lines. ED_{50} values were calculated from the dose-response curves fitted with the Hill's equation.

However, when comparing the results obtained by patch-clamp experiments with the data of cells viability, we were unable to find a close correlation between hERG1 current inhibition and the decrease in leukaemia cells viability. Indeed, effective dose values for different analogues are almost in the same concentration range, independently from the effect on hERG1 currents. The decrease in leukaemia cell viability could therefore be explained not by the direct block of the hERG1 currents, as in the case of E4031, but rather by a reduction of the trafficking of hERG protein to the cell membrane, as already demonstrated for arsenic trioxide, pentamidine and probucol (Vandenberg et al, 2012).

The discrepancy between hERG1 current blockade IC_{50} and leukaemic cell viability reduction obtained with dofetilide analogues could be also explained by a direct effect of these molecules on the macromolecular complex between hERG1 and β1 integrins. Indeed, as discussed before, at least three integrin/hERG1 channel complexes have been identified so far (Pillozzi & Arcangeli, 2010), being able to modulate intracellular signalling cascade and to trigger different biological effects, such as cell survival and migration. In this view, leukaemic cell viability reduction exerted by dofetilide analogues could be explained by the unlocking of such multiprotein membrane signalling complexes.

In conclusion, data gathered with patch-clamp technique using different dofetilide analogues provided useful information about the chemical feature that can increase or decrease both hERG1 channel affinity and blockade ability of a molecule. These findings may be valuable for the design and the subsequent validation of novel compound with different affinity for the hERG1 channels, looking for a balance between the therapeutic effects and the absence of cardiotoxicity.

2.2. Macrolides: erythromycin and clarithromycin.

Our screening of hERG1 blockers was then focused on two molecules, erythromycin and clarithromycin, belonging to the macrolides class of antibiotics.

Erythromycin and clarithromycin are both US FDA approved antibiotics, widely used in the treatment against Gram-positive bacteria. Both compound have been associated with an increased risk of proarrhythmic effects, including acquire long QT syndrome, ventricular arrhythmias and *Torsades de Pointes* (Kundu et al, 1997) (Katapadi et al, 1997) (Kamochi et al, 1999) (Mishra et al, 1999). The molecular basis for the pro-arrhythmogenic effects have been reported to reside in the block of the rapid component of the delayed rectifier potassium current, I_{Kr}, in guinea pig-isolated cardiomyocytes at clinical relevant concentrations (Daleau et al, 1995). Moreover, erythromycin, clarithromycin and other macrolides have been demonstrated to block the hERG1 current also in heterologous systems (Volberg et al, 2002) (Stanat et al, 2003). Interestingly, despite the reported side effects, in the last decade macrolides have been proposed as useful adjuvant to chemotherapy and radiotherapy treatment of cancer and are now used in clinical trials for the treatment of different tumours, in particular myelomas and chronic myeloid leukaemia (Mikasa et al, 1997) (Morris et al, 2001) (Niesvizky et al, 2008) (Morris et al, 2008) (Carella et al, 2012) (Komatsu et al, 2013). In chronic myeloid leukaemia clarithromycin potentiates the therapeutical effects of the tyrosine kinase inhibitor (Carella et al, 2012), probably through the inhibition of the late stage of autophagy (Schafranek et al, 2013).

Based on these findings, we evaluated whether macrolides could be useful compound for the treatment of leukaemia, by targeting the hERG1B channels. The initial identification of the blockade of hERG1 channels by erythromycin and clarithromycin was achieved on hERG1A current elicited in the outward direction (Volberg et al, 2002) (Stanat et al, 2003). As discussed above, to be able to made a comparison between the effects on heterologous systems and in native tumour cell lines, we evaluated the effects of both macrolides on the hERG1 current elicited in the inward direction. We initially examined the effect on the hERG1A blockade of increasing concentrations (1-350 μM) of erythromycin and clarithromycin. Both compounds revealed a concentration-

response relationship (Figure 2.8), but none of them completely blocked the hERG1A current even at saturating concentrations (Figure 2.9).
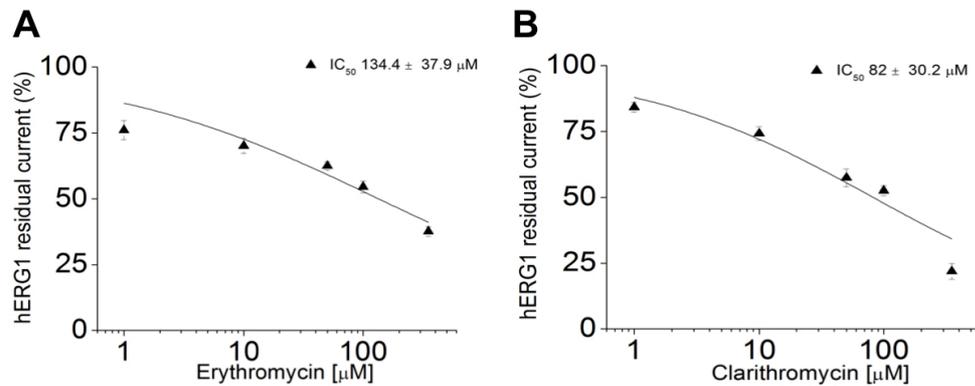

Figure 2.8. **Panel A:** concentration-response curves and IC_{50} value obtained with erythromycin on hERG1A currents elicited inward direction. **Panel B**: concentration-response curves and IC_{50} value obtained with clarithromycin on hERG1A currents elicited inward direction.
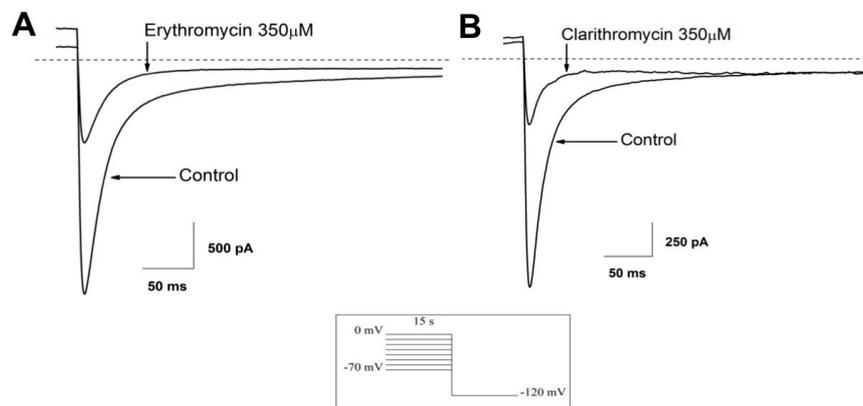

Figure 2.9. **Panel A:** representative hERG1 currents, elicited in the inward direction, obtained in HEK 293 hERG1A and effect of 350 μM erythromycin; **Panel B:** representative hERG1 currents, elicited in the inward direction, obtained in HEK 293 hERG1A and effect of 350 μM clarithromycin. For briefness, the drugs effect was reported on the tail currents elicited after conditioning at 0 mV for 15 seconds. The stimulation protocol is reported in the inset and detailed in Materials and Methods.

For erythromycin the concentration-response relationship could be best fit with an $IC_{50}=$ 134.4 ± 37.9 μM, while for clarithromycin we obtained a $IC_{50}=$ 82 ± 30.2 μM. These values resulted to be higher than those reported by Stanat et al. (Stanat et al, 2003). Such discrepancies could be due to the difference in both the stimulus pattern applied for the activation of hERG1 current (outward currents in Stanat et al., inward current in

our experiments) or in the temperature at which recordings are performed (Zhou et al, 1998); indeed, it has been demonstrated that erythromycin, as well as D,L-sotalol, blockade of hERG1 channels is highly temperature-sensitive, resulting in more than 3 fold change in IC_{50} value and in underestimated IC_{50}, at room temperature, by a factor of about 7 (Kirsch et al, 2004).

We then evaluated the effect of erythromycin and clarithromycin on the hERG1B currents in HEK 293 transfected cells. Surprisingly, erythromycin did not inhibit hERG1B current in a dose-dependent manner: indeed, even at saturated concentrations (350 μM) erythromycin exerted approximatively a 20% blockade of hERG1B currents (Figure 2.10A and Figure 2.11A). Conversely, clarithromycin reduced the hERG1B currents in HEK 293 cells in a concentration-dependent manner, producing an overall inhibition at saturated concentration similar to that obtained on hERG1A currents; moreover, the clarithromycin data was best fitted with a $IC_{50}= 66.8 \pm 9.8$ μM, resulting in a slight decrease as compared to IC_{50} value obtained of hERG1A (Figure 2.10B).
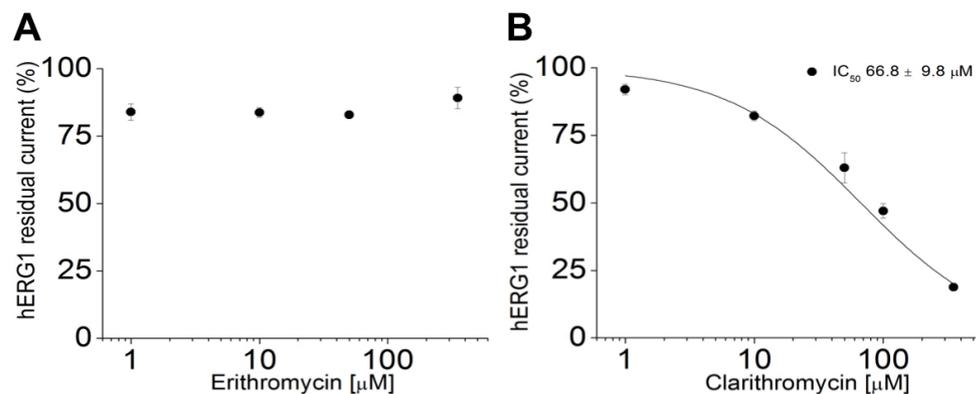
Figure 2.10. **Panel A:** concentration-response data obtained with erythromycin on hERG1B currents in HEK 293 transfected cells. **Panel B**: concentration-response curves and IC_{50} value obtained with clarithromycin on hERG1B currents.
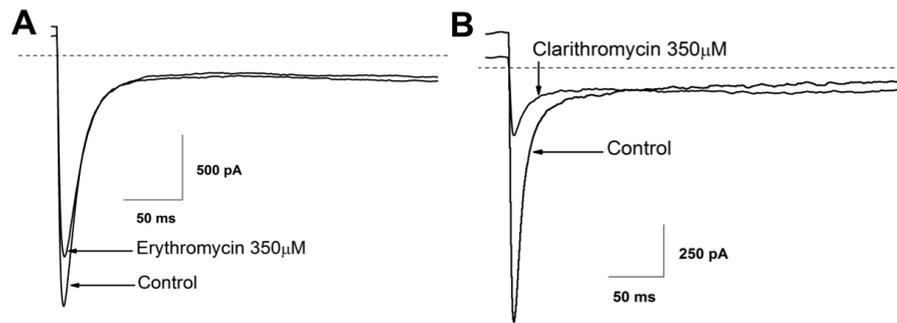
Figure 2.11. **Panel A:** representative hERG1B currents, elicited in the inward direction, obtained in HEK 293 hERG1B and effect of 350 μM erythromycin; **Panel B:** representative hERG1B currents, elicited in the inward direction, obtained in HEK 293 hERG1B and effect of 350 μM clarithromycin. For briefness, the drugs effect was reported on the tail currents elicited after conditioning at 0 mV for 15 seconds. The stimulation protocol is the same reported in Figure 2.9.

An explanation of the lack of inhibitory effect of erythromycin on hERG1B current, could reside in the difference in the aminoacidic sequence between hERG1A and hERG1B channels, with the latter having a a shortened N-terminus, constituted by only 34 aminoacid residues, with no homology with the N-terminus of hERG1A (Lees-Miller et al, 1997) (Morais Cabral et al, 1998). As demonstrated by Robertson's group the hERG1A/hERG1B heteromer has a reduced sensitivity to the blockade by E4031 (which act as an open channel blocker like erythromycin), due to differences in the N-terminal structure (Sale et al, 2008). The authors also proposed, in their kinetic model, that the presence of extended N-termini on all four subunits in the hERG1A "allows for many more states that can also be bound by drug, thus enhancing efficacy". The reduced sensitivity to drug block could therefore be due to the fewer (for heteromer channels, or absent in the case of hERG1B) extended N-termini available.

We finally evaluated whether both erythromycin and clarithromycin also blocked hERG1 in leukaemia cells. To this purpose, we used FLG 29.1, a human myeloid leukaemia (AML) cell line whose hERG1 currents are mainly sustained by the hERG1B isoform (Crociani et al, 2003). As shown in Figure 2.12, both erythromycin and clarithromycin inhibited hERG1 current in FLG 29.1 in a concentration dependent manner, with the IC_{50} being respectively 97 ± 3.1 μM and 38.5 ± 7.0 μM. However, as already demonstrated for hERG1A currents, erythromycin reached only a 60-65% blockade even at saturated concentrations (Figure 2.13A). Conversely, clarithromycin

almost totally inhibited hERG1 current in FLG 29.1 (Figure 2.13B), and revealed an IC_{50} value even lower the one gathered on heterologous systems.
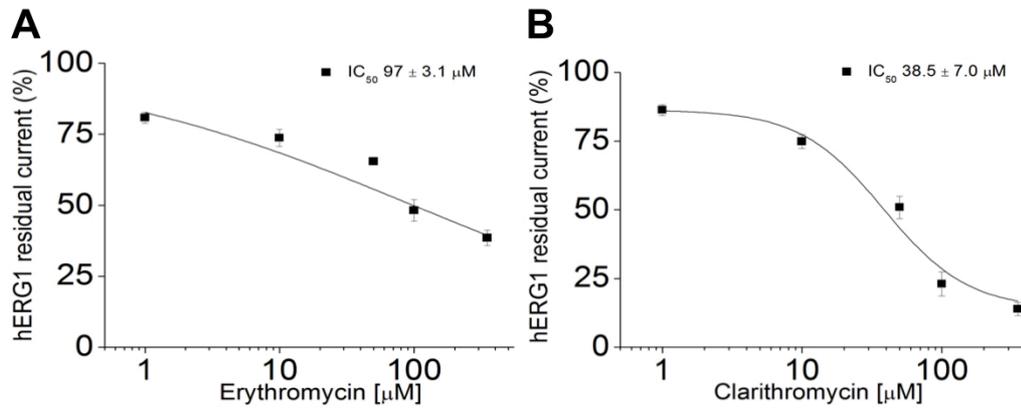

Figure 2.12. **Panel A:** concentration-response curves and IC_{50} value obtained with erythromycin on hERG1 currents elicited in FLG 29.1. **Panel B**: concentration-response curves and IC_{50} value obtained with clarithromycin on hERG1 currents in FLG 29.1.
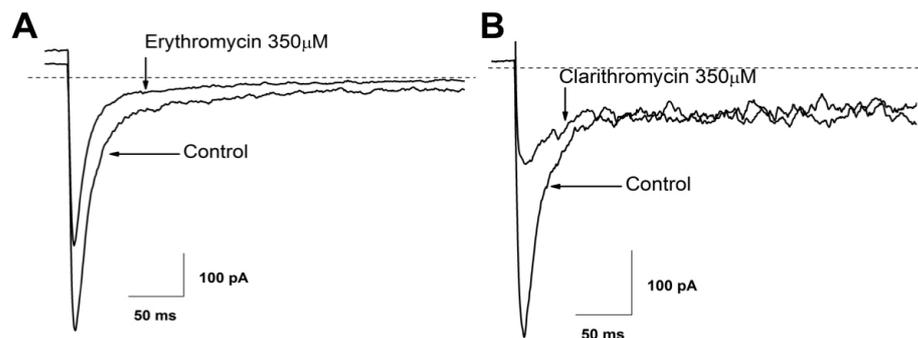

Figure 2.13. **Panel A:** representative hERG1 currents obtained in FLG 29.1 and effect of 350 μM erythromycin; **Panel B:** representative hERG1 currents obtained in FLG 29.1 and effect of 350 μM clarithromycin. For briefness, the drugs effect was reported on the tail currents elicited after conditioning at 0 mV for 15 seconds. The stimulation protocol is the same reported in Figure 2.9.

The above reported results clearly indicates that clarithromycin exert an inhibitory effect on both hERG1A and hERG1B currents in heterologous systems, being however slightly more effective on hERG1B channels. Moreover, we demonstrated that clarithromycin is able to maintain its blockade ability in endogenous hERG1 expressing cell line, i.e. the FLG 29.1, revealing also an increased potency as compared to heterologous systems. Based on these findings, and considering the crucial role of hERG1 channels in tumours, we may propose that clarithromycin is a promising useful adjuvant in chemotherapy treatment, by targeting the hERG1B channels. The significant

reduction of the IC_{50} value obtained in the FLG 29.1 could be even more advantageous from the perspective of the use of clarithromycin as adjuvant in cancer therapy, since lowering the dose could reduce or, even better, eliminate the above mentioned cardiac side effects.

2.3 NAMI-A, a ruthenium compound.

Since the discovery of anti-cancer properties of cisplatin and other platinum compounds, such as carboplatin and oxaliplatin, metal drug based compounds have gained great interest in both medicinal chemistry and in drug design (Barry & Sadler, 2013).

NAMI-A (imidazolium trans-[tetrachloro(DMSO)(imidazole) ruthenate(III)]) is an anticancer Ru(III) complex discovered by Sava et al. (Sava et al, 1998), which was found to be negligibly cytotoxic toward many cancer cell lines but instead revealed a remarkable and specific activity against metastases (Alessio et al, 2004) in various animal cancer models (Cocchietto et al, 2003) (Bergamo et al, 2004). Indeed, due to its encouraging pharmacological profile, to the low systemic toxicity and to the relevant antimetastatic activity, NAMI-A entered and completed a phase I clinical trial (Rademaker-Lakhai et al, 2004) and is actually under phase 1/2 combination study with gemcitabine (Barry & Sadler, 2013). At date, the molecular mechanism through which NAMI-A exerts its biological actions is not understood and several hypothesis have been made (Alessio et al, 2004) (Frausin et al, 2005) (Bergamo & Sava, 2007).

We gathered evidences that NAMI-A (i) exerts a strong antiproliferative effect against different leukaemic cell lines; (ii) causes cell cyle arrest in the G2/M phase and (iii) induces cell death through apoptosis in leukaemia cells (Pillozzi et al., submitted). Moreover, the citotoxic effect of NAMI-A is not dependent on ruthenium uptake or a direct damage to DNA (Pillozzi et al., submitted).

Looking for an reliable mechanism explaining the antiproliferative activity, we thus investigated whether NAMI-A could affect plasma membrane ion channels, as already reported for other ruthenium compounds (Jara-Oseguera et al, 2011).

At first, since all the tested leukaemia cell lines were reported to express hERG1 channels, we investigated whether NAMI-A could exert its effect by blocking hERG1 channels. To this purpose, we evaluated the blockade ability of NAMI-A in both heterologous system and in the hERG1-expressing leukaemic cell line FLG 29.1.

As shown in Figure 2.14, NAMI-A did not inhibit hERG1 currents in FLG 29.1 in a dose-dependent manner, producing only a 25-30% inhibition even at saturated

concentrations (i.e. 100 μM). The same results were obtained on hERG1A currents elicited in HEK 293 transfected cells (data not shown).
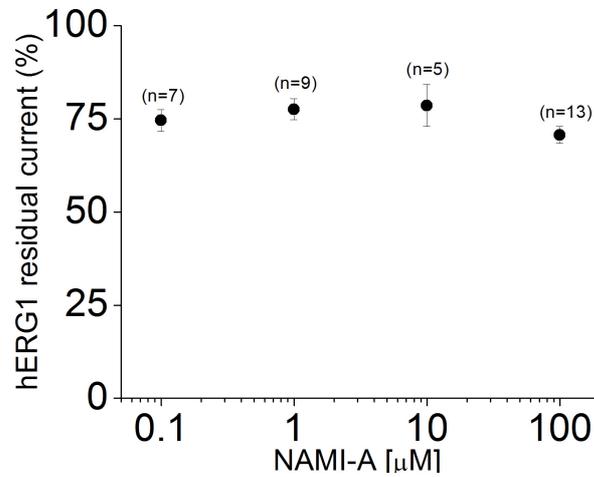

Figure 2.14. Concentration-response data obtained with NAMI-A on hERG1 currents elicited in leukaemia cell line FLG 29.1.

We then carried out other patch-clamp experiments in whole-cell mode on FLG 29.1 cells, perfused with an extracellular solution containing physiological ion concentrations (E_K was -80 mV; E_{Cl} was -50 mV). We applied a voltage ramp protocol, in the absence or in the presence of saturated concentrations of NAMI-A (100 μM). NAMI-A produced an inhibitory effect on the whole-cell current with a reversal potential around -70mV (Figure 2.15). The effect of the drug was very similar to that produced by 5mM TEA (Figure 2.16), suggesting that NAMI-A mostly affects a K^+ current.
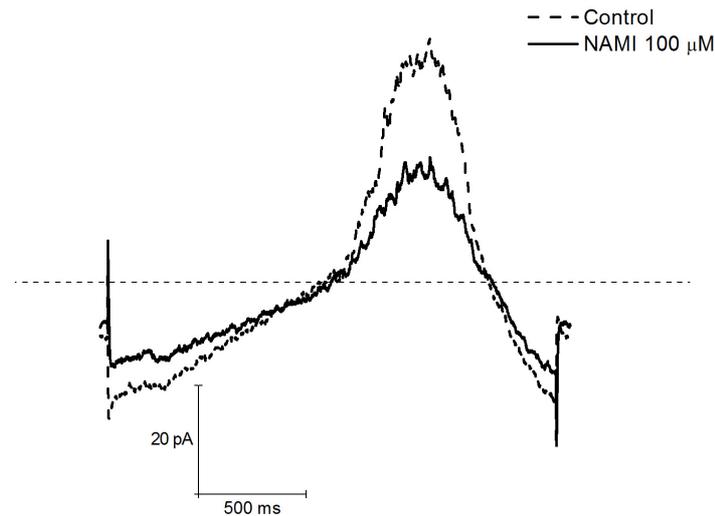
Figure 2.15. Representative current obtained in FLG 29.1 cells with a voltage ramp protocol in the absence (dashed line) and in presence of 100 μM NAMI-A (continuous line). The holding potential of -70 mV rules out the contribution of hERG channels, which are fully deactivated at this Vm.
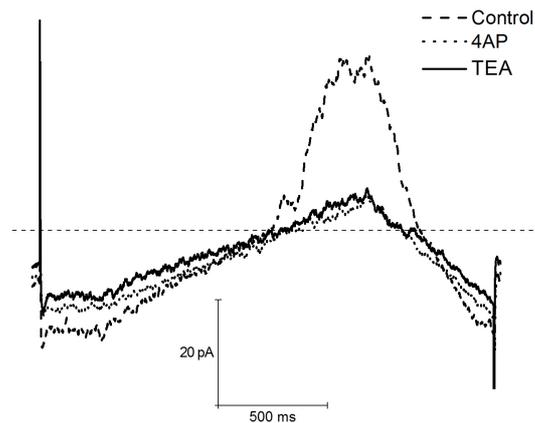

Figure 2.16. Ramp protocol obtained in FLG 29.1 cells in the absence (dashed line) and in presence of 5mM TEA (continuos line) or 200 μM 4-AminoPiridine (dotted line).

The concentration-dependent effect of the NAMI-A was then tested on outward currents, by applying voltage steps between -80 mV and +60 mV (the conditioning potential being -80 mV). Figure 2.17 shows that both 2 and 100 μM NAMI-A reduced the outward currents. In particular 2 μM NAMI-A produced an approximately 36.5 ± 4.4% (n=9) block of the current inhibited by 100 μM NAMI-A.
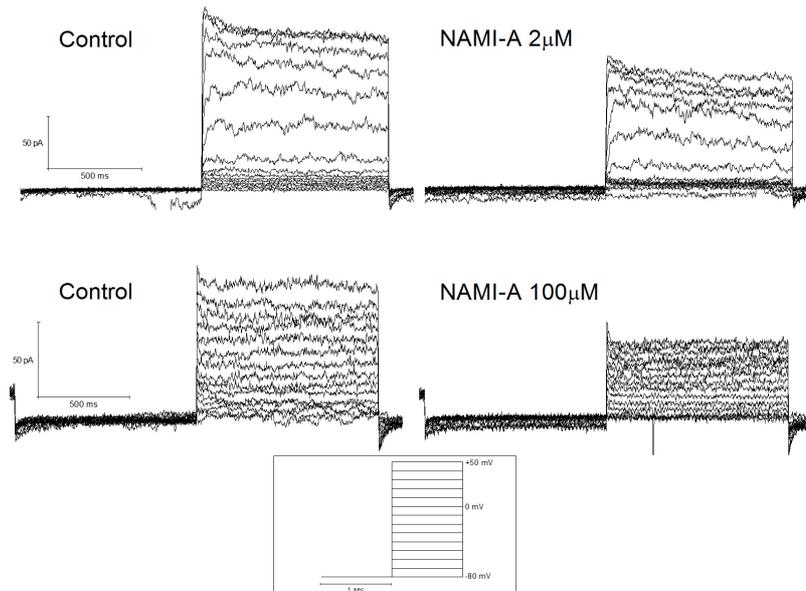
Figure 2.17. Outward currents elicited in FLG 29.1 cell line and effects of NAMI-A 2 μM (top) or 100 μM (bottom). The stimulation protocol is shown in the inset.

As a subsequent step, we try to identify the K^+ channel type affected by NAMI-A. RT-PCR analysis revealed that, besides hERG1, FLG 29.1 express mRNA encoding the Ca^{2+} dependent K^+ channel K_{Ca} 3.1, but not the K_V 1.3 and K_V 1.5. (Figure 2.18). As a positive control we used the cDNA obtained form Peripheral Blood Mononuclear cells (PBMC), which have been reported to express all the three channel types (Cahalan et al, 1985) (Grissmer et al, 1993).
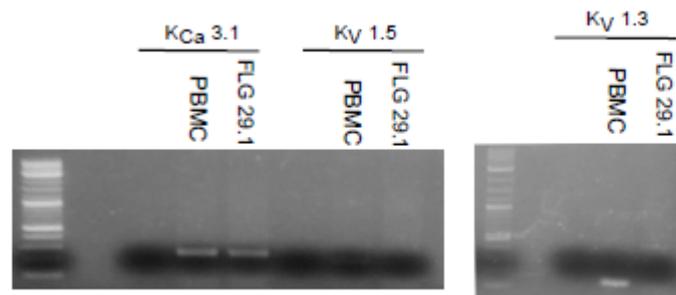

Figure 2.18. RT-PCR relative to K_{Ca} 3.1, K_V 1.3 and K_V 1.5 expression in FLG 29.1 and Peripheral Blood Mononuclear Cells (PBMC). The first lane of each gel shows the negative control of the PCR reaction.

Based on the evidence of K_{Ca} 3.1 expression in FLG 29.1, we tested whether NAMI-A inhibited K_{Ca} 3.1 channels heterologously expressed in HEK 293 cells. In these cells, as

expected, the specific K_{Ca} 3.1 inhibitor TRAM 34 produced a strong inhibition of the whole-cell currents, indicating that these are largely constituted by K_{Ca} 3.1 (Figure 2.19). Moreover, 2 µM NAMI-A significantly reduced the K_{Ca} 3.1 currents, as evidenced by the decrease of the slope of the current elicited by the voltage ramp protocol reported in Figure 2.20A. Collectively, NAMI-A (Figure 2.20B) inhibited about 30% of the K_{Ca} 3.1 current at the concentrations (1-2 µM) that were demonstrated to reduce leukaemia cell proliferation (Pillozzi et al., submitted).
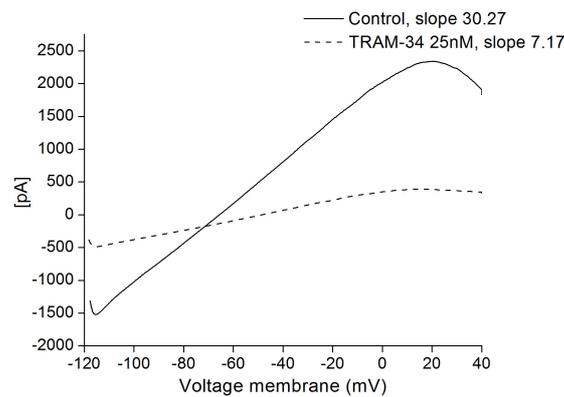

Figure 2.19. K_{Ca} 3.1 currents elicited in HEK 293 K_{Ca} 3.1 transfected and effect of TRAM 34 25 nM (dashed line).
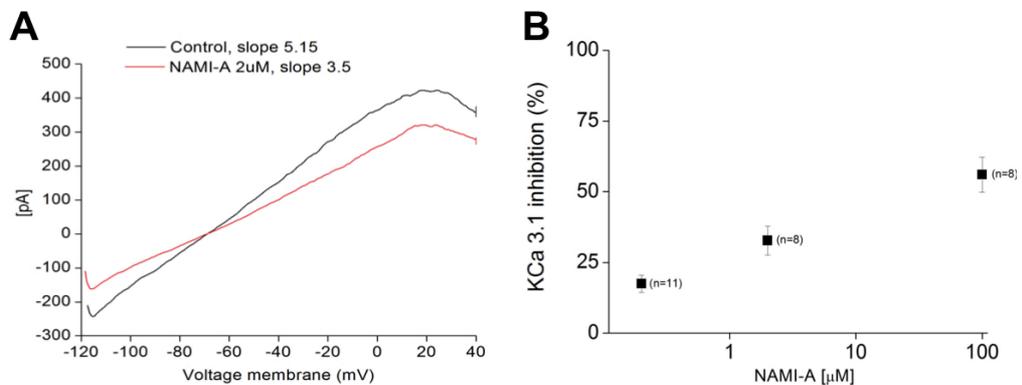

Figure 2.20. Panel A: Currents elicited in HEK 293 cells transfected with K_{Ca} 3.1 in the presence or absence of NAMI-A 2 µM. The stimulation protocol is detailed in Materials and Methods section. **Panel B**: Inhibitory effect of NAMI-A (0.2, 2 and 100 µM) on K_{Ca} 3.1 currents. The fold decrease of slope conductance was taken as a measure of channel block.

Overall, these results clearly indicates that NAMI-A exert an inhibitory effect on plasma membrane ion channels, and particularly on K_{Ca} 3.1 channels. The evidence of a blockade ability of NAMI-A toward K_{Ca} 3.1 channels seems also to account for the antileukemic effects reported by Pillozzi et al. (Pillozzi et al., submitted). K_{Ca} 3.1 channels are overexpressed in a wide variety of cancer cells including leukaemias

(D'Amico et al, 2013) and are involved in numerous hallmarks of cancer (for further details see Introduction). Very interestingly, in leukaemia and lymphoma cells, K_{Ca} 3.1 currents mainly regulate cell proliferation, whereas they are pivotal regulators of cell migration in epithelial and glial cancer cells (D'Amico et al, 2013). Such different functional behaviour of K_{Ca} 3.1 channels in the mentioned cell types seems to account very well for the pronounced cytotoxicity of NAMI-A in leukaemia cells and for its low cytotoxicity but large antimetastatic effect in solid tumours.

These findings further reinforced the notion that different ion channels play a crucial role in numerous features of tumour cells behaviour and that targeting them could represent a valuable and promising strategy for antineoplastic therapy. Moreover, it is increasingly evident that ion channels could be targeted by extremely different class of molecules, including antibiotics, antihistamines and metal based drugs, and that the same compound may exert completely opposite effects in different tumour types, as in the case of NAMI-A. The availability of compounds already proven to be safe may also accelerate the introduction into routinely clinical treatments.

2.4 CD-160130 (by BlackSwan Pharma)

CD-160130 is a pyrimido-indole compound, originally developed as a phosphodiesterase (PDE)-4 inhibitor with the aim of developing a drug able to promote apoptosis in leukemic cells through an increase in intracellular cAMP levels (Kim & Lerner, 1998) (Tiwari et al, 2004) (Lerner & Epstein, 2006). Indeed, CD-160130 was shown to possess a killing effect on Chronic Lymphocytic Leukaemia (CLL) cell (Weinberg JB, 2007). However, discrepancies between the PDE-4 inhibitory activity and leukemia cell killing efficacy for CD-160130 and some of its close analogues emerged (see Table 2.3), suggesting that the inhibition of PDE-4 unlikely plays a major role in the killing actions of CD-160130 on leukemias. Table 2.3 also shows that several of these compounds also bind hERG1 channels expressed in HEK 293 cells, as measured by the astemizole binding assay. As evident from Figure 2.21, hERG1 binding efficacy better correlated with leukemia cell killing than PDE-4 inhibition. In particular, CD-160130 had a high hERG1 binding affinity (B_{50} = 1.89 µM), and a high killing capacity and yet low PDE-4 inhibition, whereas CD-140793 (a structural analog of CD-160130, which differs by only a single substitution in the R4 position of the molecule) did not bind hERG1 and did not show any anti-leukemic effect, besides similar inhibitory activity on PDE-4 (see Table 2.3).

These data prompted us to evaluate whether CD-160130 could have an antileukemic effect due to a blocking effect on hERG1 currents.
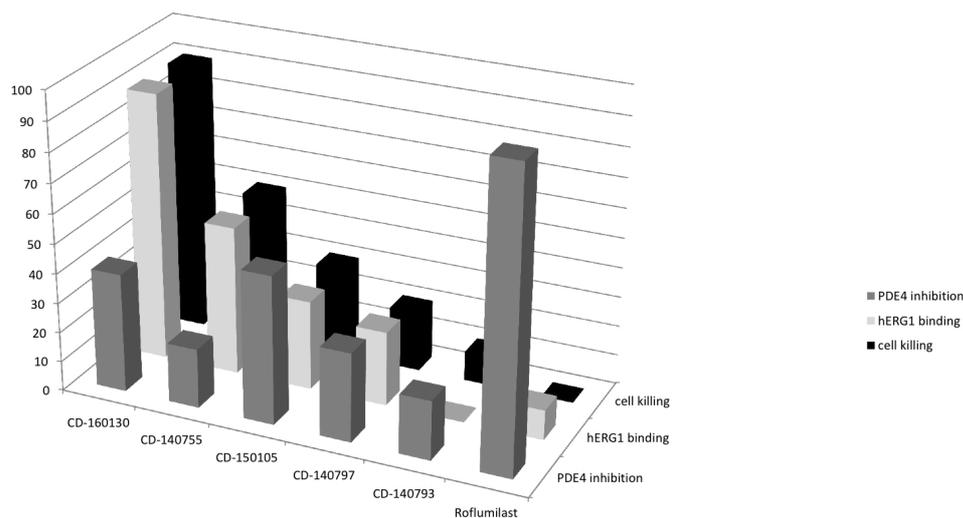
Figure 2.21. Disparity between CLL killing activities and PDE-4 inhibition. 3D graph shows the comparison between CLL killing, PDE-4 inhibition and hERG1 binding for CD-160130 and some analogues. Original values of EC50, IC50 and B50 for each analogous are reported in table 2.3.

Assay	CD-160130 μM	CD-150126 μM	CD-150105 μM	CD-140755 μM	CD-140797 μM	CD-140793 μM	Roflumilast μM
PDE-4A inhibition	0.021	0.870	0.011	0.200 μM	0.034	0.210	0.0008 (Hatzelmann et al., 2001)
CLL cell killing	2.220	1.570	39% maximum killing at 5 μM	3.52 (65% maximum killing)	39% maximum killing at 8 μM	13% maximum killing at 10 μM	42% maximum killing at 100 μM
hERG1 binding	1.890	1.740	19% at 5 μM	7.210	38% at 8 μM	0% at 10 μM	9% at 10 μM

Table 2.3: EC_{50} values (if available) of primary CLL (Chronic Lymphoid Leukemia) killing, IC_{50} of phosphodiesterase-4A inhibition and B_{50} of hERG binding obtained for CD-160130 and some other analogues. CLL cell killing was evaluated with CellTiter 96 Aqueous One Solution Cell Proliferation Assay kit; PDE-4 inhibition was analyzed with SPA assay and hERG1 binding was performed with [^{3}H] astemizole binding assay (see in Material and Methods).

Leukemia cells aberrantly express both the hERG1A and the hERG1B isoforms of hERG1, and particularly hERG1B, whose over-expression strongly contributes to sustain hERG1 currents in these cells (Hofmann et al, 2001) (Crociani et al, 2003); (Pillozzi et al, 2002) The main functional difference between hERG1A and hERG1B isoforms consists of the more rapid deactivation kinetics of hERG1B, which is apparent when comparing the upper (hERG1A) and the lower (hERG1B) panels in Figure 2.22. Hence, we tested the effect of CD-160130 on either hERG1A or hERG1B currents, expressed in HEK 293 cells (Figure 2.22). Currents were studied by measuring tail currents at -120 mV, after depolarizing voltage steps ranging from -70 to 0 mV and lasting 15 s (Figure 2.22, inset).
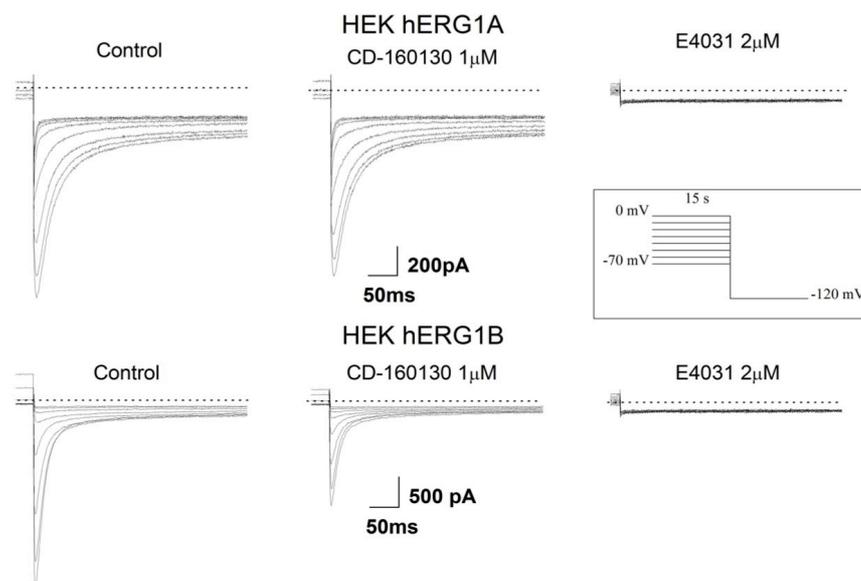

Figure 2.22. Typical hERG1A and hERG1B currents in stably transfected HEK 293 cells and the effect of the selective hERG1 inhibitor E4031 and CD-160130. The inset shows the protocol used to record the tail current; Both currents were fully blocked by 2 μM E4031, a class III antiarrhythmic drug considered the prototype of hERG1 blockers.

E4031 produced similar effects ($p > 0.05$ at both 50 nM and 100 nM; n=6) on both channel isoforms (Fig. 2.23A). On the other hand, CD-160130 was more effective in

blocking hERG1B than hERG1A (p < 0.01, at 1 µM; n=6). As shown in Fig. 2.23B, the IC$_{50}$ values for CD-160130 were approximately 13.0 ± 3.0 µM for hERG1A and 1.8 ± 0.26 µM for hERG1B. Hence, CD-160130 turned out to have an almost 10-fold higher selectivity for hERG1B. Importantly for the comparison with the antileukemic effect *in vivo* (discussed later), the difference between the effect on the two channel isoform is more pronounced at concentrations between 1 and 20 µM (i.e. the quasi-linear range of the concentration-response curve). At the maximum concentrations of CD-160130 tested, the current inhibition was removed after 258 ± 20 sec of washing (n=5). This is different from what was normally observed with E4031, whose block is notoriously difficult to fully reverse by wash-out (Faravelli et al, 1996). As a further control, we tested CD-140793: this compound produced negligible (on hERG1A) or small (on hERG1B) current inhibition, even when added at very high concentrations (50 µM) (Fig. 2.23C). Nonetheless, both CD-160130 and CD-140793 produced significantly stronger inhibition on hERG1B (p < 0.01; at 50 µM; n=6).
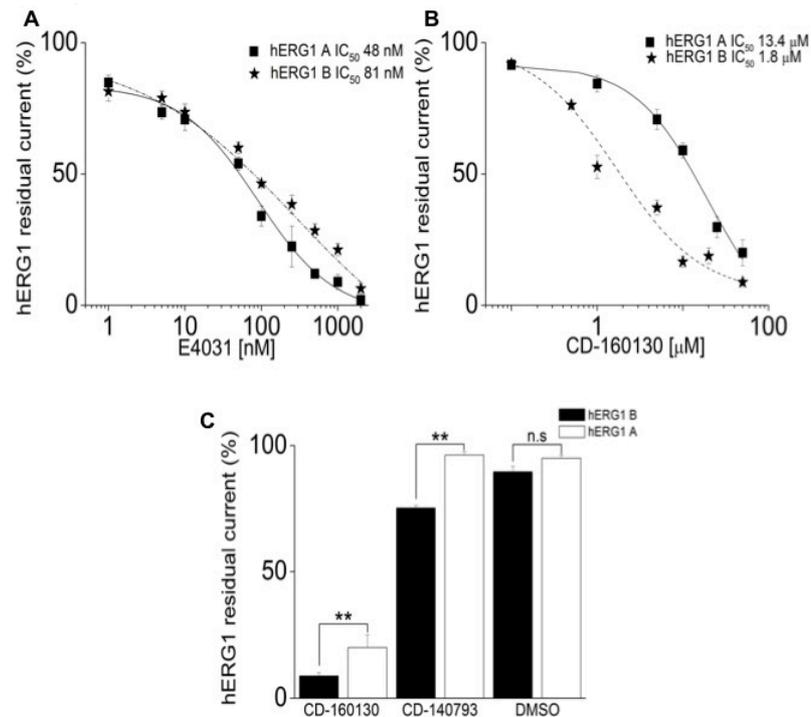
Figure 2.22. Panel A: Concentration-response curves and IC50 values obtained with E4031 on transfected HEK 293 cells. Full concentration-response relations were obtained for both E4031 and CD-160130, by measuring the percentage residual tail currents at different drug concentrations, after a 15-s pulse at 0 mV. At both 50 nM and 100 nM, no significant difference was observed between the effects produced on hERG1A or hERG1B (respectively p = 0.407 and p = 0.426; n=6). **Panel B**: Concentration-response curves and IC50 obtained with CD-160130 on transfected HEK 293 cells; **Panel C**: Bars give hERG1 residual current in presence of CD-160130 (50μM), CD-140793 (50μM) and DMSO. A significant difference was found between inhibition of hERG1A and hERG1B with both compounds (p < 0.01 for CD-160130 and p < 0.01 for CD-140793; n=6) although the degree of inhibition was higher in the CD-160130 group. DMSO, utilized for the solubilization of CD-160130 and CD-140793, produced no effect on either hERG1 isoform at the maximum concentration used (1% v/v).

To further characterise the mechanism of action of CD-160130, we first tested CD-160130 and E4031 on currents sustained by the hERG1-Δ2-370 mutant, in which the entire N-terminal domain is deleted, to determine the role of this domain in the effect of CD-160130. This mutant channel shows a deactivation kinetics similar to the one observed in hERG1B. The effects produced by CD-160130 on the hERG1-Δ2-370 currents were similar to those observed on hERG1B (Figure 2.23A). Likewise, E4031 produced similar blockade on hERG1-Δ2-370, hERG1A and hERG1B (Fig. 2.23B). These data suggest that the different efficacies of CD-160130 and E4031 on the two hERG1 isoforms do not depend on the different N-terminal domains.
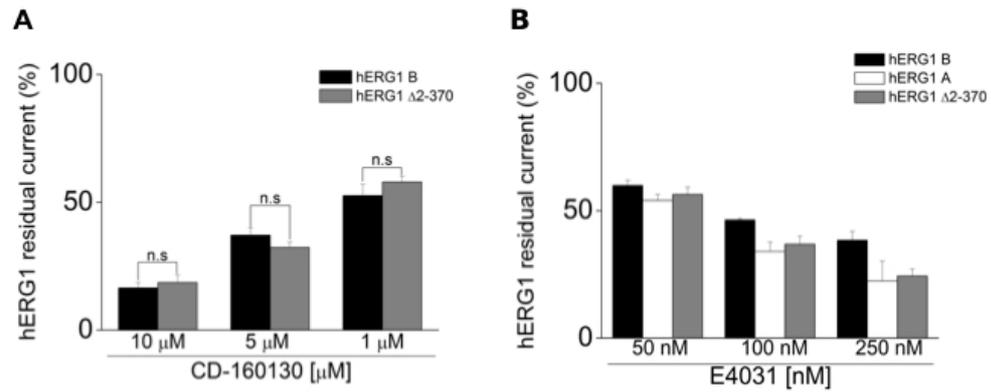
Figure 2.23. Panel A: Bars show the hERG1 residual current after addition of CD-160130 (1-5-10 μM) on hERG1 Δ2-370 and hERG1B. No significant difference, at all tested concentrations, was observed between hERG1B versus hERG1 Δ2-370 ($p > 0.05$; n=6); **Panel B**: Bars show the hERG1 residual current after addition of E4031 (50, 100, 250 nM) on hERG1 Δ2-370, hERG1A and hERG1B. No significant difference was observed between hERG1A versus hERG1 Δ2-370 ($p > 0.05$; n=6). For each drugs we choose the three concentrations with the highest difference in inhibitory level between hERG1A and hERG1B, to better highlight the effects on hERG1 Δ2-370.

We investigated whether the effect of CD-160130 was voltage-dependent. To this purpose we applied a stimulation protocol previously used to analyze the voltage-dependence of erg toxin (Gurrola et al, 1999) The blocker was applied at different conditioning potentials (between +30 and -110 mV). Next, channels were briefly (250 ms) held at +40 mV to obtain full activation, and then Vm was brought to -120 mV, to measure the hERG1 tail current (see protocol in Figure 2.24). To avoid the complete block of hERG1B currents, CD-160130 was tested at a sub-optimal concentration (5 μM). CD-160130 revealed no voltage-dependent block on either hERG1A or hERG1B currents (Figure 2.24).
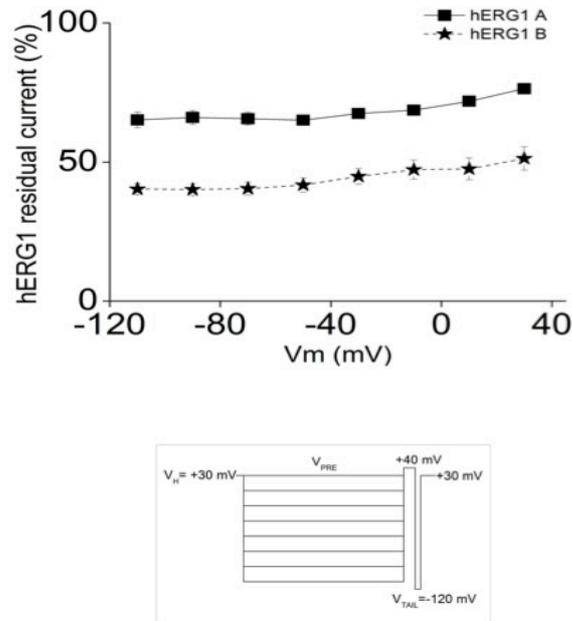
Figure 2.24. hERG1A and hERG1B residual currents after addition of 5 μM CD-160130. The following protocol (see the inset) was applied: from a holding potential of +30 mV, the cell was preconditioned for a fixed time (tPRE= 3.5 s) at different VPRE values from +30 mV to -110 mV. Then, the membrane potential was kept at +40 mV for 250 ms (for hERG1A) or for 100 ms (for hERG1B), and then at -120 mV for 150 ms. The values refer to tail currents at -120 mV.

We then studied whether CD-160130 had the same binding site on the hERG1 protein as E4031 and similar drugs, e.g. the Phe656 residue (Kamiya et al, 2006). Phe656 is located in the channel inner cavity (see Introduction for further details), and is present in both hERG1A and hERG1B. To study whether CD-160130 acts with a similar mechanism, we compared the inhibition produced by saturating concentrations of either E4031 (5 μM) or CD-160130 (100 μM) on F656A-hERG1A and wild type (wt) hERG1A channels. The Phe656Ala substitution is expected to drastically reduce the inhibitory effect of E4031. As shown in Figure 2.25A, E4031 almost abolished the wt-hERG1A currents, while producing only 25% inhibition of the F656A-hERG1A current. In contrast, CD-160130 strongly inhibited both wt-hERG1A and F656A-hERG1A (Figure 2.25B). The average inhibition observed on F656A-hERG1A was 75.5 ± 1.5 % with 100 μM CD-160130 (n=10) and 25.5 ± 1.9 % with the higher E4031 concentration (n=5) (Figure 2.25C). These results suggest that Phe656 is not part of the main binding site for CD-160130.
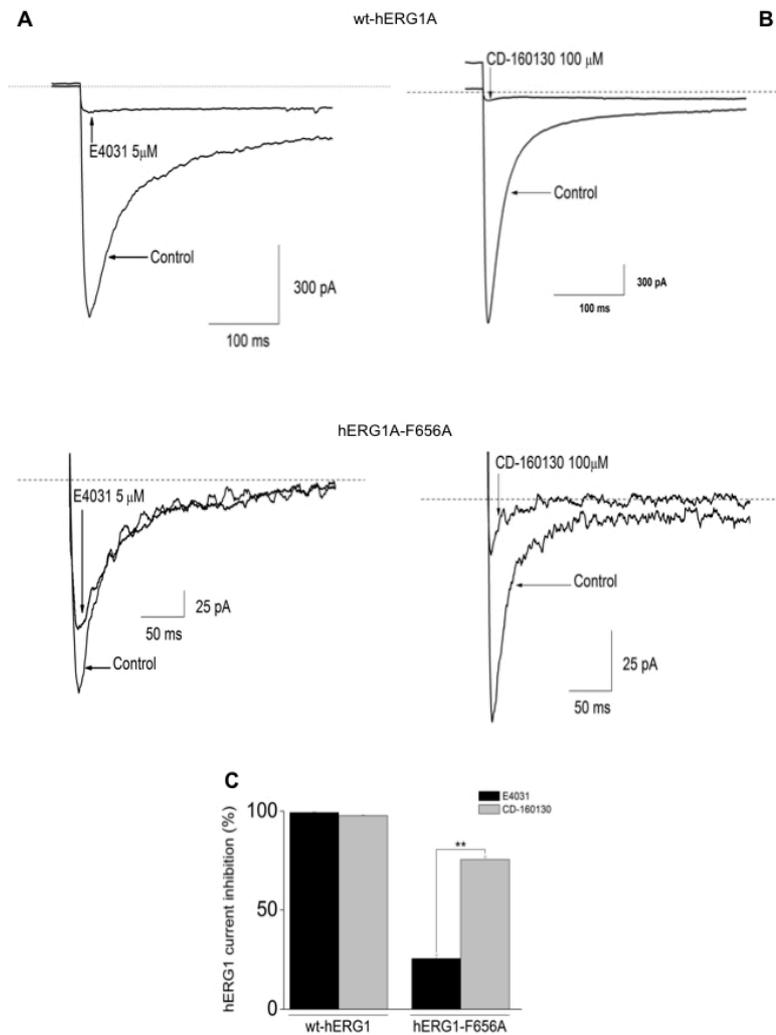
Figure 2.25 Panel A: Effect of E4031 (5 μM) and CD-160130 (100 μM) on wild type hERG1A channels transiently expressed in CHO cells; **Panel B**: Effect of E4031 (5 μM) and CD-160130 (100 μM) on mutant F656A hERG1 channels transiently expressed in CHO cells; **Panel C**: Bars give the percentage of hERG1 current inhibition with CD-160130 and E4031. A significant difference was found between the effects of E4031 and CD-160130 on hERG1-F656A current (p < 0.01; n=5 for E4031; n=10 for CD-160130).

Because the above results indicate that the blocking mechanism of CD-160130 is different from that of E4031, we studied the CD-160130 effect on the non-inactivating G628C:S631C hERG1 mutant (Jiang et al, 1999). The absence of channel inactivation enabled us to i) study the kinetics of onset of channel block and ii) compare the effects of outward and inward ion fluxes on CD-160130 potency. In these experiments, E_K was set to -30 mV, to make it practical to compare inhibition of both outward and inward

currents. Currents were elicited, from a holding potential of -80 mV, by a 120 s step to +40 mV. Next, Vm was stepped back to -80 mV, to reveal the inward tail currents. Either CD-160130 (10 μM) or E4031 (1 μM) were applied after the current had reached the steady-state at +40 mV. Typical current traces are shown in Figure 2.26A. For clarity, the tail currents at -80 mV are magnified in Figure 2.26B. In a series of representative experiments carried out in the same batch of cells, CD-160130 took about 7.4 ± 1.25 (n=6) s to start blocking hERG1 current. In contrast, the effect of E4031 had a latency of 18 ± 1.4 s (n=5). The difference between these values is statistically significant (p < 0.01; n=6). We next tested the current inhibition produced by E4031 and CD-160130 on outward (at +40 mV) and inward (at -80 mV) currents (Fig. 2.26C). For E4031, inverting the current flow by reversing the Vm polarity produced no difference in channel block (p > 0.05; n=5), whereas in the presence of CD-160130, the block on inward currents was more pronounced (55.1 ± 3.9, n=7) (p < 0.05; n=9)
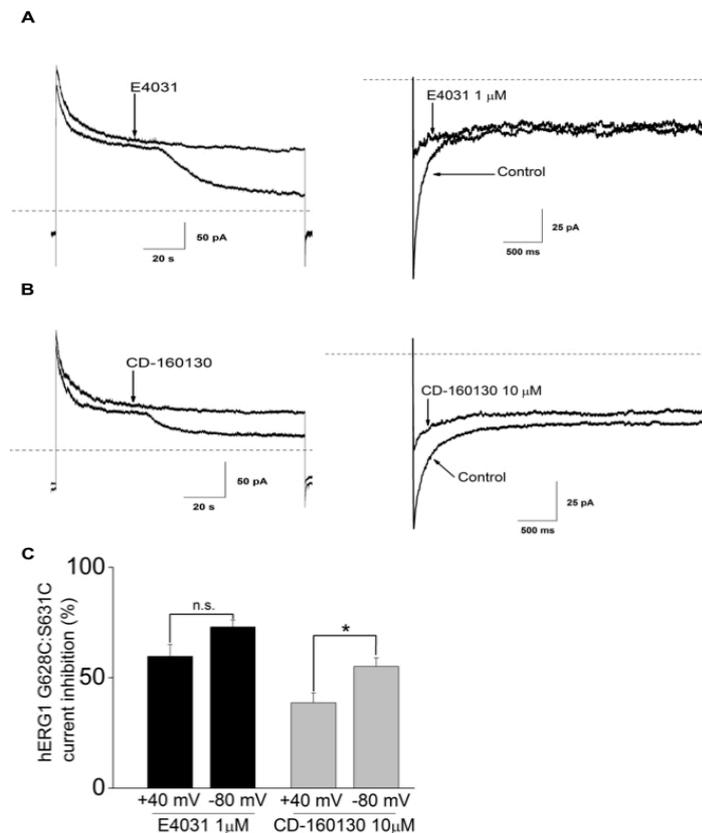
**Figure 2.26**. **Panel A-B:** currents elicited in the G628C:S631C hERG mutant and effects of 1 μM E4031 and 10 μM CD-160130; **Panel C**: hERG1 current inhibition by E4031 and CD-160130 at the two tested potential (+40 mV and -80 mV); for E4031 the difference between the inhibition at +40 mV and -80 mV was not statistically significant (p > 0.05; n=5), while a significative difference was obtained for CD-160130 (p < 0.05; n=9).

Although the specific binding sites of CD-160130 are still unknown, these results suggest that the site of CD-160130 interaction with the channel pore may be located on the extracellular side of the selectivity filter, rather than the inner cavity where most hERG inhibitors bind.

We then verified whether CD-160130 also blocked hERG1 in leukemia cells. To this purpose, we used FLG 29.1, a human myeloid leukemia (AML) cell line whose hERG1 currents are mainly sustained by the hERG1B isoform (Crociani et al, 2003) (see the inset in Figure 2.27). As shown in Figure 2.27, the IC_{50} obtained for CD-160130 on FLG 29.1 cells (1.62 ± 0.35 μM) was very similar to that obtained on HEK 293 cells transfected with hERG1B, supporting the notion that CD-160130 presents isoform selectivity.
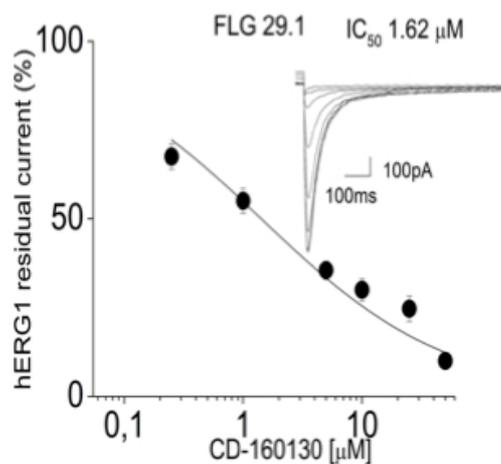
**Figure 2.27.** Concentration-response curves and IC_{50} values obtained with CD-160130 on FLG 29.1; the inset shows typical hERG1B current in FLG 29.1 cells.

Next, we investigated the effects of CD-160130 (0.1-50 μM) on FLG 29.1 cell viability, evaluated by WST-1 assay. FLG 29.1 cell viability was markedly reduced by CD-160130 at micromolar concentrations. Representative data relative to FLG 29.1 cells are shown in Figure 2.28A where the experimental data points are fitted by a Hill-type function. The effective dose (ED_{50}) obtained is 3.48 ± 0.88 μM. On the other hand, CD-140793, which does not block hERG1 currents, produced little effect on FLG 29.1 cell viability at concentrations where CD-160130 produced the highest effects (20 μM and 50 μM) (Figure 2.28B). The isoform-non selective hERG1 blocker E4031 reduced

FLG 29.1 cell viability, although with a significantly higher ED_{50} (55.7 ± 2.0 μM) (Figure 2.28C).
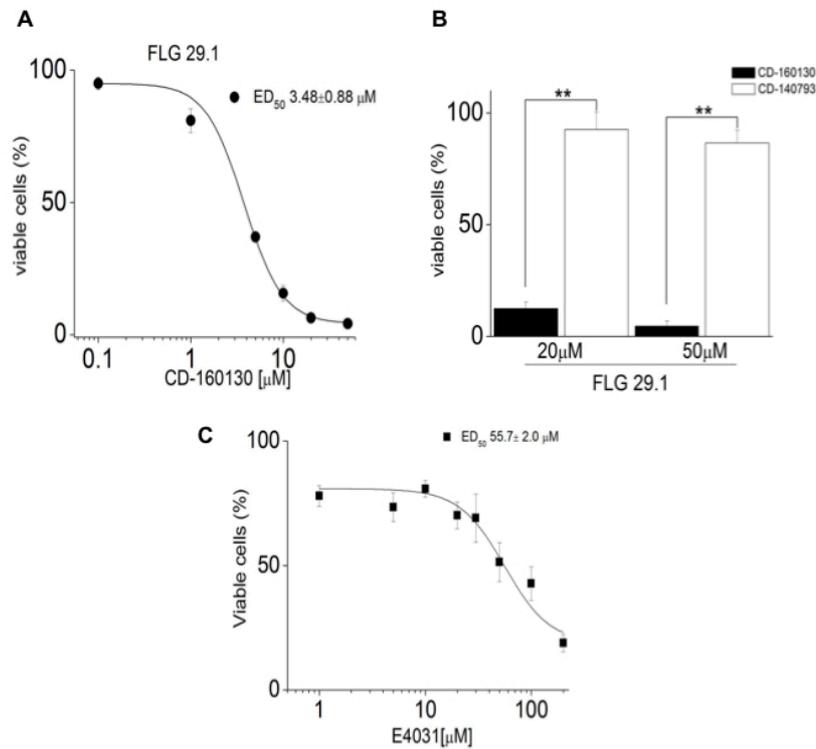

Figure 2.28. Panel A: Concentration-response curves and ED50 (Efficacy Dose 50) values obtained with WST-1 cell viability assay on FLG 29.1; **Panel B**: Bars give the results obtained with WST-1 cell viability assay of CD-160130 and CD-140793 on FLG 29.1 cells. A significant difference was found between the effects of CD-160130 and CD-140793 ($p < 0.01$ at 20 μM and $p < 0.01$ at 50 μM; n=9); **Panel C**: Concentration-response curves and ED50 values obtained with E4031 on FLG 29.1.

To investigate whether effect of CD-160130 on FLG 29.1 was related to the blocking of hERG1B currents, we tested the effects of hERG1 silencing, using small interfering (si) RNAs. Since no hERG1B-specific siRNA can be identified, we used a siRNA which encompasses a hERG1 sequence common to both hERG1A and hERG1B. FLG 29.1 were transiently transfected with anti-hERG1 siRNAs (and scramble siRNAs as a control) and current density was measured at different times from transfection: a significant reduction of hERG1 current density was observed in anti-hERG1 siRNA-treated cells, compared to scramble siRNA-transfected cells starting from 24 hours from transfection ($p < 0.001$ at both 24 hours, n=15, and 48 hours, n=23). The decrease in hERG1 current was maintained at least until 72 hours (Figure 2.29A). We then tested

the effects of CD-160130 (0.1-50 μM) on the viability of FLG 29.1 cells treated with either anti-hERG1 or scramble siRNAs. The ED_{50} of CD-160130 on anti-hERG1 siRNA-treated cells was significantly higher compared to that obtained in scramble siRNA-treated cells (Figure 2.29B). In particular, a significant difference in the percentage of viable cells could be detected at 10 μM concentration of CD-160130 (p< 0.05, n=9).
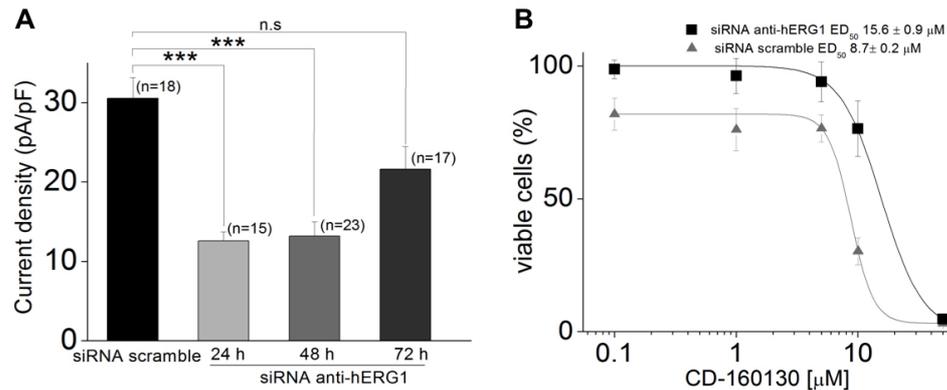

Figure 2.29 Panel A: Bars give the results of the siRNA mediated silencing of hERG1 channel obtained in FLG 29.1 at 24, 48 and 72 hours after transfection. A significant difference in current density (pA/pF) was found between siRNA scramble transfected cells and siRNA anti hERG1 at both 24 and 48 hours (p < 0.001 at 24 h, p < 0.001 at 48 h). **Panel B:** Concentration-response curves and ED50 values obtained with CD-160130 on siRNA anti-hERG1 (black) and siRNA scramble (grey) transfected FLG 29.1 cells. A significant difference was found between the effects of CD-160130 at 10 μM (p < 0.05, n=9)

Furthermore, we tested the effect of CD-160130 on leukaemia cell viability on different cell lines as well as on primary samples (both acute myeloid (AML) and acute lymphoid (ALL)). Results are summarised in Table 2.4. CD-160130 turned out to exert a cytotoxic effect at micromolar concentration toward all the tested cell lines and in almost all the primary samples; Conversely, CD-160130 did not affect cell viability of either normal peripheral blood mononuclear cells (PBMCs) or Epstein Barr Virus (EBV)-infected B lymphocytes (Table 2.4). Interestingly, CD-160130 seems to be more effective in high hERG1B expressing cell lines and primary samples.

PS / Cell line	FAB (Immunophenotype)	Cytogenetics	*h1B* gene expression (arbitrary units)	Mean ED$_{50}$ (±SEM) of CD-160130
Myeloid primary samples and cell lines				
AML-1	AML - M4 (CD13+, CD33+, CD14+, CD11b+, CD34+)	UNK	0.92 (h1A: 12.20)	20% maximum killing at 50 μM
AML-2	AML - M1 (CD13+, CD34+, HLDRA+)	Complex	68.10 (h1A: 18)	40.4 ± 11.2 μM
KG-1	AML - M6 (CD34+, CD15+, Cd13+, HLA A30+, A31+, B35+)	Complex	0.62 (h1A: 24.76)	7.6 ± 0.55 μM
FLG 29.1	AML - M5 (CD9+, CD13+, CD32+, CD42b+, CD51+, CD54+, CD44+, CD61+, CD45+, CD31+)	polyploidy, 3p+	3413 (h1A: 1086)	3.48 ± 0.88 μM
HL60	AML - M2[ref2] (CD3-, CD13+, CD14-, CD15+, CD19-, CD33+, HLA-DR-)	Pseudodiploid	94.70 (h1A: 13.70)	6.65 ± 0.26 μM
NB4	AML - M3 (CD3 -, CD4 +, CD11b -, CD13 +, CD14 -, CD15 +, CD19 -, CD33 +, CD34 -, CD38 +, HLA-DR -)	t(15;17) (q22;q11-12)	196.72 (h1A: 80.44)	7.02 ± 0.31 μM
Lymphoid primary samples and cell lines				
B-ALL-1	L2 (early B) (CD34+, CD33+, CALLA+)	t(8;14)	6.68 (h1A: 0.03)[§]	5.6 ± 1.5 μM
T-ALL-1	L2 (T) (Aberrant expression of CD34, CD117 and CD13)	UNK	5.11 (h1A: 0.76)[#]	0.6 ± 0.2 μM
REH	pro-B ALL (CD3 -, CD10 +, CD13 -, CD19 +, CD34 -, CD37 -, CD38 +, cyCD79a+, CD80 -, CD138 +, HLA-DR +, sm/cyIgG -, sm/cyIgM -, sm/cykappa -, sm/cylambda -)	t(12; 21) (p13;q22)	120 (h1A: 6.5)	6.66 ± 0.22 μM
697	pre-B ALL (CD3 -, CD10 +, CD13 -, CD19 +, CD34 -, CD37 -, CD38 +, CD80 -, HLA-DR +, sm/cyIgG -, smIgM -, cyIgM +, sm/cykappa -, sm/cylambda -)	t(1;19)	1200 (h1A:85)	3.78 ± 0.37 μM
RS	pre-B ALL - L2 (HLA DR +; CD9 +; CD24 +)	t(4;11) (q21; q23) and i(7q)	0.16 (h1A: 0.005)	7.0 ± 0.2 μM
Normal cells				
PBMNC	-	-	Normal	0 (h1A: 0)	37% maximum killing at 10 μM
EBV-infected B lymphocytes	-	-	Normal	0 (h1A: 0)	17% maximum killing at 10 μM

Table 2.4 Mean ED50 values and SEM obtained with CD-160130 on both myeloid and lymphoid primary samples as well as in a panel of leukaemic cell lines (AML, ALL and CLL). For each primary sample and cell line the French-American-British (FAB) classification, the immunophenotype and the cytogenetics (if available) are also reported, along with hERG1B and hERG1A genes expression. Data gathered with CD-160130 on two normal cell lines (PBMNC and EBV-infected B-lymphocytes) were also reported, together with the hERG1B and hERG1A transcripts expression.

To further investigated this evidence, we analysed, by Western Blot, the hERG1B protein expression in four of the tested cell lines, both AML and ALL. For each cell line, the ED_{50} value obtained with CD-160130 is reported along with the corresponding expression of the hERG1B isoform (Figure 2.30). Consistent with the hypothesis that CD-160130 exerts its effects on viability mainly by targeting hERG1B, the ED_{50} values inversely correlated with the hERG1B protein expression.
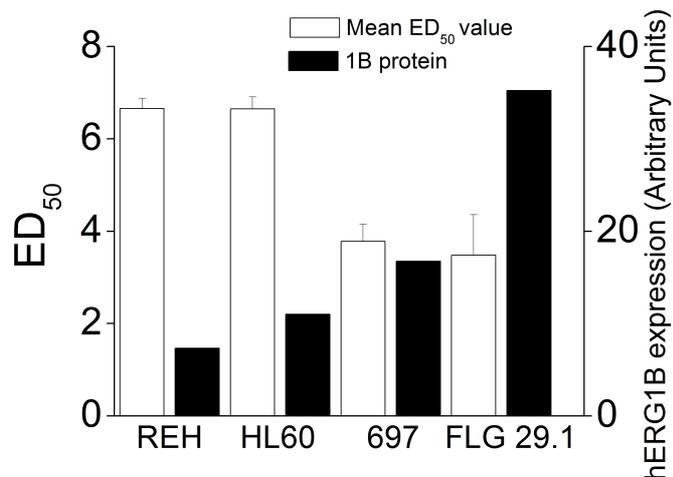

Figure 2.30. Bars report the mean ED_{50} values and the hERG1B expression level on four leukemia cell lines. The mean intensity of the bands for hERG1B protein is reported as arbitrary units and is normalised to the intensity of the bands that corresponds to the α-tubulin protein.

Finally, we evaluated whether CD-160130 had an inhibitory effect on leukaemia cell proliferation, measured as the total number of viable, Trypan blue negative cells at different times of incubation, to better define the time course of the effects on leukaemia cell growth. In this set of experiments FLG 29.1, HL60, REH and 697 were used as a model, and four CD-160130 concentrations (0.1, 1, 5 and 10 μM) were tested. After a single treatment, concentrations above 5 μM completely abolished cell proliferation in

all the tested cell lines (Figure 2.31A). At lower concentrations, after an initial block (lasting about 24 hours), both FLG and HL60 cells started again to proliferate, whilst a more pronounced cytostatic effect of CD-160130 was evident for both REH and 697 cells.
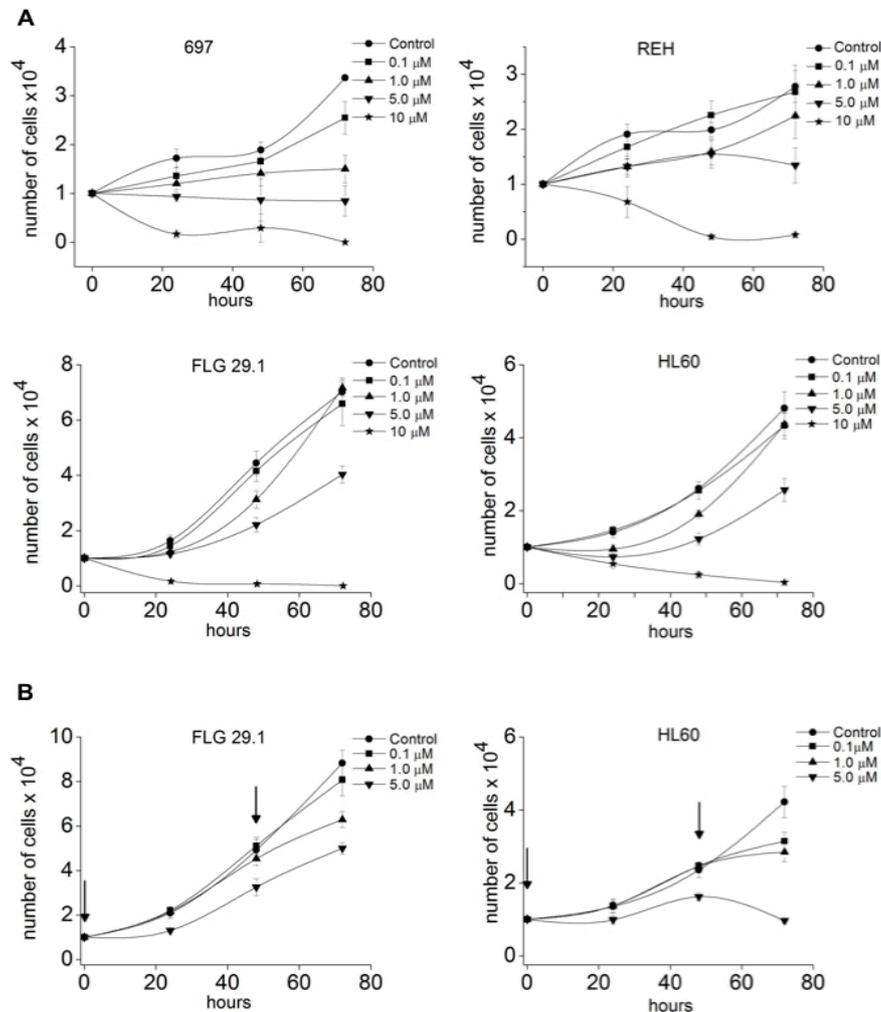
Figure 2.31. Panel A: Effects of CD-160130 on FLG 29.1, HL60, 697 and REH proliferation, after a single treatment at time 0; **Panel B**: Effects of CD-160130 on HL60 proliferation, after a a double treatment at time 0 and after 48 given as number of Trypan Blue negative cells;

For these reasons, another set of experiments was performed, in which CD-160130 was re-added to both FLG 29.1 and HL60 cells after 48 hours of incubation. We found that this treatment schedule produce a slowdown of FLG 29.1 cell proliferation, whilst it almost abolished HL60 cells proliferation (Figure 2.31B).

We then investigated the effects of a 24 hours treatment with CD-160130 on apoptosis, analysed through the Annexin-V-FLUOS Staining Kit, testing a concentration range (1.75 to 14 μM) which encompasses the ED50 value (3.5 μM), as well as half, double and four times the ED50. The mean percentage numbers of early apoptotic (annexin V positive and propidium iodide negative) FLG 29.1 cells are summarised in Figure 2.32. CD-160130 significantly induced cell apoptosis at concentrations above 5 μM (control versus CD-160130 7 μM p < 0.01; n=9).
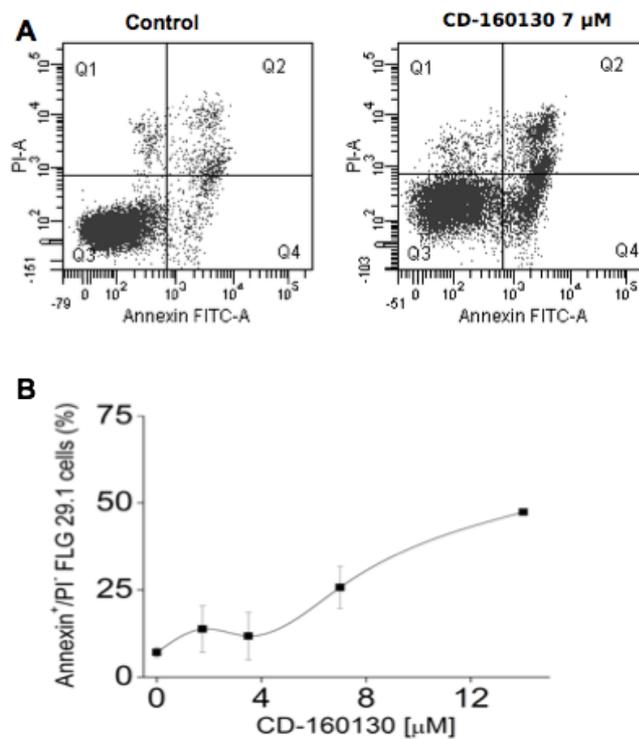
Figure 2.32 Panel A: Representative Dot Blots obtained with FLG 29.1 treated with CD-160130. A clear increase in the number of apoptotic cells (both early and late apoptosis) is evident in cells exposed to 7 μM CD-160130, as compared to control untreated cells (left panel). **Panel B**: mean percentage of FLG 29.1 early apoptotic (Annexin+/PI-) cells at different concentrations of CD-160130, after 24 hours treatment. A significant difference in percentage of early apoptotic cells was found between control and CD-160130 7 μM (p < 0.01; n=9).

As discussed in the Introduction (see "hERG channels and cancer" section), it has been demonstrated that hERG1 channels plays a critical role in the development of chemotherapy resistance in acute lymphoblastic leukaemia (ALL). A macromolecular complex between hERG1 channels, β1 integrins and CXCR4 was found to be expressed

on the plasma membrane of leukaemia cells and to be activated by culture of leukaemic cells with MSCs. The activation of such complex modulates downstream signalling pathways, including ILK, ERK1/2 MAP kinases and Akt, which in turn produces anti-apoptotic effects thus counteracting the effects of classical chemotherapeutic drugs such as doxorubicin, prednisone or methotrexate (Pillozzi et al, 2011). The importance of hERG1 channels in this process is further reinforced by the demonstration that hERG1 specific blockers, such as E-4031, WAY and erythromycin, resulted in a reduction of the protective effect of MSCs and, more important, in an enhancement of the effect of chemotherapeutic drugs (Pillozzi et al, 2011).

We thus tested the effect of CD-160130 (5 μM) in the same experimental approach. Both leukaemic cell lines (FLG, HL60, NB4, 697 and REH) and primary samples (either ALL or AML) were tested. In primary samples, hERG1 expression was evaluated by flow cytometry, using an anti-hERG1 monoclonal antibody (Lastraioli et al., 2004) and is reported as Mean Intensity of Fluorescence (MFI).

CD-160130 induced leukaemia cell apoptosis, both when tested on suspended cells and on cells cultured onto MSCs. As expected, MSCs protected leukaemia cells from the apoptosis induced by chemotherapeutic drugs, as well as from apoptosis induced by CD-160130, although at a lesser extent. Interestingly, CD-160130 potentiated the pro-apoptotic effect of chemotherapeutic drugs when leukaemic cells were co-cultured with MSCs. These effects were evident in both ALL and AML cell line, as well as in ALL and AML primary samples (Figure 2.33-2.34)
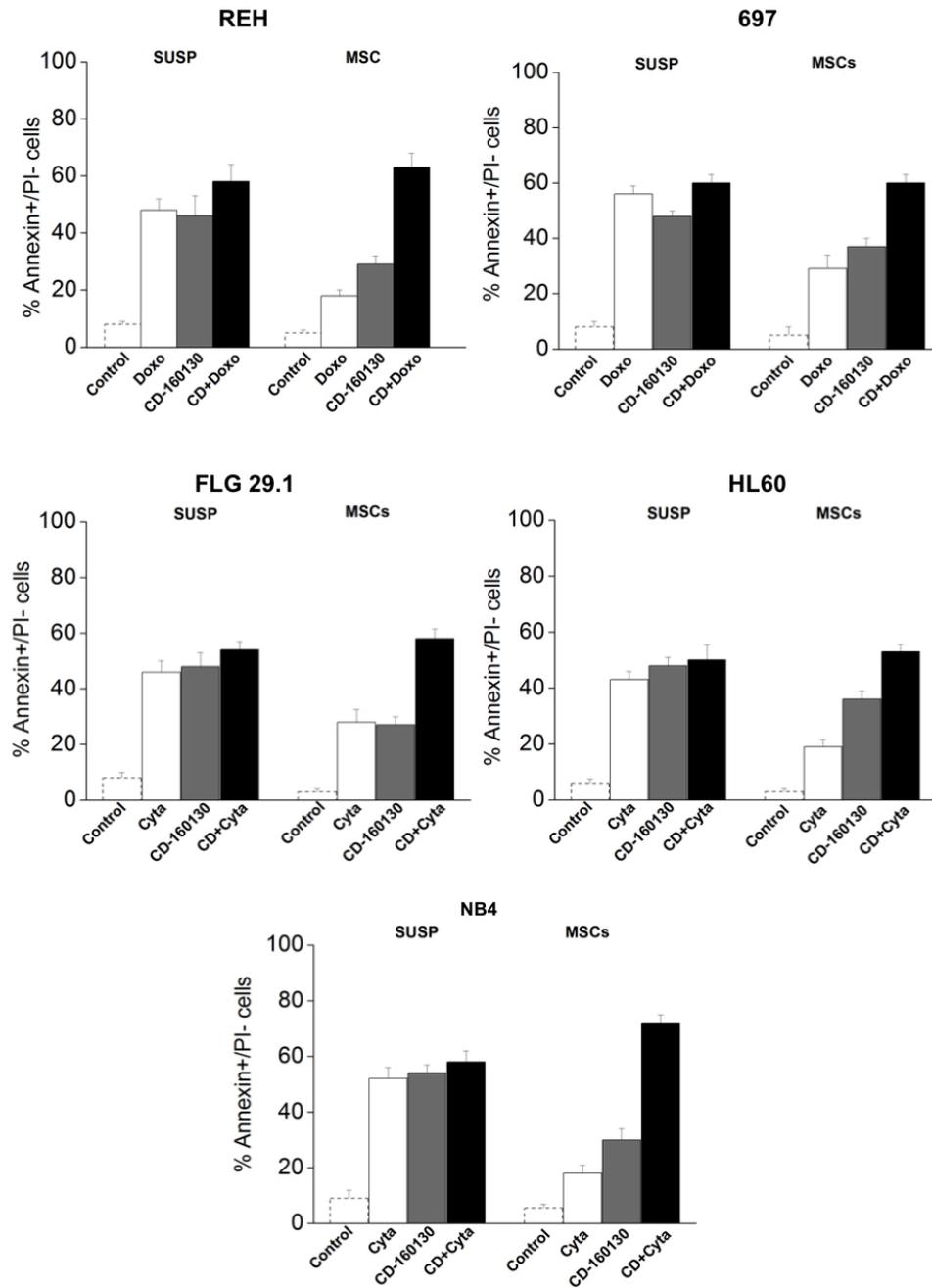
**Figure 2.33.** 697, REH, FLG 29.1, HL60 and NB4 cell line were cultured with or without MSCs (suspension) and treated with either LD$_{50}$ doses of doxorubicin (0.1 μg/mL) or cytarabine (45 nM) and CD-160130 (5μM) for 48 hours. The effects of the treatment were evaluated on early apoptosis (Annexin +/ Propidium Iodide - cells). The values of the untreated controls are reported as dotted bars in each graph.
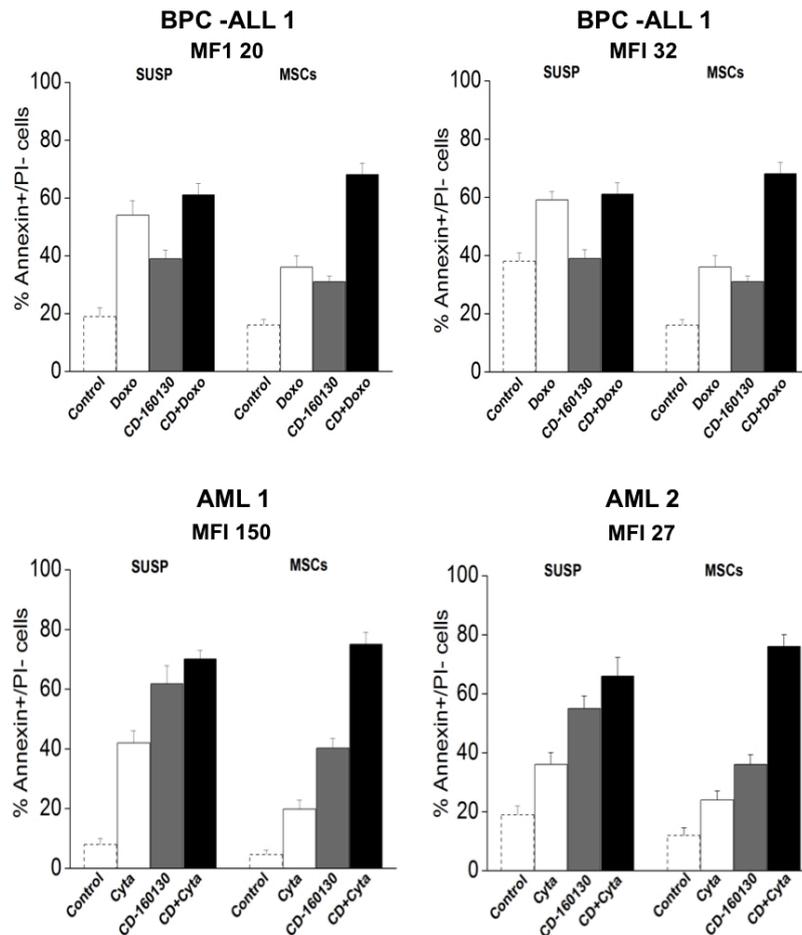
Figure 2.34. Two representative BPC-ALL primary samples (top panels) and two representative AML primary samples were cultured with or without MSCs (suspension) and treated with LD_{50} doses of either doxorubicin (0.1 μg/mL), cytarabine (45 nM) or CD-160130 for 48 hours. hERG1 expression in primary samples, evaluated by flow cytometry using the anti-hERG1 antibody, is reported as Mean Intensity of Fluorescence (MFI). BCP-ALL1 MFI= 20; BCP-ALL2 MFI= 32. AML1 MFI=150 AML2 MFI=27.

Using the same experimental model, we also tested whether CD-160130 has any effect on the signalling pathways, triggered by MSCs co-culture, previously described in both ALL and AML (Tabe et al, 2007) (Pillozzi et al, 2011). Indeed, MSCs are able to promote growth, survival and drug resistance of leukaemic cell, by providing cytokines and cell contact-mediate signals (Konopleva et al, 2009). In particular we focus our attention on the Akt - GSK3β pathway, which is modulated by the integrin ligation through the action of the integrin-linked kinase (ILK) and whose activation promotes survival of leukaemic cells (Tabe et al, 2007), as well as on the ERK1/2 and STAT 3 pathways, which in turn mediates the anti-apoptotic effect of MSCs (Konopleva et al, 2009). For these experiments we tested three cell lines, NB4, FLG 29.1 (AML) and 697

(ALL). Cells were seeded on MSCs and incubated with or without CD-160130 for different time (30-60 and 180 minutes). Representative Western Blot are shown in Figure 2.35. As summarised in the time curses in Figure 2.36, ERK1/2 phosphorylation turned out to be significantly inhibited by the addition of CD-160130 in all the tested cell lines at different time: in both 697 and NB4 cells it is clearly visible a reduction of ERK phosphorylation after 180 minutes, while in FLG 29.1 it reached a significant difference at 60 minutes. Both Akt and GSK3β phosphorylation are in turn modulated by CD-160130 treatment only in 697 cells: CD-160130 addition significantly inhibited Akt phosphorylation at both 60 and 180 minutes and GSK3β phosphorylation after 30 and 60 minutes. Conversely, in NB4 and FLG 29.1 cells neither Akt nor GSK3β phosphorylation resulted to be significantly modulated by CD-160130 treatment. We also evaluated the effects of CD-160130 treatment on the phosphorylation of STAT3 protein: STAT3 protein resulted to be not phosphorylated by co-culture with MSCs in 697 cells, while in both NB4 and FLG 29.1 we observed an increase in STAT3 phosphorylation after 180 minutes. CD-160130 treatment significantly reduced STAT3 phosphorylation only in NB4 cells.
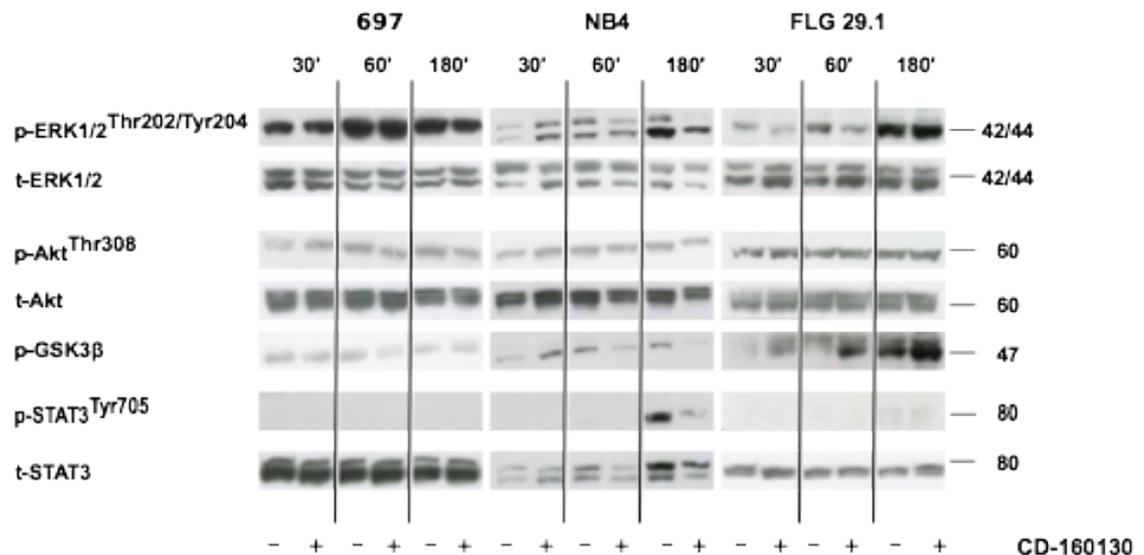
Figure 2.35. Western blot analysis of the protein levels of p-GSK3α/β[Ser9/21], p-Akt[Ser473], p-ERK1/2[Thr202/Tyr204], p-STAT3[Tyr705] in 697 cells, NB4 and FLG 29.1 cells after coculture for 30 minutes, 60 minutes and 180 minutes with MSCs in the absence or presence of CD-160130. The membrane were then reprobed with an anti-ERK1/2 or anti-Akt antibody and anti-STAT3 antibody. Experiments shown are representative of at least two independent experiments.
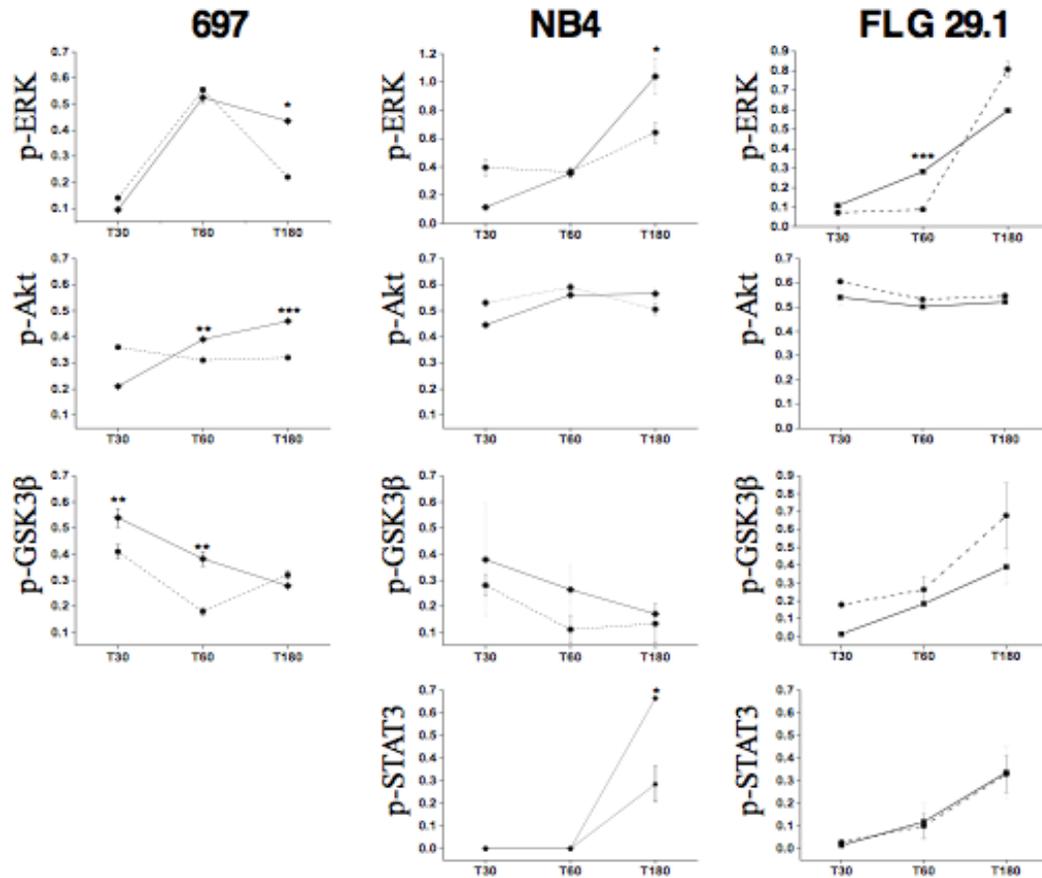
Figure 2.36. Time course analysis of the protein levels of p-GSK3α/β$^{Ser9/21}$, p-Akt^{Ser473}, p-ERK1/2$^{Thr202/Tyr204}$, p-STAT3^{Tyr705} in 697 cells, NB4 and FLG 29.1 cells after coculture for 30 minutes, 60 minutes and 180 minutes with MSCs in the absence (straight lines) or in the presence (dashed lines) of CD-160130. Experiments shown are the mean of at least two independent experiments. *** p< 0.001, ** p< 0.01, * p< 0.05. Values in Y-axis are reported as ratio between phosphorylated and total protein.

To demonstrate that the effects of CD-160130 on cell signalling were related to its inhibition of hERG1B currents, we analysed FLG 29.1 cells treated with hERG1 siRNAs, as in Figure 2.29. hERG1 silencing produced a significant decrease of ERK 1/2 phosphorylation, after 60 minutes, as compared to siRNA scramble transfected cells. Moreover, the addition of CD-160130 to hERG1-silenced FLG 29.1 cells did not produce any further effect on cell signalling (Figure 2.37).
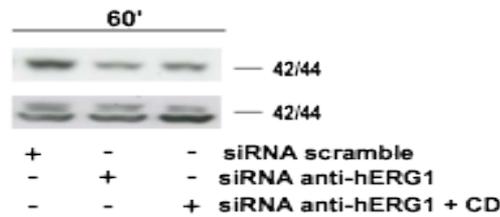
Figure 2.37. Western blot analysis of the protein levels of p-ERK1/2$^{Thr202/Tyr204}$ in siRNA transfected FLG 29.1 cells after coculture for 60 minutes with MSCs in the absence or presence of CD-160130. The membrane were then reprobed with an anti-ERK1/2 antibody.

On the whole, results gathered on the signalling pathways seem to suggest that the pro-apoptotic effects of CD-160130 treatment can be traced back to the reduction of both ERK1/2 and Akt phosphorylation in 697 cells, to the dephosphorylation of only ERK1/2 in FLG 29.1 and to reduction of both ERK1/2 and STAT3 phosphorylation in NB4 cells. GSK3β was dephosphorylated by CD-160130 in 697 and NB4 cells, while was hyperphosphorylated in FLG 29.1 cells. This suggests that GSK3β triggers different mechanisms to induce cellular apoptosis, in the different cell lines (Beurel & Jope, 2006). We also demonstrated that the effects of CD-160130 on leukaemic cell signalling are mediated by the inhibition of hERG1 channels.

Finally, we evaluated the efficacy of CD-160130 on a preclinical leukemia model, consisting of SCID mice injected intraperitoneally (i.p.) with human leukemia cells (HL60) transfected with the firefly luciferase gene (HL60-luc2 cells). HL60-luc2 cells are easily traceable *in vivo* through Photon Imager acquisition (see Methods section). Mice were monitored weekly and the luciferase activity signal was measured as counts per minutes (CPM). Two different CD-160130 doses (1 mg/Kg and 10 mg/Kg) were tested; the drug was administered orally by daily gavage administration, starting from day 5 (e.g. when leukemia cells started to engraft in the mice). This administration route was adopted based on previous experiments in Wistar rats showing that CD-160130 reached a well detectable plasma concentration, with a maximum peak after 4 hours after a single p.o. dose (50 mg/kg). The schedule (e.g. daily) was determined taking into account both the biodistribution results, which showed a half-life of about 30.9 hours (Figure 2.37) and the data of CD-160130 re-addiction reported in Figure 2.31.
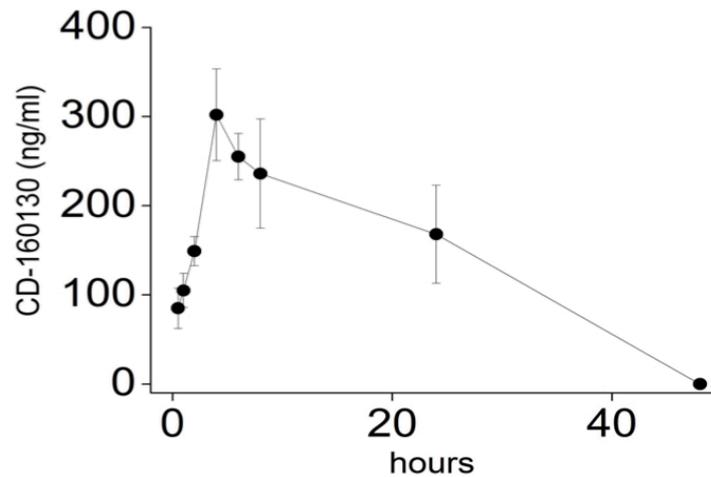
Figure 2.37. CD-160130 distribution. Pharmacokinetics of CD-160130 (ng/ml) analyzed in Wistar rats' plasma after a single oral administration (50 mg/kg). Blood samples were collected at different time point, (n=3) and analyzed by HPLC (see Materials and Methods).

The effects of CD-160130 were compared with those observed in control mice (treated with PBS) and mice treated with the chemotherapeutic drug cytarabine used at a recognised therapeutic dose (6.25mg/kg i.p.). Figure 2.38B shows that CD-160130 treatment effectively reduced the leukaemia burden, in a dose dependent manner. In particular, at 10 mg/kg, the leukaemia disease progression (as documented in panel A pictures in Figure 2.38) was comparable to, or even slower than, that occurring in the mice group treated with cytarabine. Moreover, mice survival was strongly affected by CD-160130 treatment (at 10 mg/kg), with survival times longer than those obtained with cytarabine (Figure 2.38C).
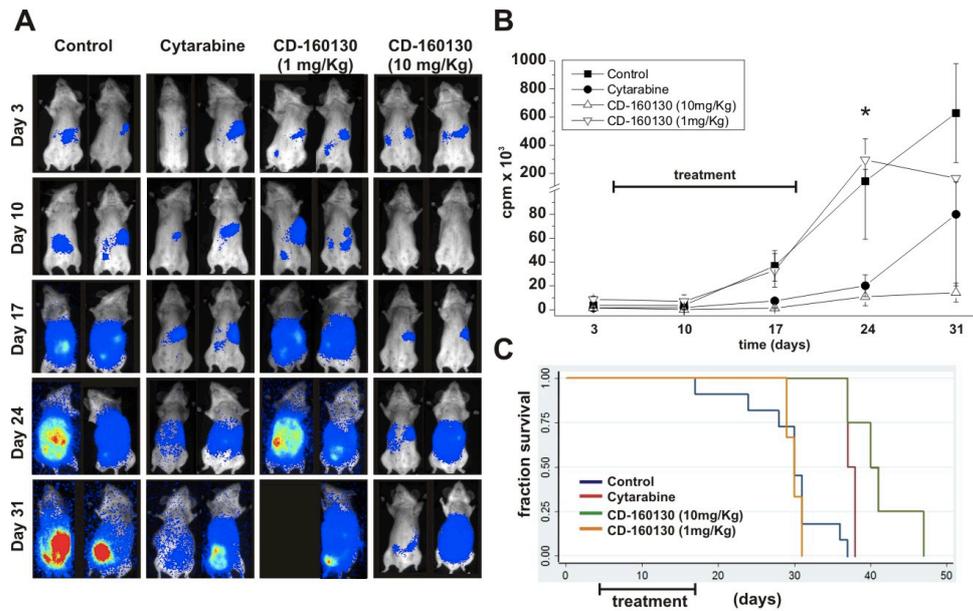
Figure 2.38. **Panel A**: SCID mice were injected with HL60-luc2 cell line (5x106 cells i.p.). Starting from day 5, animals were treated daily for fourteen consecutive days with Ora-Plus® (Control, n=9), cytarabine 6.25 mg/Kg, n=4; CD-160130 1 mg/Kg, n=3; CD-160130 10 mg/Kg, n=4. Images were acquired with Photo Acquisition software (Biospace Lab, Paris, France) and processed with M3 Vision software (Biospace Lab). **Panel B**: Cpm as in A, reported as time scale. At day 24, the signal relative to CD-160130 group was significantly reduced from the controls (p<0.05). **Panel C**: Survival curves of each experimental group, estimated by Kaplan and Meier analysis.

One of the major setback for considering hERG1 as a therapeutic target in oncology is the cardiac side effects that many hERG1 blockers exert (see Introduction, "hERG as an anti-target" section). Such effects mainly consist of a lengthening of the cardiac action potential (cAP), which can resulted in the lengthening of the QT interval. Therefore, we tested the QT liability of CD-160130, by measuring its effects on the cAP stimulated in acutely isolated left ventricular guinea pig cardiomyocytes recorded at physiologically relevant temperatures. Guinea-pig myocytes were chosen because (unlike smaller rodent animal models) they exhibit the depolarised and long duration cAP plateau, and heavy reliance on delayed rectifier potassium currents that are features repolarisation of human cAPs. CD-160130 failed to reveal a lengthening of Action Potential Duration (Figure 2.39A). In particular, 1 μM CD-160130 shortened the APD_{90} (i.e. the duration of action potential at 90% repolarisation) by less than 1 ms (-0.8 ± 2.3 ms, n=6), while 10 μM CD-160130 lengthened the APD_{90} by 2.7 ± 7.4 ms (n=7).

We also evaluated whether CD-160130 displayed any bone marrow toxicity, testing the effect of the compound on colony formation from hematopoietic stem cells isolated from the bone marrow of three healthy donors, measuring the number of colony forming units (CFU). As shown in Figure 2.39B, CD-160130 did not affect the number of CFUs (nor the percentage of different CFUs), at 5 μM, while it only produced a weak, not significant, reduction in the overall number of colonies at 10 μM.
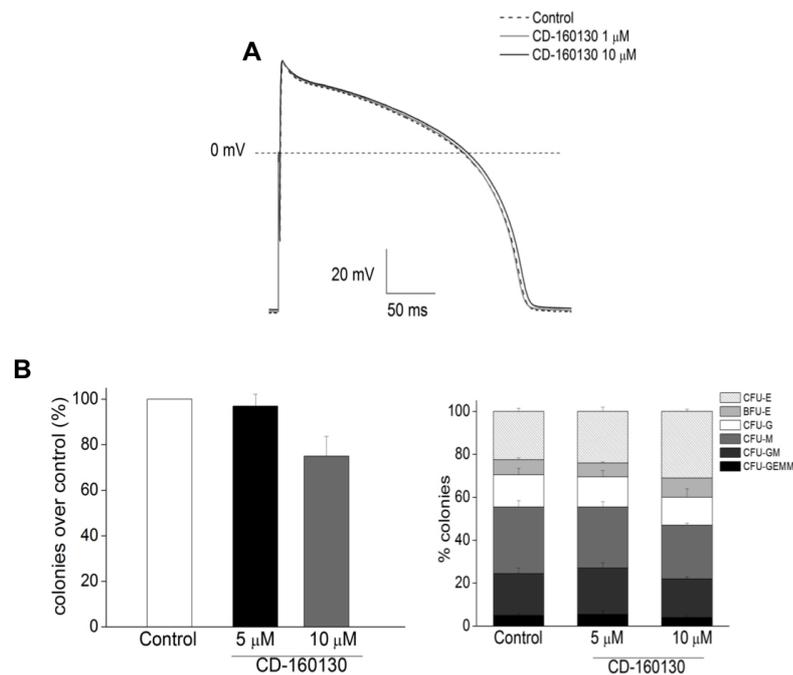
Figure 2.39. Panel A: Representative action potentials (APs) elicited in isolated ventricular cardiomyocytes of guinea pig, in the presence or in the absence of CD-160130 1μM and CD-160130 10 μM. Under all conditions, 20 APs were averaged and used to measure the APD90 values. **Panel B (upper)**: Bars give the results of the overall colonies number obtained with clonogenic assay of three samples of healthy bone marrow treated with two different concentration of CD-160130 (5μM and 10μM). No significant different was found between the control and CD-160130 at both concentrations. **Panel B (bottom)**: Bars give the results of the effect of CD-160130 on Colony forming units (CFU-GEMM, CFU-GM, CFU-G, CFU-M, CFU-E) and Burst forming units (BFU-E). No significant difference was found on CFU-E (p= 0.056) or CFU-M (p= 0.27) between control and CD-160130 10μM.

Overall data gathered with CD-160130 demonstrated that this compound behave has a hERG1 blocker, and in particular it displays almost 10-fold higher selectivity for hERG1B isoform, a selectivity also maintained in hERG1B expressing leukaemia cells FGL 29.1. Moreover, CD-160130 exert a cytotoxic effect on both primary samples and cell lines, either acute myeloid and acute lymphoid, and turned out to impair leukaemic cell proliferation *in vitro,* by inducing cellular apoptosis. The induction of apoptosis can be tracked back, as demonstrated by signalling experiments, to the inhibition of Akt, ERK1/2 and STAT3 phosphorylation by CD-160130, although with time courses and overall effects which depended on the cell line examined. Furthermore, in an "*in vitro* model" of chemoresistance CD-160130 turned out to potentiate the pro-apoptotic effect of chemotherapeutic drugs when leukaemic cells were co-cultured with MSCs. These results further confirm and strengthen the crucial role of hERG1 channels in the hallmarks of cancer cells, and in particular in "sustaining proliferative signals" and "resisting cell death" (see Introduction), thus suggesting a rationale for targeting hERG1 channels in cancer.

As stated in the introduction (see "hERG1 as a target in oncological diseases: a needed balance between therapeutical and side effects") some different strategies have been proposed to circumvent the problems that therapeutic use of hERG1 blockers may cause. Our aim to circumvent the serious cardiac side effects, was specifically targeting the hERG1B isoform, which prevails in leukemias. Our results indicate that, in principle, CD-160130, by selectively blocking the hERG1B channels, might be a promising tool for the treatment of leukemias.

From a more biophysical point of view CD-160130 displayed blocking features considerably different from those shown by classical hERG1 blockers, such as the type III antiarrhythmics. In fact, (i) CD-160130 inhibited hERG1B (i.e. the "tumour" hERG1 isoform) with a 10-fold higher potency, compared to hERG1A, and (ii) did not bind the same residue as E4031, namely Phe656, located in the channel inner cavity. Furthermore, when compared to E4031, CD-160130 (iii) was considerably quicker in producing hERG1 current block, (iv) its effect was promptly reversible on washout, thus preventing the use-dependent block, and (v) the blockade was more pronounced on inward currents. Regardless of the detailed blocking mechanism, the CD-160130 properties appear to make it particularly suitable to target hERG1 currents in leukemias,

because these cells preferentially express the hERG1B isoform (Crociani et al, 2003) (Pillozzi et al, 2007). Moreover, compared to cardiac cells, leukemia cells express higher hERG1 steady state currents because of their stable depolarised resting V_m (Schonherr et al, 1999). The high expression of hERG1B in leukemias could further enhance this effect by increasing the fraction of heteromeric hERG1A/hERG1B currents, which are known to be larger than hERG1A currents (Sale et al, 2008). The fact that a significant fraction of the channels should be in the open state at rest in leukemias should facilitate cumulative channel block at low drug concentrations.

These results are further reinforced by the demonstration that antileukemic effect of CD-160130 also occurs *in vivo* in an AML xenograft mouse model. This action is evident when the drug is administered daily at 10 mg/kg, whereas it disappears at 1 mg/kg. Taking into account the biodistribution data obtained in the rat, the plasma concentration after 50 mg/kg administration should be around 1 μM and thus the range of effective dose concentration in rodents should be between 20 and 200 nM. The ratio between these values and the drug's IC_{50} for hERG1A *in vitro* (13.4 μM) turns out to be far higher than 30, a threshold suggested by Redfern (Redfern et al, 2003) to be a safety factor to avoid cardiotoxicity with hERG1 blockers.

Finally, to fully ruled out a possible cardiac side effect, we demonstrated that CD-16130, even at concentrations in the range of those found to be effective in killing leukaemia cells *in vitro* (1 and 10 μM), did not lengthen the APD_{90} of guinea pig cardiomyocytes. This result is relevant for translation in the human setting, since the guinea pig cardiac AP has properties comparable to those observed in human cells and is currently considered an effective early cardiovascular de-risking and lead optimisation model (Morissette et al, 2013).

CONCLUSIONS

A growing body of evidences indicated a crucial role of ion channels in the hallmarks of cancer (Prevarskaya et al, 2010), thus suggesting a rationale for targeting them in anticancer therapies. Among these channels, hERG1 turned out to be aberrantly expressed in numerous human cancers (Arcangeli et al, 2009) and to regulate several aspects of cancer cell behaviour (D'Amico et al, 2013). In the first section of this thesis we provided some evidences concerning the importance of hERG1 channels in colorectal cancer, showing that hERG1 channels are activated by β1 integrin activation, being the first step of a signalling cascade that sustains angiogenesis and progression; furthermore, while looking for a strategy to overcome chemotherapy resistance to cisplatin treatment, we demonstrated that both hERG1 and K_{Ca} 3.1 channels can be targeted by riluzole treatment in HCT116 cells. Moreover, data gathered with dofetilide analogues and even more with CD-160130 on leukaemic cell viability, proliferation and apoptosis corroborate all the previous findings on the crucial role of hERG1 channels in cancer. For these reasons, targeting hERG1 channels could represents a very promising tool for new anticancer therapeutic approaches.

However, hERG1 is considered as an anti-target for drugs development, due to the serious cardiac side effects, including long QT syndrome and TdPs, that follow its blockade; indeed hERG1 channels plays a crucial role during cardiac action potential (cAP), being one of the major regulator of the action potential repolarisation in cardiac cells (Sanguinetti & Tristani-Firouzi, 2006). For these reasons, there is an urgent need to identify or synthesise newly hERG1 blockers, devoid of cardiotoxicity and pro-arrhythmogenic effects, to be used in cancer therapy.

To avoid cardiotoxicity, we proposed developing therapeutic strategies aimed at specifically targeting the hERG1B channels, i.e the "tumour" hERG1 isoform. To this purpose we screened, by both electrophysiological and "biological" assays, numerous different compounds, looking for specific hERG1B blockers.

Data reported in this thesis show that hERG1 (both hERG1A and hERG1B isoforms) channels can be targeted with different class of molecules, either analogues of the

classic antiarrhythmic drugs, already FDA approved antibiotics or novel compounds initially developed with other targets, such as CD-160130. A possible explanation of such surprisingly "pharmacological promiscuity" of the hERG channels is the presence of a large inner cavity with both aromatic and polar residues that can interact with a wide pharmacological range of molecules (Mitcheson, 2008). Despite this apparent complexity, which can hinder the identification of highly specific compounds, we demonstrated that drugs affinity for hERG1 channels can be dramatically modified even by small modification in the chemical structure, as clearly proved by either dofetilide analogues and CD-140793. Moreover, we showed that higher affinity for hERG1 channels, as revealed by different binding assays, does not strictly correlate with a higher blockade of hERG currents, as in the case of Dofetilide analogous D34.

The screening of such chemical different compounds as well as of different analogues also gave us valuable informations regarding the binding sites of these molecules within hERG channels, thus confirming and widening our knowledge of the crucial aminoacidic residues in hERG structure. From a more biophysical point of view, we gathered preliminary data concerning a possible open channel affinity of Dofetilide analogous D79; this evidence, if further corroborate by more biophysical analysis, may allow us to perform additional studies on its mechanism of action as well as on both *in vitro* and *in vivo* effects in different cancer models, as already done for R-roscovitine. The evidences gathered with dofetilide analogues could also represent a valuable starting point for medicinal chemistry, with the aim of developing new antiarrhythmic drugs devoid of the severe side effects reported for Dofetilide.

We provided indications that clarithromycin, a widely used antibiotic belonging to macrolides class of molecules, is, at least in our experimental conditions, slightly more effective on hERG1B channels, maintaining also its blockade ability in endogenous hERG1 expressing cell line (the FLG 29.1) with an increased potency as compared to heterologous systems. We therefore propose that clarithromycin is a promising useful adjuvant in chemotherapy treatment, by targeting the hERG1B channels. The significant reduction of the IC_{50} value obtained in the FLG 29.1 could be even more advantageous from the perspective of the use of clarithromycin as adjuvant in cancer therapy, since lowering the dose could reduce or eliminate clarithromycin's cardiac side effects.

Finally, we demonstrated that the proposed strategy of specifically targeting hERG1B channels in leukaemia was successful by using a novel pyrimido-indole compound, CD-160130. Indeed we demonstrated a significant antileukaemic effect, both *in vitro* and *in vivo,* of CD-160130 in either myeloid and lymphoid acute leukaemias, combined with pro-apoptotic effect of CD-160130 alone and in even better in combination with well known chemotherapeutic drugs. We also gathered evidences of a good bioavailability and a lack of both myelotoxicity and potential QT liability, thus suggesting a safety pharmacological profile of CD-160130. This makes CD-160130 a potential first-in-class hERG1 channel inhibitor for the treatment of leukemias, and in particular of chemotherapy resistant patients.

On the whole, data reported in this thesis provided valuable knowledge for the development of compounds with a well-defined selectivity for the different isoforms of the hERG1 channels.

REFERENCES

Afrasiabi E, Hietamaki M, Viitanen T, Sukumaran P, Bergelin N, Tornquist K (2010) Expression and significance of HERG (KCNH2) potassium channels in the regulation of MDA-MB-435S melanoma cell proliferation and migration. *Cell Signal* **22:** 57-64

Akhavan A, Atanasiu R, Shrier A (2003) Identification of a COOH-terminal segment involved in maturation and stability of human ether-a-go-go-related gene potassium channels. *The Journal of biological chemistry* **278:** 40105-40112

Al-Owais M, Bracey K, Wray D (2009) Role of intracellular domains in the function of the herg potassium channel. *European biophysics journal : EBJ* **38:** 569-576

Alessio E, Mestroni G, Bergamo A, Sava G (2004) Ruthenium antimetastatic agents. *Current topics in medicinal chemistry* **4:** 1525-1535

Andre T, de Gramont A (2004) An overview of adjuvant systemic chemotherapy for colon cancer. *Clinical colorectal cancer* **4 Suppl 1:** S22-28

Arcangeli A, Becchetti A (2010) Integrin structure and functional relation with ion channels. *Advances in experimental medicine and biology* **674:** 1-7

Arcangeli A, Bianchi L, Becchetti A, Faravelli L, Coronnello M, Mini E, Olivotto M, Wanke E (1995) A novel inward-rectifying K+ current with a cell-cycle dependence governs the resting potential of mammalian neuroblastoma cells. *The Journal of physiology* **489 (Pt 2):** 455-471

Arcangeli A, Crociani O, Lastraioli E, Masi A, Pillozzi S, Becchetti A (2009) Targeting ion channels in cancer: a novel frontier in antineoplastic therapy. *Current medicinal chemistry* **16:** 66-93

Arcangeli A, Faravelli L, Bianchi L, Rosati B, Gritti A, Vescovi A, Wanke E, Olivotto M (1996) Soluble or bound laminin elicit in human neuroblastoma cells short- or long-term potentiation of a K+ inwardly rectifying current: relevance to neuritogenesis. *Cell adhesion and communication* **4:** 369-385

Arcangeli A, Pillozzi S, Becchetti A (2012) Targeting ion channels in leukemias: a new challenge for treatment. *Current medicinal chemistry* **19:** 683-696

Arcangeli A, Romoli MR, Boni L, Gerlini G, Tofani L, Urso C, Borgognoni L (2013) High hERG1 expression in advanced melanoma. *Melanoma research* **23:** 185-190

Arcangeli A, Yuan JX (2011) American Journal of Physiology-Cell Physiology theme: ion channels and transporters in cancer. *American journal of physiology Cell physiology* **301:** C253-254

Barry NP, Sadler PJ (2013) Exploration of the medical periodic table: towards new targets. *Chemical communications (Cambridge, England)* **49:** 5106-5131

Becchetti A (2011) Ion channels and transporters in cancer. 1. Ion channels and cell proliferation in cancer. *Am J Physiol Cell Physiol* **301:** C255-265

Bell IM, Bilodeau MT (2008) The impact of I(Kr) blockade on medicinal chemistry programs. *Current topics in medicinal chemistry* **8:** 1128-1139

Bentzen BH, Bahrke S, Wu K, Larsen AP, Odening KE, Franke G, Storm vans Gravesande K, Biermann J, Peng X, Koren G, Zehender M, Bode C, Grunnet M, Brunner M (2011) Pharmacological activation of Kv11.1 in transgenic long QT-1 rabbits. *Journal of cardiovascular pharmacology* **57:** 223-230

Bergamo A, Sava G (2007) Ruthenium complexes can target determinants of tumour malignancy. *Dalton transactions (Cambridge, England : 2003)***:** 1267-1272

Bergamo A, Stocco G, Casarsa C, Cocchietto M, Alessio E, Serli B, Zorzet S, Sava G (2004) Reduction of in vivo lung metastases by dinuclear ruthenium complexes is coupled to inhibition of in vitro tumour invasion. *Int J Oncol* **24:** 373-379

Beurel E, Jope RS (2006) The paradoxical pro- and anti-apoptotic actions of GSK3 in the intrinsic and extrinsic apoptosis signaling pathways. *Progress in neurobiology* **79:** 173-189

Bianchi L, Wible B, Arcangeli A, Taglialatela M, Morra F, Castaldo P, Crociani O, Rosati B, Faravelli L, Olivotto M, Wanke E (1998) herg encodes a K+ current highly conserved in tumors of different histogenesis: a selective advantage for cancer cells? *Cancer research* **58:** 815-822

Binggeli R, Weinstein RC (1986) Membrane potentials and sodium channels: hypotheses for growth regulation and cancer formation based on changes in sodium channels and gap junctions. *J Theor Biol* **123:** 377-401

Boulikas T, Vougiouka M (2003) Cisplatin and platinum drugs at the molecular level. (Review). *Oncol Rep* **10:** 1663-1682

Cahalan MD, Chandy KG, DeCoursey TE, Gupta S (1985) A voltage-gated potassium channel in human T lymphocytes. *The Journal of physiology* **358:** 197-237

Carella AM, Beltrami G, Pica G, Carella A, Catania G (2012) Clarithromycin potentiates tyrosine kinase inhibitor treatment in patients with resistant chronic myeloid leukemia. *Leukemia & lymphoma* **53:** 1409-1411

Carmeliet E (1992) Voltage- and time-dependent block of the delayed K+ current in cardiac myocytes by dofetilide. *The Journal of pharmacology and experimental therapeutics* **262:** 809-817

Casis O, Olesen SP, Sanguinetti MC (2006) Mechanism of action of a novel human ether-a-go-go-related gene channel activator. *Molecular pharmacology* **69:** 658-665

Cherubini A, Hofmann G, Pillozzi S, Guasti L, Crociani O, Cilia E, Di Stefano P, Degani S, Balzi M, Olivotto M, Wanke E, Becchetti A, Defilippi P, Wymore R, Arcangeli A (2005) Human ether-a-go-go-related gene 1 channels are physically linked to beta1 integrins and modulate adhesion-dependent signaling. *Molecular biology of the cell* **16:** 2972-2983

Cherubini A, Taddei GL, Crociani O, Paglierani M, Buccoliero AM, Fontana L, Noci I, Borri P, Borrani E, Giachi M, Becchetti A, Rosati B, Wanke E, Olivotto M, Arcangeli A (2000) HERG potassium channels are more frequently expressed in human endometrial cancer as compared to non-cancerous endometrium. *Br J Cancer* **83:** 1722-1729

Chiesa N, Rosati B, Arcangeli A, Olivotto M, Wanke E (1997) A novel role for HERG K+ channels: spike-frequency adaptation. *The Journal of physiology* **501 (Pt 2):** 313-318

Choi BY, Kim HY, Lee KH, Cho YH, Kong G (1999) Clofilium, a potassium channel blocker, induces apoptosis of human promyelocytic leukemia (HL-60) cells via Bcl-2-insensitive activation of caspase-3. *Cancer letters* **147:** 85-93

Chouabe C, Drici MD, Romey G, Barhanin J, Lazdunski M (1998) HERG and KvLQT1/IsK, the cardiac K+ channels involved in long QT syndromes, are targets for calcium channel blockers. *Molecular pharmacology* **54:** 695-703

Clarke CE, Hill AP, Zhao J, Kondo M, Subbiah RN, Campbell TJ, Vandenberg JI (2006) Effect of S5P alpha-helix charge mutants on inactivation of hERG K+ channels. *The Journal of physiology* **573:** 291-304

Cocchietto M, Zorzet S, Sorc A, Sava G (2003) Primary tumor, lung and kidney retention and antimetastasis effect of NAMI-A following different routes of administration. *Investigational new drugs* **21:** 55-62

Cordero-Morales JF, Jogini V, Lewis A, Vasquez V, Cortes DM, Roux B, Perozo E (2007) Molecular driving forces determining potassium channel slow inactivation. *Nature structural & molecular biology* **14:** 1062-1069

Crociani O, Guasti L, Balzi M, Becchetti A, Wanke E, Olivotto M, Wymore RS, Arcangeli A (2003) Cell cycle-dependent expression of HERG1 and HERG1B isoforms in tumor cells. *The Journal of biological chemistry* **278:** 2947-2955

Crociani O, Zanieri F, Pillozzi S, Lastraioli E, Stefanini M, Fiore A, Fortunato A, D'Amico M, Masselli M, De Lorenzo E, Gasparoli L, Chiu M, Bussolati O, Becchetti A, Arcangeli A (2013) hERG1 channels modulate integrin signaling to trigger angiogenesis and tumor progression in colorectal cancer. *Scientific reports* **3:** 3308

Cuddapah VA, Sontheimer H (2011) Ion channels and transporters [corrected] in cancer. 2. Ion channels and the control of cancer cell migration. *American journal of physiology Cell physiology* **301:** C541-549

Cuello LG, Jogini V, Cortes DM, Pan AC, Gagnon DG, Dalmas O, Cordero-Morales JF, Chakrapani S, Roux B, Perozo E (2010) Structural basis for the coupling between activation and inactivation gates in K(+) channels. *Nature* **466:** 272-275

D'Amico M, Gasparoli L, Arcangeli A (2013) Potassium channels: novel emerging biomarkers and targets for therapy in cancer. *Recent patents on anti-cancer drug discovery* **8:** 53-65

Daleau P, Lessard E, Groleau MF, Turgeon J (1995) Erythromycin blocks the rapid component of the delayed rectifier potassium current and lengthens repolarization of guinea pig ventricular myocytes. *Circulation* **91:** 3010-3016

De Bruin ML, Pettersson M, Meyboom RH, Hoes AW, Leufkens HG (2005) Anti-HERG activity and the risk of drug-induced arrhythmias and sudden death. *Eur Heart J* **26:** 590-597

de la Pena P, Alonso-Ron C, Machin A, Fernandez-Trillo J, Carretero L, Dominguez P, Barros F (2011) Demonstration of physical proximity between the N terminus and the S4-S5 linker of the human ether-a-go-go-related gene (hERG) potassium channel. *The Journal of biological chemistry* **286:** 19065-19075

Diochot S, Loret E, Bruhn T, Beress L, Lazdunski M (2003) APETx1, a new toxin from the sea anemone Anthopleura elegantissima, blocks voltage-gated human ether-a-go-go-related gene potassium channels. *Molecular pharmacology* **64:** 59-69

Diss JK, Stewart D, Pani F, Foster CS, Walker MM, Patel A, Djamgoz MB (2005) A potential novel marker for human prostate cancer: voltage-gated sodium channel expression in vivo. *Prostate cancer and prostatic diseases* **8:** 266-273

Doyle DA, Morais Cabral J, Pfuetzner RA, Kuo A, Gulbis JM, Cohen SL, Chait BT, MacKinnon R (1998) The structure of the potassium channel: molecular basis of K+ conduction and selectivity. *Science (New York, NY)* **280:** 69-77

Eckhardt LL, Rajamani S, January CT (2005) Protein trafficking abnormalities: a new mechanism in drug-induced long QT syndrome. *British journal of pharmacology* **145:** 3-4

Eiras S, Fernandez P, Pineiro R, Iglesias MJ, Gonzalez-Juanatey JR, Lago F (2006) Doxazosin induces activation of GADD153 and cleavage of focal adhesion kinase in cardiomyocytes en route to apoptosis. *Cardiovascular research* **71:** 118-128

Enyedi P, Czirjak G (2010) Molecular background of leak K+ currents: two-pore domain potassium channels. *Physiological reviews* **90:** 559-605

Fan JS, Jiang M, Dun W, McDonald TV, Tseng GN (1999) Effects of outer mouth mutations on hERG channel function: a comparison with similar mutations in the Shaker channel. *Biophysical journal* **76:** 3128-3140

Faravelli L, Arcangeli A, Olivotto M, Wanke E (1996) A HERG-like K+ channel in rat F-11 DRG cell line: pharmacological identification and biophysical characterization. *The Journal of physiology* **496 (Pt 1):** 13-23

Farrelly AM, Ro S, Callaghan BP, Khoyi MA, Fleming N, Horowitz B, Sanders KM, Keef KD (2003) Expression and function of KCNH2 (HERG) in the human jejunum. *American journal of physiology Gastrointestinal and liver physiology* **284:** G883-895

Fermini B, Fossa AA (2003) The impact of drug-induced QT interval prolongation on drug discovery and development. *Nature reviews Drug discovery* **2:** 439-447

Finlayson K, McLuckie J, Hern J, Aramori I, Olverman HJ, Kelly JS (2001a) Characterisation of [(125)I]-apamin binding sites in rat brain membranes with HE293 cells transfected with SK channel subtypes. *Neuropharmacology* **41:** 341-350

Finlayson K, Turnbull L, January CT, Sharkey J, Kelly JS (2001b) [3H]dofetilide binding to HERG transfected membranes: a potential high throughput preclinical screen. *European journal of pharmacology* **430:** 147-148

Fraser SP, Diss JK, Chioni AM, Mycielska ME, Pan H, Yamaci RF, Pani F, Siwy Z, Krasowska M, Grzywna Z, Brackenbury WJ, Theodorou D, Koyuturk M, Kaya H, Battaloglu E, De Bella MT, Slade MJ, Tolhurst R, Palmieri C, Jiang J, Latchman DS, Coombes RC, Djamgoz MB (2005) Voltage-gated sodium channel expression and potentiation of human breast cancer metastasis. *Clinical cancer research : an official journal of the American Association for Cancer Research* **11:** 5381-5389

Frausin F, Scarcia V, Cocchietto M, Furlani A, Serli B, Alessio E, Sava G (2005) Free exchange across cells, and echistatin-sensitive membrane target for the metastasis inhibitor NAMI-A (imidazolium trans-imidazole dimethyl sulfoxide tetrachlororuthenate) on KB tumor cells. *The Journal of pharmacology and experimental therapeutics* **313:** 227-233

Ganapathi SB, Kester M, Elmslie KS (2009) State-dependent block of HERG potassium channels by R-roscovitine: implications for cancer therapy. *American journal of physiology Cell physiology* **296:** C701-710

Gang H, Zhang S (2006) Na+ permeation and block of hERG potassium channels. *The Journal of general physiology* **128:** 55-71

Gessner G, Macianskiene R, Starkus JG, Schonherr R, Heinemann SH (2010) The amiodarone derivative KB130015 activates hERG1 potassium channels via a novel mechanism. *European journal of pharmacology* **632:** 52-59

Gintant GA (2000) Characterization and functional consequences of delayed rectifier current transient in ventricular repolarization. *American journal of physiology Heart and circulatory physiology* **278:** H806-817

Grissmer S, Nguyen AN, Cahalan MD (1993) Calcium-activated potassium channels in resting and activated human T lymphocytes. Expression levels, calcium dependence, ion selectivity, and pharmacology. *The Journal of general physiology* **102:** 601-630

Grunnet M (2010) Repolarization of the cardiac action potential. Does an increase in repolarization capacity constitute a new anti-arrhythmic principle? *Acta physiologica (Oxford, England)* **198 Suppl 676:** 1-48

Grunnet M, Diness TG, Hansen RS, Olesen SP (2008) Biophysical characterization of the short QT mutation hERG-N588K reveals a mixed gain-and loss-of-function. *Cellular physiology and biochemistry : international journal of experimental cellular physiology, biochemistry, and pharmacology* **22:** 611-624

Guasti L, Crociani O, Redaelli E, Pillozzi S, Polvani S, Masselli M, Mello T, Galli A, Amedei A, Wymore RS, Wanke E, Arcangeli A (2008) Identification of a posttranslational mechanism for the regulation of hERG1 K+ channel expression and hERG1 current density in tumor cells. *Molecular and cellular biology* **28:** 5043-5060

Gullo F, Ales E, Rosati B, Lecchi M, Masi A, Guasti L, Cano-Abad MF, Arcangeli A, Lopez MG, Wanke E (2003) ERG K+ channel blockade enhances firing and epinephrine secretion in rat chromaffin cells: the missing link to LQT2-related sudden death? *FASEB journal : official publication of the Federation of American Societies for Experimental Biology* **17:** 330-332

Guo D, Klaasse E, de Vries H, Brussee J, Nalos L, Rook MB, Vos MA, van der Heyden MA, Ijzerman AP (2009) Exploring chemical substructures essential for HERG k(+) channel blockade by synthesis and biological evaluation of dofetilide analogues. *ChemMedChem* **4:** 1722-1732

Gurrola GB, Rosati B, Rocchetti M, Pimienta G, Zaza A, Arcangeli A, Olivotto M, Possani LD, Wanke E (1999) A toxin to nervous, cardiac, and endocrine ERG K + channels isolated from Centruroides noxius scorpion venom. *FASEB journal : official publication of the Federation of American Societies for Experimental Biology* **13:** 953-962

Gussak I, Brugada P, Brugada J, Wright RS, Kopecky SL, Chaitman BR, Bjerregaard P (2000) Idiopathic short QT interval: a new clinical syndrome? *Cardiology* **94:** 99-102

Gustina AS, Trudeau MC (2009) A recombinant N-terminal domain fully restores deactivation gating in N-truncated and long QT syndrome mutant hERG potassium channels. *Proceedings of the National Academy of Sciences of the United States of America* **106:** 13082-13087

Gustina AS, Trudeau MC (2011) hERG potassium channel gating is mediated by N- and C-terminal region interactions. *J Gen Physiol* **137:** 315-325

Gustina AS, Trudeau MC (2013) The eag domain regulates hERG channel inactivation gating via a direct interaction. *The Journal of general physiology* **141:** 229-241

Hanahan D, Weinberg RA (2000) The hallmarks of cancer. *Cell* **100:** 57-70

Hanahan D, Weinberg RA (2011) Hallmarks of cancer: the next generation. *Cell* **144:** 646-674

Hardman RM, Stansfeld PJ, Dalibalta S, Sutcliffe MJ, Mitcheson JS (2007) Activation gating of hERG potassium channels: S6 glycines are not required as gating hinges. In *J Biol Chem* Vol. 282, pp 31972-31981. United States

Harmar AJ, Hills RA, Rosser EM, Jones M, Buneman OP, Dunbar DR, Greenhill SD, Hale VA, Sharman JL, Bonner TI, Catterall WA, Davenport AP, Delagrange P, Dollery CT, Foord SM, Gutman GA, Laudet V, Neubig RR, Ohlstein EH, Olsen RW, Peters J, Pin JP, Ruffolo RR, Searls DB, Wright MW, Spedding M (2009) IUPHAR-DB: the IUPHAR database of G protein-coupled receptors and ion channels. *Nucleic acids research* **37:** D680-685

Herzberg IM, Trudeau MC, Robertson GA (1998) Transfer of rapid inactivation and sensitivity to the class III antiarrhythmic drug E-4031 from HERG to M-eag channels. *The Journal of physiology* **511 (Pt 1):** 3-14

Hofmann G, Bernabei PA, Crociani O, Cherubini A, Guasti L, Pillozzi S, Lastraioli E, Polvani S, Bartolozzi B, Solazzo V, Gragnani L, Defilippi P, Rosati B, Wanke E, Olivotto M, Arcangeli A (2001) HERG K+ channels activation during beta(1) integrin-mediated adhesion to fibronectin induces an up-regulation of alpha(v) beta(3) integrin in the preosteoclastic leukemia cell line FLG 29.1. *The Journal of biological chemistry* **276:** 4923-4931

Horton JK, Baxendale PM (1995) Mass measurements of cyclic AMP formation by radioimmunoassay, enzyme immunoassay, and scintillation proximity assay. *Methods in molecular biology (Clifton, NJ)* **41:** 91-105

Huffaker SJ, Chen J, Nicodemus KK, Sambataro F, Yang F, Mattay V, Lipska BK, Hyde TM, Song J, Rujescu D, Giegling I, Mayilyan K, Proust MJ, Soghoyan A, Caforio G, Callicott JH, Bertolino A, Meyer-Lindenberg A, Chang J, Ji Y, Egan MF, Goldberg TE, Kleinman JE, Lu B, Weinberger DR (2009) A primate-specific, brain isoform of KCNH2 affects cortical physiology, cognition, neuronal repolarization and risk of schizophrenia. *Nature medicine* **15:** 509-518

Jara-Oseguera A, Ishida IG, Rangel-Yescas GE, Espinosa-Jalapa N, Perez-Guzman JA, Elias-Vinas D, Le Lagadec R, Rosenbaum T, Islas LD (2011) Uncoupling charge movement from channel opening in voltage-gated potassium channels by ruthenium complexes. *The Journal of biological chemistry* **286:** 16414-16425

Jehle J, Schweizer PA, Katus HA, Thomas D (2011) Novel roles for hERG K(+) channels in cell proliferation and apoptosis. *Cell death & disease* **2:** e193

Jiang M, Dun W, Tseng GN (1999) Mechanism for the effects of extracellular acidification on HERG-channel function. *Am J Physiol* **277:** H1283-1292

Jiang M, Zhang M, Maslennikov IV, Liu J, Wu DM, Korolkova YV, Arseniev AS, Grishin EV, Tseng GN (2005) Dynamic conformational changes of extracellular S5-P linkers in the hERG channel. *The Journal of physiology* **569:** 75-89

Jones EM, Roti Roti EC, Wang J, Delfosse SA, Robertson GA (2004) Cardiac IKr channels minimally comprise hERG 1a and 1b subunits. *The Journal of biological chemistry* **279:** 44690-44694

Jurkiewicz NK, Sanguinetti MC (1993) Rate-dependent prolongation of cardiac action potentials by a methanesulfonanilide class III antiarrhythmic agent. Specific block of rapidly activating delayed rectifier K+ current by dofetilide. *Circ Res* **72:** 75-83

Kamiya K, Niwa R, Mitcheson JS, Sanguinetti MC (2006) Molecular determinants of HERG channel block. *Molecular pharmacology* **69:** 1709-1716

Kamochi H, Nii T, Eguchi K, Mori T, Yamamoto A, Shimoda K, Ibaraki K (1999) Clarithromycin associated with torsades de pointes. *Japanese circulation journal* **63:** 421-422

Kang J, Chen XL, Wang H, Ji J, Cheng H, Incardona J, Reynolds W, Viviani F, Tabart M, Rampe D (2005) Discovery of a small molecule activator of the human ether-a-go-go-related gene (HERG) cardiac K+ channel. *Molecular pharmacology* **67:** 827-836

Katapadi K, Kostandy G, Katapadi M, Hussain KM, Schifter D (1997) A review of erythromycin-induced malignant tachyarrhythmia--torsade de pointes. A case report. *Angiology* **48:** 821-826

Keating MT, Sanguinetti MC (1996) Molecular genetic insights into cardiovascular disease. *Science (New York, NY)* **272:** 681-685

Kim CJ, Cho YG, Jeong SW, Kim YS, Kim SY, Nam SW, Lee SH, Yoo NJ, Lee JY, Park WS (2004) Altered expression of KCNK9 in colorectal cancers. *APMIS : acta pathologica, microbiologica, et immunologica Scandinavica* **112:** 588-594

Kim DH, Lerner A (1998) Type 4 cyclic adenosine monophosphate phosphodiesterase as a therapeutic target in chronic lymphocytic leukemia. *Blood* **92:** 2484-2494

Kirsch GE, Trepakova ES, Brimecombe JC, Sidach SS, Erickson HD, Kochan MC, Shyjka LM, Lacerda AE, Brown AM (2004) Variability in the measurement of hERG potassium channel inhibition: effects of temperature and stimulus pattern. *Journal of pharmacological and toxicological methods* **50:** 93-101

Komatsu S, Moriya S, Che XF, Yokoyama T, Kohno N, Miyazawa K (2013) Combined treatment with SAHA, bortezomib, and clarithromycin for concomitant targeting of aggresome formation and intracellular proteolytic pathways enhances ER stress-mediated cell death in breast cancer cells. *Biochemical and biophysical research communications* **437:** 41-47

Konopleva M, Tabe Y, Zeng Z, Andreeff M (2009) Therapeutic targeting of microenvironmental interactions in leukemia: mechanisms and approaches. *Drug resistance updates : reviews and commentaries in antimicrobial and anticancer chemotherapy* **12:** 103-113

Kornberg LJ (1998) Focal adhesion kinase and its potential involvement in tumor invasion and metastasis. *Head & neck* **20:** 745-752

Kumagai M, Manabe A, Pui CH, Behm FG, Raimondi SC, Hancock ML, Mahmoud H, Crist WM, Campana D (1996) Stroma-supported culture in childhood B-lineage acute lymphoblastic leukemia cells predicts treatment outcome. *The Journal of clinical investigation* **97:** 755-760

Kundu S, Williams SR, Nordt SP, Clark RF (1997) Clarithromycin-induced ventricular tachycardia. *Annals of emergency medicine* **30:** 542-544

Kunzelmann K (2005) Ion channels and cancer. *The Journal of membrane biology* **205:** 159-173

Kupershmidt S, Snyders DJ, Raes A, Roden DM (1998) A K+ channel splice variant common in human heart lacks a C-terminal domain required for expression of

rapidly activating delayed rectifier current. *The Journal of biological chemistry* **273:** 27231-27235

Larsen AP, Bentzen BH, Grunnet M (2010) Differential effects of Kv11.1 activators on Kv11.1a, Kv11.1b and Kv11.1a/Kv11.1b channels. *British journal of pharmacology* **161:** 614-628

Larsen AP, Olesen SP (2010) Differential expression of hERG1 channel isoforms reproduces properties of native I(Kr) and modulates cardiac action potential characteristics. *PloS one* **5:** e9021

Larsen AP, Olesen SP, Grunnet M, Jespersen T (2008) Characterization of hERG1a and hERG1b potassium channels-a possible role for hERG1b in the I (Kr) current. *Pflugers Archiv : European journal of physiology* **456:** 1137-1148

Lastraioli E, Guasti L, Crociani O, Polvani S, Hofmann G, Witchel H, Bencini L, Calistri M, Messerini L, Scatizzi M, Moretti R, Wanke E, Olivotto M, Mugnai G, Arcangeli A (2004) herg1 gene and HERG1 protein are overexpressed in colorectal cancers and regulate cell invasion of tumor cells. *Cancer research* **64:** 606-611

Lecchi M, Redaelli E, Rosati B, Gurrola G, Florio T, Crociani O, Curia G, Cassulini RR, Masi A, Arcangeli A, Olivotto M, Schettini G, Possani LD, Wanke E (2002) Isolation of a long-lasting eag-related gene-type K+ current in MMQ lactotrophs and its accommodating role during slow firing and prolactin release. *The Journal of neuroscience : the official journal of the Society for Neuroscience* **22:** 3414-3425

Lee EL, Hasegawa Y, Shimizu T, Okada Y (2008) IK1 channel activity contributes to cisplatin sensitivity of human epidermoid cancer cells. *American journal of physiology Cell physiology* **294:** C1398-1406

Lees-Miller JP, Duan Y, Teng GQ, Duff HJ (2000) Molecular determinant of high-affinity dofetilide binding to HERG1 expressed in Xenopus oocytes: involvement of S6 sites. *Molecular pharmacology* **57:** 367-374

Lees-Miller JP, Kondo C, Wang L, Duff HJ (1997) Electrophysiological characterization of an alternatively processed ERG K+ channel in mouse and human hearts. *Circulation research* **81:** 719-726

Lenz TL, Hilleman DE (2000) Dofetilide, a new class III antiarrhythmic agent. *Pharmacotherapy* **20:** 776-786

Lerner A, Epstein PM (2006) Cyclic nucleotide phosphodiesterases as targets for treatment of haematological malignancies. *The Biochemical journal* **393:** 21-41

Levesque MC, O'Loughlin CW, Weinberg JB (2001) Use of serum-free media to minimize apoptosis of chronic lymphocytic leukemia cells during in vitro culture. *Leukemia* **15:** 1305-1307

Li M, Xiong ZG (2011) Ion channels as targets for cancer therapy. *International journal of physiology, pathophysiology and pharmacology* **3:** 156-166

Li Q, Raida M, Kang C (2010) 1H, 13C and 15N chemical shift assignments for the N-terminal domain of the voltage-gated potassium channel-hERG. *Biomolecular NMR assignments* **4:** 211-213

Li X, Xu J, Li M (1997) The human delta1261 mutation of the HERG potassium channel results in a truncated protein that contains a subunit interaction domain and decreases the channel expression. *The Journal of biological chemistry* **272:** 705-708

Liu J, Zhang M, Jiang M, Tseng GN (2002) Structural and functional role of the extracellular s5-p linker in the HERG potassium channel. *The Journal of general physiology* **120:** 723-737

London B, Trudeau MC, Newton KP, Beyer AK, Copeland NG, Gilbert DJ, Jenkins NA, Satler CA, Robertson GA (1997) Two isoforms of the mouse ether-a-go-go-related gene coassemble to form channels with properties similar to the rapidly activating component of the cardiac delayed rectifier K+ current. *Circ Res* **81:** 870-878

Marklund L, Henriksson R, Grankvist K (2001) Cisplatin-induced apoptosis of mesothelioma cells is affected by potassium ion flux modulator amphotericin B and bumetanide. *International journal of cancer Journal international du cancer* **93:** 577-583

Masi A, Becchetti A, Restano-Cassulini R, Polvani S, Hofmann G, Buccoliero AM, Paglierani M, Pollo B, Taddei GL, Gallina P, Di Lorenzo N, Franceschetti S, Wanke E, Arcangeli A (2005) hERG1 channels are overexpressed in glioblastoma multiforme and modulate VEGF secretion in glioblastoma cell lines. *British journal of cancer* **93:** 781-792

Menendez ST, Rodrigo JP, Alvarez-Teijeiro S, Villaronga MA, Allonca E, Vallina A, Astudillo A, Barros F, Suarez C, Garcia-Pedrero JM (2012) Role of HERG1 potassium channel in both malignant transformation and disease progression in head and neck carcinomas. *Modern pathology : an official journal of the United States and Canadian Academy of Pathology, Inc* **25:** 1069-1078

Mikasa K, Sawaki M, Kita E, Hamada K, Teramoto S, Sakamoto M, Maeda K, Konishi M, Narita N (1997) Significant survival benefit to patients with advanced non-small-cell lung cancer from treatment with clarithromycin. *Chemotherapy* **43:** 288-296

Milberg P, Hilker E, Ramtin S, Cakir Y, Stypmann J, Engelen MA, Monnig G, Osada N, Breithardt G, Haverkamp W, Eckardt L (2007) Proarrhythmia as a class effect of quinolones: increased dispersion of repolarization and triangulation of action potential predict torsades de pointes. *Journal of cardiovascular electrophysiology* **18:** 647-654

Milnes JT, Crociani O, Arcangeli A, Hancox JC, Witchel HJ (2003) Blockade of HERG potassium currents by fluvoxamine: incomplete attenuation by S6 mutations at F656 or Y652. *British journal of pharmacology* **139:** 887-898

Mishra A, Friedman HS, Sinha AK (1999) The effects of erythromycin on the electrocardiogram. *Chest* **115:** 983-986

Mitcheson J, Perry M, Stansfeld P, Sanguinetti MC, Witchel H, Hancox J (2005) Structural determinants for high-affinity block of hERG potassium channels. *Novartis Foundation symposium* **266:** 136-150; discussion 150-138

Mitcheson JS (2008) hERG potassium channels and the structural basis of drug-induced arrhythmias. *Chemical research in toxicology* **21:** 1005-1010

Morais Cabral JH, Lee A, Cohen SL, Chait BT, Li M, Mackinnon R (1998) Crystal structure and functional analysis of the HERG potassium channel N terminus: a eukaryotic PAS domain. *Cell* **95:** 649-655

Morissette P, Nishida M, Trepakova E, Imredy J, Lagrutta A, Chaves A, Hoagland K, Hoe CM, Zrada MM, Travis JJ, Zingaro GJ, Gerenser P, Friedrichs G, Salata JJ (2013) The anesthetized guinea pig: an effective early cardiovascular derisking and lead optimization model. *Journal of pharmacological and toxicological methods* **68:** 137-149

Morris TC, Kettle PJ, Drake M, Jones FC, Hull DR, Boyd K, Morrison A, Clarke P, O'Reilly P, Quinn J (2008) Clarithromycin with low dose dexamethasone and thalidomide is effective therapy in relapsed/refractory myeloma. *British journal of haematology* **143:** 349-354

Morris TC, Ranaghan L, Morrison J (2001) Phase II trial of clarithromycin and pamidronate therapy in myeloma. *Medical oncology (Northwood, London, England)* **18:** 79-84

Muskett FW, Thouta S, Thomson SJ, Bowen A, Stansfeld PJ, Mitcheson JS (2011) Mechanistic insight into human ether-a-go-go-related gene (hERG) K+ channel deactivation gating from the solution structure of the EAG domain. *The Journal of biological chemistry* **286:** 6184-6191

Neusch C, Rozengurt N, Jacobs RE, Lester HA, Kofuji P (2001) Kir4.1 potassium channel subunit is crucial for oligodendrocyte development and in vivo

myelination. *The Journal of neuroscience : the official journal of the Society for Neuroscience* **21:** 5429-5438

Ng CA, Hunter MJ, Perry MD, Mobli M, Ke Y, Kuchel PW, King GF, Stock D, Vandenberg JI (2011) The N-terminal tail of hERG contains an amphipathic alpha-helix that regulates channel deactivation. *PloS one* **6:** e16191

Niesvizky R, Jayabalan DS, Christos PJ, Furst JR, Naib T, Ely S, Jalbrzikowski J, Pearse RN, Zafar F, Pekle K, Larow A, Lent R, Mark T, Cho HJ, Shore T, Tepler J, Harpel J, Schuster MW, Mathew S, Leonard JP, Mazumdar M, Chen-Kiang S, Coleman M (2008) BiRD (Biaxin [clarithromycin]/Revlimid [lenalidomide]/ dexamethasone) combination therapy results in high complete- and overall-response rates in treatment-naive symptomatic multiple myeloma. *Blood* **111:** 1101-1109

Ohya S, Kimura K, Niwa S, Ohno A, Kojima Y, Sasaki S, Kohri K, Imaizumi Y (2009) Malignancy grade-dependent expression of K+-channel subtypes in human prostate cancer. *Journal of pharmacological sciences* **109:** 148-151

Pal S, Hartnett KA, Nerbonne JM, Levitan ES, Aizenman E (2003) Mediation of neuronal apoptosis by Kv2.1-encoded potassium channels. *The Journal of neuroscience : the official journal of the Society for Neuroscience* **23:** 4798-4802

Pal SK, Takimoto K, Aizenman E, Levitan ES (2006) Apoptotic surface delivery of K+ channels. *Cell death and differentiation* **13:** 661-667

Pardo-Lopez L, Zhang M, Liu J, Jiang M, Possani LD, Tseng GN (2002) Mapping the binding site of a human ether-a-go-go-related gene-specific peptide toxin (ErgTx) to the channel's outer vestibule. *J Biol Chem* **277:** 16403-16411

Perrin MJ, Kuchel PW, Campbell TJ, Vandenberg JI (2008) Drug binding to the inactivated state is necessary but not sufficient for high-affinity binding to human ether-a-go-go-related gene channels. *Molecular pharmacology* **74:** 1443-1452

Perry M, de Groot MJ, Helliwell R, Leishman D, Tristani-Firouzi M, Sanguinetti MC, Mitcheson J (2004) Structural determinants of HERG channel block by clofilium and ibutilide. *Molecular pharmacology* **66:** 240-249

Perry M, Sachse FB, Sanguinetti MC (2007) Structural basis of action for a human ether-a-go-go-related gene 1 potassium channel activator. *Proceedings of the National Academy of Sciences of the United States of America* **104:** 13827-13832

Perry M, Sanguinetti MC (2008) A single amino acid difference between ether-a-go-go-related gene channel subtypes determines differential sensitivity to a small molecule activator. *Molecular pharmacology* **73:** 1044-1051

Phartiyal P, Jones EM, Robertson GA (2007) Heteromeric assembly of human ether-a-go-go-related gene (hERG) 1a/1b channels occurs cotranslationally via N-terminal interactions. *The Journal of biological chemistry* **282:** 9874-9882

Pillozzi S, Arcangeli A (2010) Physical and functional interaction between integrins and hERG1 channels in cancer cells. *Advances in experimental medicine and biology* **674:** 55-67

Pillozzi S, Brizzi MF, Balzi M, Crociani O, Cherubini A, Guasti L, Bartolozzi B, Becchetti A, Wanke E, Bernabei PA, Olivotto M, Pegoraro L, Arcangeli A (2002) HERG potassium channels are constitutively expressed in primary human acute myeloid leukemias and regulate cell proliferation of normal and leukemic hemopoietic progenitors. *Leukemia* **16:** 1791-1798

Pillozzi S, Brizzi MF, Bernabei PA, Bartolozzi B, Caporale R, Basile V, Boddi V, Pegoraro L, Becchetti A, Arcangeli A (2007) VEGFR-1 (FLT-1), beta1 integrin, and hERG K+ channel for a macromolecular signaling complex in acute myeloid leukemia: role in cell migration and clinical outcome. *Blood* **110:** 1238-1250

Pillozzi S, Masselli M, De Lorenzo E, Accordi B, Cilia E, Crociani O, Amedei A, Veltroni M, D'Amico M, Basso G, Becchetti A, Campana D, Arcangeli A (2011) Chemotherapy resistance in acute lymphoblastic leukemia requires hERG1 channels and is overcome by hERG1 blockers. *Blood* **117:** 902-914

Piper DR, Duff SR, Eliason HC, Frazee WJ, Frey EA, Fuerstenau-Sharp M, Jachec C, Marks BD, Pollok BA, Shekhani MS, Thompson DV, Whitney P, Vogel KW, Hess SD (2008) Development of the predictor HERG fluorescence polarization assay using a membrane protein enrichment approach. *Assay and drug development technologies* **6:** 213-223

Piper DR, Varghese A, Sanguinetti MC, Tristani-Firouzi M (2003) Gating currents associated with intramembrane charge displacement in HERG potassium channels. *Proceedings of the National Academy of Sciences of the United States of America* **100:** 10534-10539

Pommier Y, Sordet O, Antony S, Hayward RL, Kohn KW (2004) Apoptosis defects and chemotherapy resistance: molecular interaction maps and networks. *Oncogene* **23:** 2934-2949

Prevarskaya N, Skryma R, Shuba Y (2010) Ion channels and the hallmarks of cancer. *Trends in molecular medicine* **16:** 107-121

Rademaker-Lakhai JM, van den Bongard D, Pluim D, Beijnen JH, Schellens JH (2004) A Phase I and pharmacological study with imidazolium-trans-DMSO-imidazole-tetrachlororuthenate, a novel ruthenium anticancer agent. *Clinical cancer research : an official journal of the American Association for Cancer Research* **10:** 3717-3727

Rampe D, Murawsky MK, Grau J, Lewis EW (1998) The antipsychotic agent sertindole is a high affinity antagonist of the human cardiac potassium channel HERG. *The Journal of pharmacology and experimental therapeutics* **286:** 788-793

Raschi E, Vasina V, Poluzzi E, De Ponti F (2008) The hERG K+ channel: target and antitarget strategies in drug development. *Pharmacol Res* **57:** 181-195

Recanatini M, Poluzzi E, Masetti M, Cavalli A, De Ponti F (2005) QT prolongation through hERG K(+) channel blockade: current knowledge and strategies for the early prediction during drug development. *Medicinal research reviews* **25:** 133-166

Redfern WS, Carlsson L, Davis AS, Lynch WG, MacKenzie I, Palethorpe S, Siegl PK, Strang I, Sullivan AT, Wallis R, Camm AJ, Hammond TG (2003) Relationships between preclinical cardiac electrophysiology, clinical QT interval prolongation and torsade de pointes for a broad range of drugs: evidence for a provisional safety margin in drug development. *Cardiovascular research* **58:** 32-45

Roden DM (1998) Mechanisms and management of proarrhythmia. *The American journal of cardiology* **82:** 49i-57i

Rosati B, Marchetti P, Crociani O, Lecchi M, Lupi R, Arcangeli A, Olivotto M, Wanke E (2000) Glucose- and arginine-induced insulin secretion by human pancreatic beta-cells: the role of HERG K(+) channels in firing and release. *FASEB journal : official publication of the Federation of American Societies for Experimental Biology* **14:** 2601-2610

Roy J, Vantol B, Cowley EA, Blay J, Linsdell P (2008) Pharmacological separation of hEAG and hERG K+ channel function in the human mammary carcinoma cell line MCF-7. *Oncology reports* **19:** 1511-1516

Sacco T, Bruno A, Wanke E, Tempia F (2003) Functional roles of an ERG current isolated in cerebellar Purkinje neurons. *Journal of neurophysiology* **90:** 1817-1828

Sale H, Wang J, O'Hara TJ, Tester DJ, Phartiyal P, He JQ, Rudy Y, Ackerman MJ, Robertson GA (2008) Physiological properties of hERG 1a/1b heteromeric currents and a hERG 1b-specific mutation associated with Long-QT syndrome. *Circulation research* **103:** e81-95

Sanguinetti MC, Jurkiewicz NK (1990) Two components of cardiac delayed rectifier K
+ current. Differential sensitivity to block by class III antiarrhythmic agents. *The
Journal of general physiology* **96:** 195-215

Sanguinetti MC, Tristani-Firouzi M (2006) hERG potassium channels and cardiac
arrhythmia. *Nature* **440:** 463-469

Sankaranarayanan A, Raman G, Busch C, Schultz T, Zimin PI, Hoyer J, Kohler R,
Wulff H (2009) Naphtho[1,2-d]thiazol-2-ylamine (SKA-31), a new activator of
KCa2 and KCa3.1 potassium channels, potentiates the endothelium-derived
hyperpolarizing factor response and lowers blood pressure. *Molecular
pharmacology* **75:** 281-295

Sava G, Capozzi I, Clerici K, Gagliardi G, Alessio E, Mestroni G (1998)
Pharmacological control of lung metastases of solid tumours by a novel
ruthenium complex. *Clinical & experimental metastasis* **16:** 371-379

Schafranek L, Leclercq TM, White DL, Hughes TP (2013) Clarithromycin enhances
dasatinib-induced cell death in chronic myeloid leukemia cells, by inhibition of
late stage autophagy. *Leukemia & lymphoma* **54:** 198-201

Schonherr R, Heinemann SH (1996) Molecular determinants for activation and
inactivation of HERG, a human inward rectifier potassium channel. *The Journal
of physiology* **493 (Pt 3):** 635-642

Schonherr R, Rosati B, Hehl S, Rao VG, Arcangeli A, Olivotto M, Heinemann SH,
Wanke E (1999) Functional role of the slow activation property of ERG K+
channels. *The European journal of neuroscience* **11:** 753-760

Schwarz JR, Bauer CK (2004) Functions of erg K+ channels in excitable cells. *Journal
of cellular and molecular medicine* **8:** 22-30

Shah RR (2005) Drug-induced QT interval prolongation--regulatory guidance and
perspectives on hERG channel studies. *Novartis Foundation symposium* **266:**
251-280; discussion 280-255

Shao XD, Wu KC, Guo XZ, Xie MJ, Zhang J, Fan DM (2008) Expression and
significance of HERG protein in gastric cancer. *Cancer biology & therapy* **7:**
45-50

Shao XD, Wu KC, Hao ZM, Hong L, Zhang J, Fan DM (2005) The potent inhibitory
effects of cisapride, a specific blocker for human ether-a-go-go-related gene
(HERG) channel, on gastric cancer cells. *Cancer biology & therapy* **4:** 295-301

Shibasaki T (1987) Conductance and kinetics of delayed rectifier potassium channels in
nodal cells of the rabbit heart. *The Journal of physiology* **387:** 227-250

Shimizu T, Lee EL, Ise T, Okada Y (2008) Volume-sensitive Cl(-) channel as a regulator of acquired cisplatin resistance. *Anticancer research* **28:** 75-83

Siddik ZH (2003) Cisplatin: mode of cytotoxic action and molecular basis of resistance. *Oncogene* **22:** 7265-7279

Smith GA, Tsui HW, Newell EW, Jiang X, Zhu XP, Tsui FW, Schlichter LC (2002) Functional up-regulation of HERG K+ channels in neoplastic hematopoietic cells. *The Journal of biological chemistry* **277:** 18528-18534

Smith PL, Baukrowitz T, Yellen G (1996) The inward rectification mechanism of the HERG cardiac potassium channel. *Nature* **379:** 833-836

Smith PL, Yellen G (2002) Fast and slow voltage sensor movements in HERG potassium channels. *The Journal of general physiology* **119:** 275-293

Spector PS, Curran ME, Zou A, Keating MT, Sanguinetti MC (1996) Fast inactivation causes rectification of the IKr channel. *J Gen Physiol* **107:** 611-619

Stanat SJ, Carlton CG, Crumb WJ, Jr., Agrawal KC, Clarkson CW (2003) Characterization of the inhibitory effects of erythromycin and clarithromycin on the HERG potassium channel. *Molecular and cellular biochemistry* **254:** 1-7

Stuhmer W, Pardo LA (2010) K(+) channels as therapeutic targets in oncology. *Future medicinal chemistry* **2:** 745-755

Su Z, Limberis J, Souers A, Kym P, Mikhail A, Houseman K, Diaz G, Liu X, Martin RL, Cox BF, Gintant GA (2009) Electrophysiologic characterization of a novel hERG channel activator. *Biochemical pharmacology* **77:** 1383-1390

Subbiah RN, Clarke CE, Smith DJ, Zhao J, Campbell TJ, Vandenberg JI (2004) Molecular basis of slow activation of the human ether-a-go-go related gene potassium channel. *The Journal of physiology* **558:** 417-431

Subbiah RN, Kondo M, Campbell TJ, Vandenberg JI (2005) Tryptophan scanning mutagenesis of the HERG K+ channel: the S4 domain is loosely packed and likely to be lipid exposed. *The Journal of physiology* **569:** 367-379

Szabo G, Farkas V, Grunnet M, Mohacsi A, Nanasi PP (2011) Enhanced repolarization capacity: new potential antiarrhythmic strategy based on HERG channel activation. *Current medicinal chemistry* **18:** 3607-3621

Tabe Y, Jin L, Tsutsumi-Ishii Y, Xu Y, McQueen T, Priebe W, Mills GB, Ohsaka A, Nagaoka I, Andreeff M, Konopleva M (2007) Activation of integrin-linked kinase is a critical prosurvival pathway induced in leukemic cells by bone marrow-derived stromal cells. *Cancer research* **67:** 684-694

Tanaka Y, Aida M, Tanaka H, Shigenobu K, Toro L (1998) Involvement of maxi-K(Ca) channel activation in atrial natriuretic peptide-induced vasorelaxation. *Naunyn-Schmiedeberg's archives of pharmacology* **357:** 705-708

Thomas D, Bloehs R, Koschny R, Ficker E, Sykora J, Kiehn J, Schlomer K, Gierten J, Kathofer S, Zitron E, Scholz EP, Kiesecker C, Katus HA, Karle CA (2008) Doxazosin induces apoptosis of cells expressing hERG K+ channels. *European journal of pharmacology* **579:** 98-103

Tiwari S, Felekkis K, Moon EY, Flies A, Sherr DH, Lerner A (2004) Among circulating hematopoietic cells, B-CLL uniquely expresses functional EPAC1, but EPAC1-mediated Rap1 activation does not account for PDE4 inhibitor-induced apoptosis. *Blood* **103:** 2661-2667

Toro L, Wallner M, Meera P, Tanaka Y (1998) Maxi-K(Ca), a Unique Member of the Voltage-Gated K Channel Superfamily. *News in physiological sciences : an international journal of physiology produced jointly by the International Union of Physiological Sciences and the American Physiological Society* **13:** 112-117

Torres AM, Bansal PS, Sunde M, Clarke CE, Bursill JA, Smith DJ, Bauskin A, Breit SN, Campbell TJ, Alewood PF, Kuchel PW, Vandenberg JI (2003) Structure of the HERG K+ channel S5P extracellular linker: role of an amphipathic alpha-helix in C-type inactivation. *The Journal of biological chemistry* **278:** 42136-42148

Tristani-Firouzi M, Chen J, Sanguinetti MC (2002) Interactions between S4-S5 linker and S6 transmembrane domain modulate gating of HERG K+ channels. *The Journal of biological chemistry* **277:** 18994-19000

Tseng GN (2006) Linkage between 'disruption of inactivation' and 'reduction of K+ selectivity' among hERG mutants in the S5-P linker region. In *J Physiol* Vol. 577, pp 459-460; author reply 461-452. England

Tseng GN, Sonawane KD, Korolkova YV, Zhang M, Liu J, Grishin EV, Guy HR (2007) Probing the outer mouth structure of the HERG channel with peptide toxin footprinting and molecular modeling. *Biophysical journal* **92:** 3524-3540

Tsujimae K, Suzuki S, Yamada M, Kurachi Y (2004) Comparison of kinetic properties of quinidine and dofetilide block of HERG channels. *European journal of pharmacology* **493:** 29-40

Van Slyke AC, Rezazadeh S, Snopkowski M, Shi P, Allard CR, Claydon TW (2010) Mutations within the S4-S5 linker alter voltage sensor constraints in hERG K+ channels. *Biophysical journal* **99:** 2841-2852

Vandenberg JI, Perry MD, Perrin MJ, Mann SA, Ke Y, Hill AP (2012) hERG K(+) channels: structure, function, and clinical significance. *Physiological reviews* **92:** 1393-1478

Viskin S (1999) Long QT syndromes and torsade de pointes. *Lancet* **354:** 1625-1633

Volberg WA, Koci BJ, Su W, Lin J, Zhou J (2002) Blockade of human cardiac potassium channel human ether-a-go-go-related gene (HERG) by macrolide antibiotics. *The Journal of pharmacology and experimental therapeutics* **302:** 320-327

Voloshyna I, Besana A, Castillo M, Matos T, Weinstein IB, Mansukhani M, Robinson RB, Cordon-Cardo C, Feinmark SJ (2008) TREK-1 is a novel molecular target in prostate cancer. *Cancer research* **68:** 1197-1203

Wallis RM (2010) Integrated risk assessment and predictive value to humans of non-clinical repolarization assays. *British journal of pharmacology* **159:** 115-121

Wang DT, Hill AP, Mann SA, Tan PS, Vandenberg JI (2011) Mapping the sequence of conformational changes underlying selectivity filter gating in the K(v)11.1 potassium channel. *Nature structural & molecular biology* **18:** 35-41

Wang J, Myers CD, Robertson GA (2000) Dynamic control of deactivation gating by a soluble amino-terminal domain in HERG K(+) channels. *The Journal of general physiology* **115:** 749-758

Wang J, Trudeau MC, Zappia AM, Robertson GA (1998) Regulation of deactivation by an amino terminal domain in human ether-a-go-go-related gene potassium channels. *J Gen Physiol* **112:** 637-647

Weinberg JB JN, Volkheimer AD, Chen Y, Bond, KM, MooreE, JO, Gockerman JP, Diehl LF, De Castro CM, Rizzieri DA, Levesque MC, Mugridge K and Deangelo J. (2007) Cytotoxicity of the type 4 phosphodiesterase inhibitor CD160130 for freshly isolated human CLL cells in vitro. Blood supplementary, p. 3129.

Witchel HJ (2011) Drug-induced hERG block and long QT syndrome. *Cardiovascular therapeutics* **29:** 251-259

Wolpert C, Schimpf R, Giustetto C, Antzelevitch C, Cordeiro J, Dumaine R, Brugada R, Hong K, Bauersfeld U, Gaita F, Borggrefe M (2005) Further insights into the effect of quinidine in short QT syndrome caused by a mutation in HERG. *Journal of cardiovascular electrophysiology* **16:** 54-58

Wonderlin WF, Strobl JS (1996) Potassium channels, proliferation and G1 progression. *The Journal of membrane biology* **154:** 91-107

Wulff H, Castle NA, Pardo LA (2009) Voltage-gated potassium channels as therapeutic targets. *Nature reviews Drug discovery* **8:** 982-1001

Wynia-Smith SL, Gillian-Daniel AL, Satyshur KA, Robertson GA (2008) hERG gating microdomains defined by S6 mutagenesis and molecular modeling. *The Journal of general physiology* **132:** 507-520

Yang J, Jan YN, Jan LY (1995) Control of rectification and permeation by residues in two distinct domains in an inward rectifier K+ channel. *Neuron* **14:** 1047-1054

Zhang M, Korolkova YV, Liu J, Jiang M, Grishin EV, Tseng GN (2003) BeKm-1 is a HERG-specific toxin that shares the structure with ChTx but the mechanism of action with ErgTx1. *Biophysical journal* **84:** 3022-3036

Zhang M, Liu J, Tseng GN (2004) Gating charges in the activation and inactivation processes of the HERG channel. *The Journal of general physiology* **124:** 703-718

Zhang R, Tian P, Chi Q, Wang J, Wang Y, Sun L, Liu Y, Tian S, Zhang Q (2012) Human ether-a-go-go-related gene expression is essential for cisplatin to induce apoptosis in human gastric cancer. *Oncology reports* **27:** 433-440

Zheng F, Li H, Liang K, Du Y, Guo D, Huang S (2012) Imatinib has the potential to exert its antileukemia effects by down-regulating hERG1 K+ channels in chronic myelogenous leukemia. *Medical oncology (Northwood, London, England)* **29:** 2127-2135

Zhou Z, Gong Q, Ye B, Fan Z, Makielski JC, Robertson GA, January CT (1998) Properties of HERG channels stably expressed in HEK 293 cells studied at physiological temperature. *Biophysical journal* **74:** 230-241

Zou A, Xu QP, Sanguinetti MC (1998) A mutation in the pore region of HERG K+ channels expressed in Xenopus oocytes reduces rectification by shifting the voltage dependence of inactivation. *The Journal of physiology* **509 (Pt 1):** 129-137

ACKNOWLEDGEMENTS

First and foremost I want to thank my supervisor, Professor Annarosa Arcangeli for giving me the opportunity to do my P.h.D in her lab. Thank you so much for all the suggestions, the advice and discussions during these three years.

I am also very grateful to Professor Andrea Becchetti, for his patience and kindness in critically revising the experiments, and especially all the patch-clamp studies, and for providing me valuable advice for the development of my research.

I would also like to thank all the member of the Arcangeli lab, which have shared with me this experience and have contribute to my professional growth. In particular I would like to thank Angela, Francesca, Antonella and Angelica, colleagues but mainly friends, for all the good times we had together, both inside and outside the lab. I would also give a special thanks to Massimo, with whom I share the credit for part of my job, for guiding and teaching me in the beginning of my research. Thank you so much for all the time spent together.

A particular and special thanks is dedicated to Silvia, my beloved girlfriend and life parter, who shared with me, as colleague and mostly as girlfriend, this long and sometimes arduous experience. We started together this P.h.D course, we supported each other during tough times and we finished together, this experience would not be the same without you. Thank you so much for your faithful support, for all your helps and love!

Finally, I would like to thanks my family, my dad, mum and sisters, for all their support, love and trust in all these years. For these and thousand other reasons, thank you so much. This thesis is dedicated to you.

Dottorato di Ricerca in
SCIENZE BIOMEDICHE
sede amministrativa: Dipartimento di
Scienze Biomediche Sperimentali e Cliniche
coordinatore: Prof. Persio Dello Sbarba

Dottorato di Ricerca in Scienze Biomediche

Presentazione del candidato: Luca Gasparoli
Curriculum: Oncologia Sperimentale e Clinica
Ciclo: XXVI°
Titolo della tesi: hERG1 channel as a molecular target for new anticancer
therapeutic approaches

A conclusione del corso triennale del XXVI° Ciclo del Dottorato di Ricerca in Scienze Biomediche (*curriculum Oncologia Sperimentale e Clinica)*, il Collegio dei Docenti, facendo propria la relazione presentata dalla Prof.ssa Annarosa Arcangeli, in qualità di *tutor*, circa l'attività di ricerca, l'operosità e l'assiduità del candidato, rilascia con parere unanime il seguente giudizio da presentare alla Commissione Giudicatrice ai fini dell'espletamento dell'esame finale.

Il Dr. Luca Gasparoli, nato a Gallarate il 06/05/1985, laureato in Scienze Biologiche Sanitarie il 16/12/2009, discutendo una tesi dal titolo "Analisi Biomolecolare e immunoistochimica dell'espressione del canale del potassio hERG1 in una casistica di adenocarcinoma del colon-retto", con la votazione di 110 e Lode, è stato/a ammesso/a, a partire dal 01/01/2011, al Dottorato di Ricerca in Scienze Biomediche *curriculum* Oncologia Sperimentale e Clinica (XXVI° Ciclo), svolgendo la propria attività di ricerca presso il Dipartimento di Patologia e Oncologia Sperimentali, sotto il tutoraggio della Prof.ssa Annarosa Arcangeli.

Descrizione dell'attività di ricerca/Risultati ottenuti:

Scopo dell'attività di ricerca è stata l'identificazione e la validazione di nuove molecole in grado di bloccare la corrente condotta dal canale ionico hERG1, con la prospettiva di un loro possibile utilizzo in ambito clinico nella terapia antitumorale. Il canale hERG1 rappresenta infatti un target interessante

in quanto risulta essere espresso in maniera alterata in numerosi tumori umani e regolare diversi aspetti della fisiologia della cellula tumorale. Il canale hERG1 è tuttavia considerato un anti-target nello sviluppo di nuovi farmaci dal momento che esso ha un ruolo fondamentale nella fisiologia cardiaca, essendo il principale regolatore della ripolarizzazione ventricolare: il blocco della conduzione del canale hERG1 può causare severi effetti collaterali, tra cui sindrome del QT lungo e torsione di punta, una forma di aritmia con esiti spesso fatali. Risulta quindi necessario identificare o sintetizzare nuovi composti in grado di bloccare il canale hERG1, esenti da effetti cardiotossici o arritmogenici, che possano essere in futuro utilizzati in ambito clinico. Sono state proposte diverse strategie per superare i problemi che potrebbero essere causati dall'utilizzo di bloccanti di hERG1; la strategia adottata in questo progetto di ricerca si è incentrata sull'identificazione di bloccanti selettivi dell'isoforma hERG1B, la quale risulta essere maggiormente espressa in diverse forme di leucemia e nei neuroblastomi umani.

I risultati ottenuti in questo lavoro sperimentale dimostrano che il canale hERG1 può essere bloccato da composti di diversa natura chimica, sia analoghi dei classici farmaci antiaritmici, antibiotici già utilizzati nella pratica clinica o molecole inizialmente sviluppate contro altri bersagli. Lo screening, effettuato tramite la tecnica del patch-clamp, di composti chimici differenti ha fornito importanti informazioni per quanto riguarda i siti di legame di queste molecole, confermando e ampliando la nostra conoscenza dei residui aminoacidici cruciali nella struttura hERG1. I risultati ottenuti con gli analoghi della Dofetilide, un farmaco anti-aritmico di classe III, potrebbero inoltre rappresentare un punto di partenza prezioso per lo sviluppo di nuovi farmaci antiaritmici privi dei gravi effetti collaterali riportati per la Dofetilide. Abbiamo inoltre dimostrato che la claritromicina, un antibiotico appartenente alla classe dei macrolidi già utilizzato in ambito clinico, risulta essere, nelle nostre condizioni sperimentali, leggermente più efficace nel bloccare la corrente condotta dal canale hERG1B, suggerendone così un possibile utilizzo come adiuvante nella chemioterapia.

Infine, gli esperimenti condotti utilizzando il CD-160130, un composto con struttura pirimido-indolica, hanno dimostrato che è possibile inibire selettivamente l'isoforma hERG1b. Il CD-160130 ha infatti dimostrato una significativa attività anti-leucemia sia in vitro che in vivo in leucemie mielodi e linfoidi acute ed un marcato effetto pro-apoptotico in combinazione con alcuni farmaci chemioterapici, entrambi riconducibili a un'inibizione del canale ionico hERG1. Abbiamo inoltre dimostrato che il composto CD-160130 risulta essere privo di effetti collaterali sia mielotossici che cardiotossici, e che non produce allungamento della durata del potenziale d'azione cardiaco.

Nel complesso, i dati sperimentali discussi in questa tesi fornisco nuove indicazioni per lo sviluppo di composti con una ben definita selettività per le diverse isoforme dei canali hERG1.

Pubblicazioni/Presentazione dati a congressi nazionali e internazionali:

Pubblicazioni:

- Potassium Channels: Novel Emerging Biomarkers and Targets for Therapy in Cancer. D'Amico M, **Gasparoli L**, Arcangeli A. Recent Pat Anticancer Drug Discov. 2013 Jan 1;8(1): 53-65. Review.

- hERG1 channels modulate integrin signaling to trigger angiogenesis and tumor progression in colorectal cancer. Crociani O, Zanieri F, Pillozzi S, Lastraioli E, Stefanini M, Fiore A, Fortunato A, D'Amico M, Masselli M, De Lorenzo E, **Gasparoli L**, Chiu M, Bussolati O, Becchetti A, Arcangeli A. Sci Rep. 2013 Nov 25;3:3308.

- An analytical method for the quantification of hERG1 channel gene expression in human colorectal cancer. Fortunato A, **Gasparoli L**, Falsini S, Boni L and Arcangeli A. Diagn Mol Pathol. 2013 Dec;22(4):215-21.

Congressi nazionali e internazionali:

- Targeted Anticancer Therapies (TAT) 2011, Paris, France 7-9 March 2011. Arcangeli, A. Becchetti, O. Crociani, M. D'Amico, **L. Gasparoli**, M. Masselli, S. Pillozzi, K. Mugridge,W. Tiedke. HERG1 channels: from antitargets to novel therapeutic targets in oncology. Ann. Oncol.(2011) 22 (Supp.l 3): iii22-iii24

- ABCD Congress 2011 Ravenna, Italy 8-10 September 2011. **L. Gasparoli**, M. D'Amico, M. Masselli, A. Becchetti, A. Arcangeli. Identification of a MSCs induced potassium elk-like current in a B-chronic leukemia cell line, MEC1

- Joint National Ph.D. Meeting (ABCD and SIBBM), Gubbio, Italy 20-22 October 2011. **L. Gasparoli** and A. Arcangeli. hERG1 potassium channel as a molecular target for new anticancer therapeutic approaches

- Targeted Anticancer Therapies (TAT) 2012, Amsterdam, Netherlands 8-10 March 2012. **L. Gasparoli**, M. D'Amico, A.Becchetti, O. Crociani, M. Masselli, S. Pillozzi, K.Mugridge, W. Tiedke and A. Arcangeli. CD160130: a selective inhibitor of the tumor-type hERG1 channels, active in human leukemias. Ann. Oncol. (2012) 23 (Suppl. 1): i26–i44

- ASH Annual Meeting and Exposition, 2012, Atlanta, USA, 8-11 December, 2012. Marika Masselli, Serena Pillozzi, Massimo D'Amico, **Luca Gasparoli**, Olivia Crociani, Matteo Stefanini, Kennet Mugridge, Wolfang Tiedke, Andrea Becchetti, and Annarosa Arcangeli. Identification of Non-Cardiotoxic hERG1 Blockers to Overcome Chemoresistance in Acute Lymphoblastic Leukemias. Blood (ASH Annual Meeting Abstracts), Nov 2012; 120: 1506

Seminari:

- Presentazione Dottorato di Ricerca I anno: "hERG1 ionic channel as a molecular target for new anticancer therapeutic approaches" (2011)

- Presentazione Dottorato di Ricerca II anno: "hERG1 ionic channel as a molecular target for new anticancer therapeutic approaches" (2012)

- Presentazione Dottorato di Ricerca III anno: "hERG1 ionic channel as a molecular target for new anticancer therapeutic approaches" (2013)

Durante il corso di dottorato, il candidato ha seguito con il massimo impegno il programma didattico stabilito dal Collegio dei Docenti ed ha portato avanti con entusiasmo e determinazione le sue ricerche, dando prova di grande inventiva ed intraprendenza, nonché di notevole elasticità nella elaborazione dei dati sperimentali. Nel corso del triennio, il candidato ha inoltre maturato una buona cultura di base ed una vasta esperienza diretta in metodiche sperimentali.

Per quanto sopra, il Collegio dei Docenti unanime ritiene che il Dr. Luca Gasparoli possa meritatamente aspirare a conseguire il titolo di Dottore di Ricerca.

Firenze,   13/02/2014

Il Coordinatore del Corso
Prof. Persio Dello Sbarba